PoDeA

Port Development Argentina

Daan Deckers, Mathijs van Dijk, Mitchel Grund, Gijs Hendrickx, René de Koning & Niels Smit

Delft University of Technology
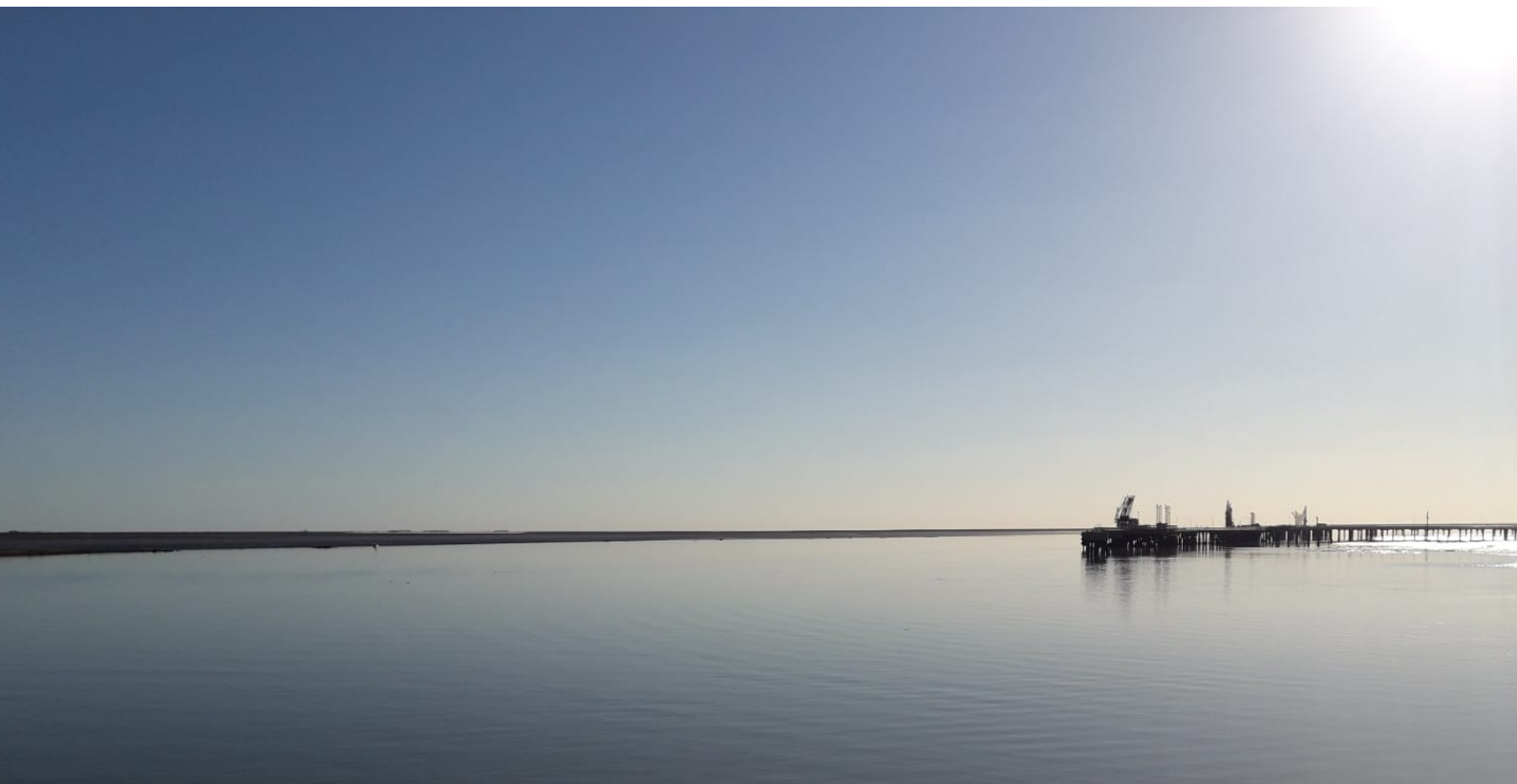
In collaboration with

PoDeA
Port Development Argentina

December 3, 2018

Authors

D. (Daan) Deckers	Hydraulic Engineering
M.H. (Mathijs) van Dijk	Structural Engineering
M. (Mitchel) Grund	Structural Engineering
G.G. (Gijs) Hendrickx	Hydraulic Engineering
R.T. (René) de Koning	Hydraulic Engineering
N.G.A. (Niels) Smit	Hydraulic Engineering

Delft University of Technology

Supervisors

T. (Tiedo) Vellinga	Delft University of Technology
P.H.E. (Pablo) Arecco	University of Buenos Aires
J.G. (Jarit) de Gijt	Delft University of Technology
M.Z. (Mark) Voorendt	Delft University of Technology

In collaboration with

Preface

This report is the outcome of a multidisciplinary project performed for the Delft University of Technology. The project is part of the master program and gives a group of students with different disciplines the change to work together to solve a problem in the field of civil engineering; enhancing the experience working in multidisciplinary groups.

This project is carried out by a group of six students from the TU Delft. Two of them specialised in the field of structural engineering and four in the field of hydraulic engineering. With the help of Tiedo Vellinga we got in contact with Pablo Arecco who helped us arranging and defining the scope of the project. Next to that, he helped us with the guidance during the project.

In the project we wanted to add our knowledge and expertise by investigating the change in hydrodynamics and morphodynamics caused by a port expansion, but also to look at structural alternatives of port construction nowadays in Argentina. Therefore we went to Argentina to do this project.

During our stay in Argentina, we worked from the office of Besna, located in the capital of the country; Buenos Aires. However, during the project we had some field trips to the port of Bahía Blanca to get a better insight on what we are working on. During these trips, we worked at the office of the port authority; Consorcio de Gestión del Puerto de Bahía Blanca. Here we had the opportunity to collaborate with experienced people working for the CGPBB and to discuss our work and findings with them.

The project was an interesting contribution on the master program; integrating multiple disciplines into one project was an enriching experience. Moreover, carrying out the project in Argentina made the work on the report both interesting and informative. For the hydraulic engineers it was next to that an interesting opportunity to work with a, on beforehand unknown, hydraulic model called MOHID.

We are thankful for the opportunity to come to Argentina. It was a fruitful experience and with our report we hope to have contributed to the development of the Port of Bahía Blanca.

PoDeA
Daan Deckers, Mathijs van Dijk, Mitchel Grund,
Gijs Hendrickx, René de Koning & Niels Smit

Buenos Aires,
October, 2018

Abstract

This report contains the conceptual lay-out for two possible expansions of the port of Bahía Blanca (Figures 2 and 3[1]). To determine the best conceptual lay-outs, emphasis is drawn to understand the physical system to determine the effect of the expansion of the port on the natural system. The port of Bahía Blanca is situated at the end of a ria, or tidal basin.

For the designs, different conceptual lay-outs are developed and simulated in a hydrodynamic model called MOHID. This is a 2D depth-averaged model (2DH), which uses a rough bathymetry grid of the ria to determine the effect of the port development.

There are three mutations of the different port expansions on the environment, which are investigated using the MOHID-model: (1) the East expansion, containing reclamation of tidal flats and closure of a side channel; (2) the South expansion, containing a widening and elongation of the channel and reclamation of tidal flats; and (3) the deepening of the entire navigation channel to various minimum depths.

From the results of the MOHID-model on the East expansion conclusions on the mutations of the different port expansions are drawn. For the East expansion, only small changes are predicted; only local erosion in the navigation channel near the expansion may occur. For the South expansion, the flow velocities reduce in the entire stretch and there seems to be sedimentation at the eastern part of the expansion. It is and the widening of the channel is the dominant causation of the changes. For the deepening, the forcing determines the impact of a larger depth and differs along the channel.

As a conclusion the best and most feasible designs are chosen. The best design is the lay-out that obtained the highest score in the MultiCriteria- Analysis (MCA). The most feasible design is the design having the highest cost/benefit ratio determined by a Cost-Benefit Analysis (CBA).

The east bank is located close to the current port, Ingeniero White, on tidal flats which are inundated at high-water and dry at low-water. For the East expansion, different port lay-outs are developed mainly differing in amount of reclaimed land, length of viaducts and the presence of a mooring basin. The best design on the east is characterised as being very compact and having small viaducts between the dry bulk and agribulk terminals and jetties (Figure 1a). The main advantage of this design is the small expected increase of siltation, good safety and sufficient future expansion possibilities. The most feasible design, however, is characterised by long viaducts reducing the costs of the design (Figure 1b).

The other appointed location for the port expansion is the south bank, opposite of the current port development. This location, however, is characterised by two main disadvantages; the proximity of the natural reserve limits the available space and it is far from any form of connection with

---

[1]For the larger figures see Appendix O

(a)Best lay-out for east bank. (b)Most feasible lay-out for east bank.
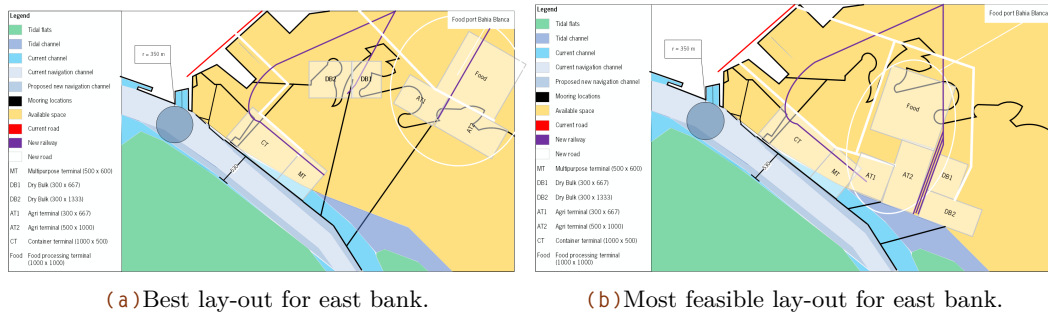
Figure 1. Overview of the designs for the expansion on the east bank.
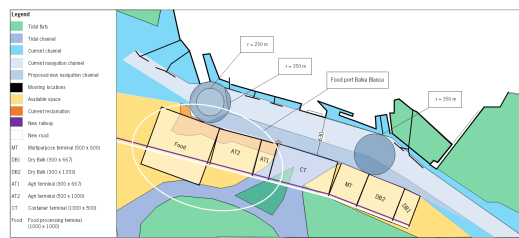
Figure 2. Most feasible lay-out for south bank.

the hinterland. Nevertheless, in 2013, the port authority (CGPBB) initiated the start of small reclamation works. The best and most feasible design fully utilises this reclaimed portion of land (Figure 2). Moreover, the best design has a small expected increase of siltation in the port area.

As a final design for the east bank, all four designs are combined to create a design in which all the advantages of each of the designs is fully incorporated. Therefore, this design has little reclamation as well as viaducts with only intermediate lengths, presented in Figure 3.

Figure 3. Optimized design for the east bank.

Table of Contents

V   Conclusion

Appendix

List of Figures

List of Tables

List of Scripts

1
Introduction

The Bahía Blanca ria is situated at the south of the province of Buenos Aires, Argentina (Figure 1.1). It is located at the southern boundary of the agricultural belt of Latin America, of which its majority lays in Argentina. The ria has the most complex set of geomorphological and dynamic conditions of Argentina, which makes it a difficult location to predict effects of new developments (Piccolo et al., 2008). Bahía Blanca currently has one of the most important ports of Argentina, mostly in solid and liquid bulk.

Figure 1.1. Bahía Blanca's location in Argentina.

1.1. Problem statement

The port of Bahía Blanca has aspirations to expand and has multiple possibilities to achieve this. The port authorities have bought multiple areas of land surrounding the current port (Figure 2.1). A market research has been conducted in which the wish for multiple new port areas is concluded. These areas can be build either south or east of the current port. Both have their own advantages and disadvantages. A conceptual design will be made to give insight in the expansion possibilities. Multiple designs will be considered on both sides and the effect on bathymetry and the required hinterland connections will be examined.

1.2. Goal

The goal of this project is to develop two conceptual lay-outs for the port expansion of Bahía Blanca (one east of the existing port, and one south – at the other side of the main channel), based on an understanding of the ria. Both structural and hydraulic engineering matters will be taken into account.

1.3. Methodology

The project is divided into four different parts which are executed consecutively. It should be noted that this is a design cycle and therefore includes different feedback loops on several moments. The methodology is shown in Figure 1.2.

Analysis – The main part of the analysis is to explore and state the requirements of the designs. In the analysis the main elements of characteristics of the ria system is covered. This includes the hydrodynamic conditions, the soil characteristics and bathymetry and the port as it is now. Also previous dredging activities and the design parameters for the conceptual designs will be discussed.

Synthesis – In this phase the different port lay-outs are developed. This is done in multiple design cycles to continuously improve the conceptual designs. In each of the cycles, different aspects are included and taken into account. Here, also the design of the proposed caissons are treated. On a hydraulic point of view, adaption to the ria due to the expansions will be considered and how this will be modelled.

Simulation – In the simulation phase the port lay-outs are tested. Testing in this case enhances determining the scores for each of the criteria, e.g. the dredging volumes and impact on the environment are determined. Beside this, the results of the hydrodynamic modelling are presented.

Evaluation – In the last phase of the design cycle, the evaluation, the different lay-outs are evaluated. This enhances a cost-benefit analysis, with as a final outcome one design for the east and one design for the south side.

It should be noted that throughout the design cycle, improvements on the designs are made, using the knowledge of later design phases. Not all these back- and forward movements through the design
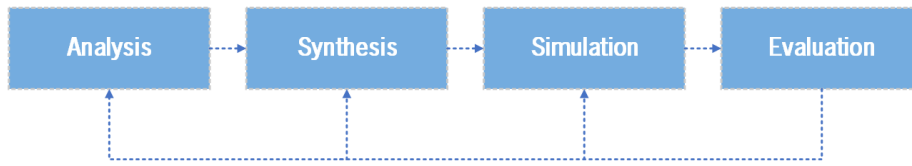
Figure 1.2. Schematisation of the methodology.

cycle are mentioned in this report for clarity and readability. The implications of the results of the modelled adjustments on the ria are examined to clarify the effects on the ria.

1.4. Port Vision 2040

In the port vision written by Port Consultants Rotterdam (2017a,b), the future plans of the port of Bahía Blanca are described up to 2040. It links the path to 2040 through five key success factors. These are, in no particular order, the following:

- Investment climate

- Work, laws and regulations

- Environment, safety and quality of life

- Accessibility and logistics

- City and region

These cornerstones and the effect they have on the development of the port are all briefly discussed below.

Investment climate – Yearly, millions of dollars are invested in the port, making it one of the main drivers of economic development in the region. The Port Authority has an enormous influence on its investment climate. A favourable climate benefits the entire region. This would mean the Port Authority needs:

- Strategic Stakeholder Management

- Transparency, Predictability and Stability

- Commercial Expansion

Work, laws and regulations – The port should make an active effort in continuing to increase efficiency, professionalism and transparency in port management. in 2040 it should have tools and human resources to plan and extend both its fore land and hinterland. To achieve this, the Port Authority needs:

- Professionalisation of Human Resources

- Port Planning

- Research, Development and Innovations

Environment, safety and quality of life – Our changing environment is one of the biggest global issues of the 21st century. The Port Authority already has started several initiatives on the

preservation of the surrounding environment, and should keep doing so in the future. Within the expansion it should also be kept in mind that the Port Authority should have:

- Environmental Management
- Energy Sustainability
- Protecting Biodiversity

Accessibility and logistics – The current railway and road connections are one of the main weaknesses of the port. In order to grow further, the current system must be improved, and enlarged. Not only close to the port, but also to the hinterland. The quality of life of the city should always be kept in mind. Traffic through the city is undesirable. The Port Authority should improve or construct:

- Nearby Infrastructure
- Hinterland Connection Infrastructure

City and region – The last key success factor is the connection with the city and the region. The improvement of the port should also positively affect the quality of life of the population, the attractiveness of the region and Bahía Blanca's place as one of the main innovators of the country. The port aims to increase:

- Quality of Life in the Surrounding Area
- Human Development

1.5. Structure

This report follows the same steps as the design cycle as shown in Section 1.3. It is divided in the same four sections. Firstly, in the analysis, the current situation is extensively described. All properties of the ria, the soil, and the possible expansion areas are analysed. Moreover the requirements of the port designs are described.

The next phase, the simulation, consists of three different parts. Firstly, four different conceptual designs for the east, and three designs for the south expansion are presented. Next the MOHID-model is constructed for the simulation of the ria and lastly the possibility for the use of caissons in investigated.

Thirdly, in the simulation, the three different parts of the synthesis come together. The constructed MOHID-model is used to predict what the expansion will do to the properties of the ria and a possible caisson is calculated.

Next, in the evaluation, the results of the simulation are evaluated on different criteria. Grades are given to all aspects of the design. In the final chapter the best design for each of the two expansion areas is presented.

The conclusion of this report contains the final design and recommendations for further studies.

Analysis

2

System analysis

In order to investigate the influence of possible port expansions into the ria, a proper understanding of the ria is needed. In this chapter an elaboration of the system analysis is given.

First the analysis of the current port lay-out is described (Section 2.1) followed by the assessment of the bathymetry (Section 2.2). Thereafter the soil characteristics (Section 2.3) and the sediment characteristics are discussed (Section 2.4). Last the Hydrodynamics (Section 2.5) are discussed.

2.1. Port lay-out

Figure 2.1 shows the current situation of the port area. The current port areas can be seen in green. The orange and the yellow highlighted areas show the possible expansion areas. The orange area, east of the current port, could partly be placed on current existing land, and partially on reclaimed land. The yellow part, on the south side of the current port, can utilise reclaimed land from the 2013 reclamation works and be extended by reclaiming more land.

2.2. Bathymetry

Vast areas of the Bahía Blanca ria are covered by salt marshes, as is clearly visible in Figure 2.2 (green colour). These areas will be partly flooded during high tide, and above the water line during ebb.

The channel in front of the ria has a depth of around 13–14 metres, which is maintained in Canal Principal via dredging up to Puerto Galván, which is 4–5 kilometres west of Ingeniero White (visible in Figure 2.3); this is up to where the current port of Bahía Blanca is situated. The other two bays
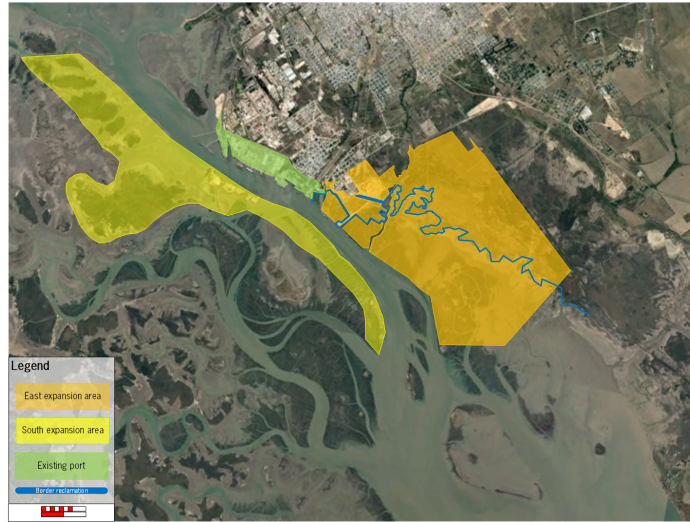
Figure 2.1. The possible expansion areas.
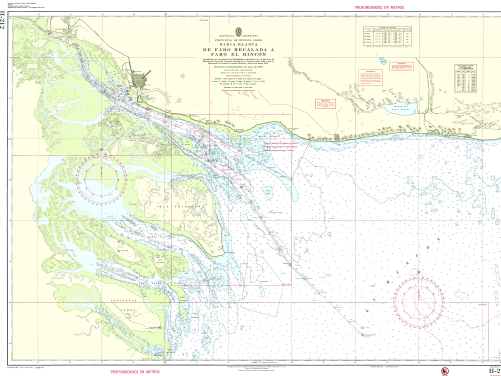
(a)Map of Faro Recalada to Faro El Rincon (Larrondo, 2000b).
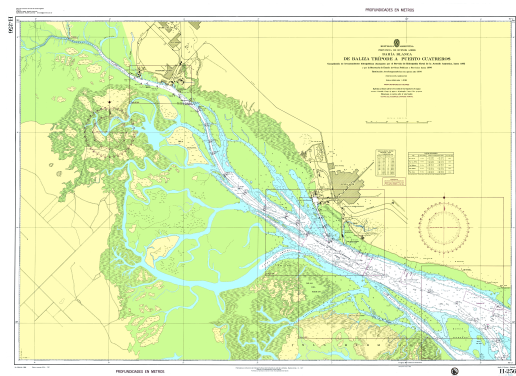
(b)Map of Bahía Blanca ria (Larrondo, 2000a).

Figure 2.2. Maps of the southern coastline of the province of Buenos Aires.
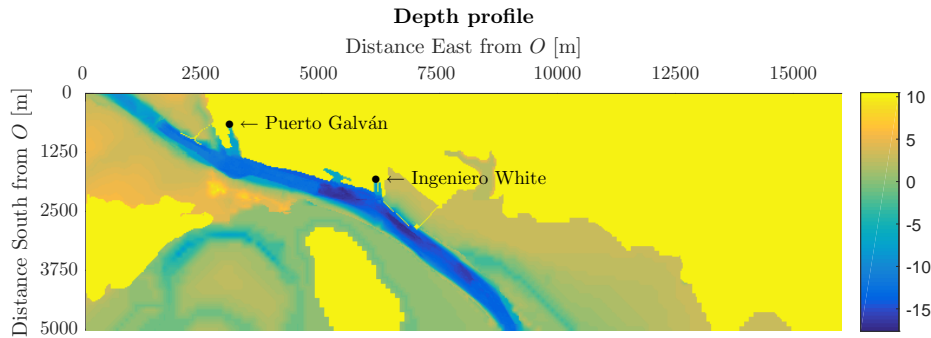
Figure 2.3. Depth profile of the port area. Areas with an elevation of 10 m are land sides.

– Bahía Falsa and Bahía Verde – get shallower just as the ria starts. At the mouth of the estuaries a couple of islands are situated after which the area becomes mainly salt marshes with clear channels running across the area.

Furthermore, the ria shows a clear funnel shape and becomes significantly wider towards the mouth, starting with a width of approximately 200 metres at the head to 53 kilometres at the mouth. The longest channel is the Canal Principal, which has a length of 60 kilometres and a width ranging from 200 metres at the head – with a depth of 3 metres – to a width of 3-4 kilometres, where a depths of 22 metres are found (Piccolo et al., 2008). According to Perillo and Piccolo (1991), the Canal Principal's width and depth increase exponentially from head to mouth. At the mouth, Canal Principal is partly closed due to a modified ebb delta (Cuardrado and Perillo, 1997). The cross-section of the channel varies over its length; from U-shaped up to Puerto Galván to V-shaped from there on, due to dredging activities by the port of Bahía Blanca.

At the mouth of the ria, the approach channel for the port areas of Bahía Blanca manoeuvres through sandbanks just east of Isla Bermejo. The route has frequently changed due to large geomorphological changes at this location and the occasional stranding of a ship as a result of this (Cuardrado and Perillo, 1997). After the study performed by NEDECO (1983), the port authority of Bahía Blanca has chosen to have the approach channel of the port through Canal Del Toro, which is a dynamic part of the mouth of the ria – some studies are performed on the movements of sediment enhancing sedimentation of the current route (e.g. Cuardrado and Perillo, 1997; Aliotta and Perillo, 1987). An elaboration on the historical and current dredging activities is given in Appendix B.

The main point of interest is the port area of Bahía Blanca. In this area, survey campaigns are regularly executed by the port authority to check the needed depth for the vessels. Data from such a campaign is shown in Figure 2.3. The datum in use is the lowest amplitude tide (LAT), which is 0 in the data. The location of point O is set to be $38'49'09.724'' \, S$, $62'20'03.882'' \, W$.

In the area of interest more than 60% of the area that is not land side is tidal flat, which shows the importance of the tidal flats, also around the port. Figure 2.3 shows clearly the main channel but also two other, shallower channels in the port area: (1) south-west from Ingeniero White; and (2) south of Puerto Galván. Due to the vast amounts of salt marshes, the port makes use of a lot of jetties to get from the main land (yellow) to the main channel (blue). During ebb, these two deeper areas are (partly) closed of from the main channel.
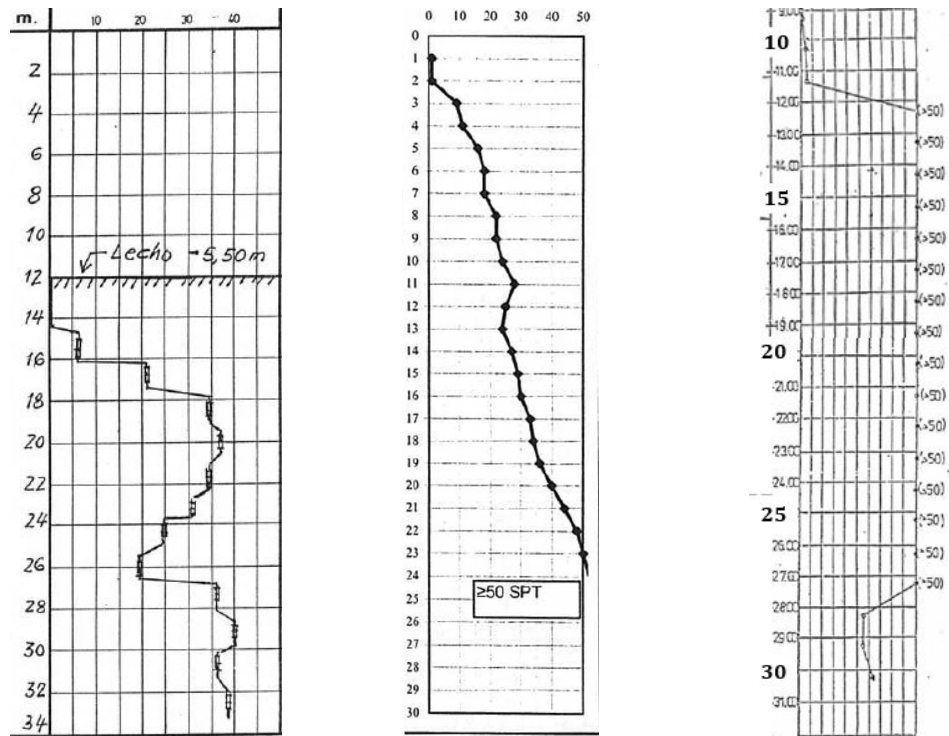
(a) Subsoil at the waterfront.   (b) Water under the inter tidal zones.   (c) subsoil strength at land.

Figure 2.4. Three types of subsoil at Ingeniero White.

2.3. Soil characteristics

No tests have been conducted on the exact locations of the possible expansion areas, but data is available on sights nearby. From this data, the expected soil characteristics of the relevant soils can be estimated. On these locations standard penetration tests have been done. In conclusion these results show roughly three different subsoil types: (1) soil at the waterfront; (2) soil under the intertidal flats; and (3) soil under the current land. These three types show three different subsoil profiles, shown in respectively Figures 2.4a to 2.4c.

These differ significantly in their strength. The soil under the excising land is quite strong from $-12\ m$ and below. The soil under the inter tidal zones slowly increases in strength and reaches a decent firmness from $20\ m$ and below. The soil at the waterfront has the lowest quality of the three considered. This soil never gets to the strength of the other two types, and only reaches a significant firmness from $28\ m$ and below.

These are not the exact values and evidently more investigation is needed, but for a first conceptual design this will provide as a sufficient estimation.

| Station | Percentages | | Sediment size (μm) | | | | | | Density |
	Sand	Fines	D_m	D_{10}	D_{35}	D_{50}	D_{65}	D_{90}	($kg m^{-3}$)
F 1	88	12	660	310	630	800			2640
F 2	38	62	150	80	130	170	210	310	2645
CS 1 S	5	95	115	70	100	120	140	180	2620
CS 2 S	92	8	190	100	165	185	225	320	2640
CS 2 C	8	92	215	105	170	215	260	390	2695
CS 3 C	97	3	210	180	215	225	235	270	2650
CS 3 S	97	3	215	176	220	235	250	285	2630

Table 2.1. Sediment gradation in the Bahía Blanca ria (NEDECO, 1983), location specification in Figure N.1.

2.4. Sediment characteristics

The runoff of the rivers into the Bahía Blanca ria is very little, implying a very small, negligible sediment supply. The sediment input from the continental shelf (ocean) is blocked due to ebb tidal delta. Therefore the high concentration of suspended sediments in the ria is due to erosion of tidal flats and island shores (Ginsberg and Perillo, 1990).

According to Campuzano et al. (2008), the process of erosion is characterised by little sediment import into the ria but relatively more sediment loss into the open ocean. This explains partly the wide ranges of values for turbidity and sediments in the inner areas of ria where the tide covers up an larger area compared to the main channel. Turbidity varies constantly during the tidal cycle.

Because most sediments in the ria are silts and clays, deposition depends on slack times. However in the Bahía Blanca ria strong currents and short slack water intervals hinder deposition of silt and clays in channels and on the tidal flat. Physical interactions like waves and tide in the system are rather important in the development of tidal creeks and playing a role in the erosion processes. Short, local generated waves erode old sediment and prevent the settling of new sediments. Crabs and plants together are responsible for eroding large parts of the tidal flats. These processes combined explain why the ria is mostly erosion dominated. (Piccolo et al., 2008)

During the NEDECO study in 1983 the sediment characteristics were investigated. The result is an overview of the sediment characteristics at fixed locations in the ria.

According to the studies of NEDECO (1983), by enhanced drilling, variability of depth of lithified (coarse) material is large. It is found in the range from 5 m on the tidal flats to more than 15 m in the areas of the Main Canal. This layer is originally covered by a layer of loose granular material of a few meters. Soil characteristics can be seen in Table 2.1.

2.5. Hydrodynamics

Since the bay has a horizontal dimension of around 70 km and the average depth is approximately 10 m, the circulations are mainly horizontal. This implies that vertical accelerations can be ignored (Campuzano et al., 2008).

Tidal component	Frequency ($° \ h^{-1}$)	Amplitude (cm)	Phase ($°$)
Z_0	0.00	263.54	0.00
M_2	28.98	169.12	186.07
L_2	29.53	25.48	255.36
N_2	28.44	23.98	103.59
M_4	57.97	22.76	178.28
S_2	30.00	21.59	307.35
K_1	15.04	21.15	61.18
O_1	13.94	15.53	0.70
MU_2	27.97	14.52	291.53
NU_2	28.51	10.95	137.92

Table 2.2. Principal tidal components for Ingeniero White (Table 2, Campuzano et al., 2014).

The hydrodynamics are divided into six categories: (1) tide; (2) water levels; (3) currents; (4) waves; (5) wind; and (6) salinity. All these topics are elaborated on below.

Tide

Recently, a harmonic analysis was performed by Campuzano et al. (2014) on the water levels. This resulted in 62 tidal components of which the principal tidal components at Ingeniero White are listed in Table 2.2. These are presented in Figure 2.5; the mean flood and ebb water levels are also presented. Out of this data becomes clear that the semi-diurnal components are dominant and so one can state that there is a semi-diurnal tide in the ria, which is confirmed by other studies (e.g. Perillo and Sequeira, 1989; Campuzano et al., 2008; Pierini et al., 2013). Of the semi-diurnal components, the M2 is most important as it represents more than 90% of the tidal energy (Pierini et al., 2008). After the semi-diurnal components, the diurnal components are most significant (Campuzano et al., 2008, 2014). The influence of the diurnal components decreases towards the head of the ria (Campuzano et al., 2008, 2014). Furthermore, the overtides become more important towards the head due to the interaction with the tidal flats (Campuzano et al., 2008; Pierini et al., 2013; Campuzano et al., 2014), which is in line with the decreasing importance of the diurnal components.

Moreover, the tidal amplitude increases towards the heads of the three bays of the Bahía Blanca ria (Pierini et al., 2013), with the biggest amplitude in the head of Canal Principal (Campuzano et al., 2008): the mean tidal amplitude varies between the head and the mouth between 3.5 m and 2.2 m, respectively (Piccolo et al., 2008). At the head, the spring tidal amplitude equals 4.0 m, and the neap tidal amplitude 3.0 m. At the mouth, the spring and neap equal 2.7 m and 1.8 m, respectively (Perillo and Piccolo, 1991). The increase in tidal amplitude towards the heads of the bay can be addressed to the funnel shape of the bays, as further discussed in Section 2.2. Thereby, the Bahía Blanca ria can be addressed to as a hyperchronous type ria, whereas the friction effect on the tidal wave is smaller than the convergence effect (Piccolo et al., 2008).

The increased amplitudes result in interaction between the bays during high tides, resulting in an exchange of water and sediment (Campuzano et al., 2008). The just-mentioned fact that overtides gain importance towards the head, results in the transition of a flood dominant tide at the mouth towards ebb dominance towards the head (Campuzano et al., 2008, 2014; Perillo et al., 2001). Due
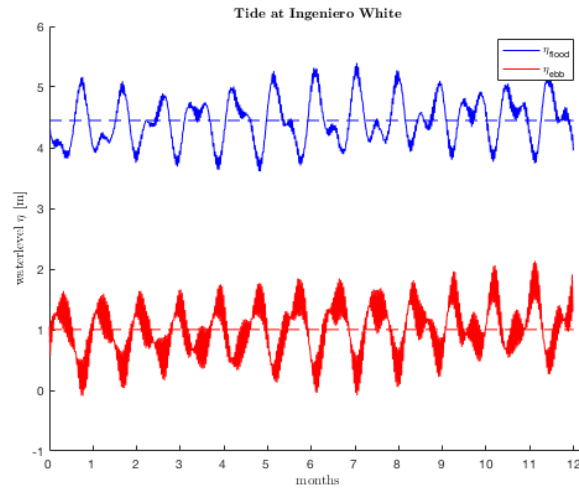
Figure 2.5. Flood and ebb levels at Ingeniero White, based on the tidal components listed in Table 2.2.

to the fact that the system is mainly ebb dominant, there is an ebb-orientated transport in Canal Principal (Perillo and Sequeira, 1989; Campuzano et al., 2008).

The tidal wave has in general the characteristics of a damped progressive wave that enters the ria from the southern margin and behaves more like a standing wave on the shallow areas; i.e. the tidal flats (Perillo et al., 2001; Pierini et al., 2013). Interestingly, Perillo and Sequeira (1989) mentions that the tidal wave can be described as a standing semi-diurnal wave, which is in contradiction with more recent studies. Possible explanations to this difference are (1) the measurement techniques improved, which results in a different view on the behaviour; or (2) due to the capital dredging that took place after the research of Perillo and Sequeira (1989), as mentioned in more detail in Appendix B. All in all, the tidal wave is taken as damped progressive wave in general and as standing wave in the shallow areas, whereas this is suggested by more recent studies.

The tidal wave as measured differs much from the predicted astronomical tide, which is due to the interaction with the tidal flats, river runoffs, and the influence of wind (Piccolo et al., 2008). The salt marshes in the ria result in a dampening of the tidal wave, just as the river runoffs do. The winds either push the tidal wave down – in case of winds from the NW – or increase the tidal wave – in case of winds from the SE. In general the winds are from the N and NW (as mentioned in Section 2.5), which according to Perillo and Piccolo (1991) result in the greatest tidal variations: (1) the time of low water is longer; (2) the time of high water is shorter; and (3) the water levels at high as well as low tide are reduced. Thereby, the tidal wave is referred to as a distorted wave (Pierini et al., 2013; Perillo et al., 2001).

Even though the time of low water is increased, still the new tidal wave already enters the system before the previous has left, which is due to the time needed for the water retreating from the tidal flats at which they scour the flats (Campuzano et al., 2008; Pierini et al., 2013; Campuzano et al., 2014). Because the next tidal wave is coming in before the system is fully drained, the slack duration is very short, which is also mentioned by Perillo et al. (2001). Hence, high concentrations of fine sediments that have no time to settle.

Location	Ebb		Flood	
	Velocity (m/s)	Direction $(° N)$	Velocity (m/s)	Direction $(° N)$
Km 70 | CF3	0.55	135	0.55	325
Km 47 | CF2	0.95	155	0.80	350
Km 45 | CF4	1.05	155	0.95	305
Km 70 | CS7	0.75	115	0.75	295
Km 70 | CS6C	0.75	80	0.60	270
Km 70 | CS5	0.95	110	0.95	290
Km 70 | CS4	0.85	110	0.70	310
Km 70 | CF1	0.95	135	0.75	315
Km 70 | CS2	1.00	170	0.80	330
Km 70 | CS1	0.55	105	0.40	280

Table 2.3. Mean current velocity and direction (Reyes et al., 2017).

Water levels

When the tide comes in, it starts with a water level of 1.2 m in the channels and a water level of 3.2 m at the head. The tide then rises until the water levels rise to 3.4 m. Then the tide retreats and water levels go down again, with at the heads a late response while maintaining higher water levels of around 3.2 m (Campuzano et al., 2008).

Depending on the wind direction, the mean sea level differs from 1.94 m without wind to 2.44 m as a result from the setup caused by the with wind from the southeast (Campuzano et al., 2008).

Currents

When flood comes in, waterlevel increases, the amount of land under water increases and velocities reduce (Campuzano et al., 2008). By modelling, it has been found that peak velocities on the intertidal areas during flow were generally under 0.3 ms^{-1}. In the Canal Principal, the maximum flow velocities during ebb are near the upper reaches, being between 0.7 and 1.4 ms^{-1} (Campuzano et al., 2008). Peak velocities during flood are 1 ms^{-1}.

The currents are related to the tide only. Since the tidal wave is mostly reflected within the ria, it exhibits the characteristics of a standing wave. Therefore the tidal currents are close to zero at high tide and low tide.

Residual velocities can get larger than $0.2ms^{-1}$ in both the inner area as the outer area of the ria. As the Canal Principal is connected with the other channels via the tidal flats, there are locations where the residual flow reverses towards these channels perpendicular to the Canal Principal. According to table Table 2.3, the tidal current may exceed velocities > 1 ms^{-1}.

Because the Coriolis force directs the flow to the left on the southern hemisphere, the currents in the Canal Principal are coming in at the southern bank and leave the channel at the northern bank.

Considering the residual velocities, there have been observed recirculation patterns at the mouth of the ria. When there is ebb flow, there are currents present directed towards the centre of the

channel. This is due to the slope of the flank, directed towards the centre of the channel flowing in a non-channelised way (Perillo and Sequeira, 1989).

Waves

On present mud-flats, wind induced waves are of high importance. Significant wave heights on the tidal flats never exceeded 0.2 m and produced bottom shear stress of maximum 4 Nm^{-2}. The hydrodynamics of the intertidal flats during high tide are characterised as wind waves of 10 cm in height, maximum wavelengths of $1 - 3\ m$, and periods of $1 - 3\ s$ (Pratolongo et al., 2010). The tidal wave is originally a progressive wave, but reflection on the channel flanks and head convert it to a standing wave (Piccolo et al., 2008). Oceanic waves are only important on the coast outside the ria and on the outer banks. Generated waves inside the channel due to the interaction of incoming tide with northern wind are up to 1.5 m steep with wavelengths in the order of $10 - 30\ m$ (Piccolo et al., 2008).

Wind

The dominant wind directions are from the North and Northwest. Strong winds are over 43 $km\ h^{-1}$ and occurs significant times a year (196 times a year). The end of spring and summer present the highest wind velocities. (Piccolo, 2008).

Predominant winds affecting the tidal variations are coming from the NW and N. These winds advance the time of low water, delay the time of high water and reduce the predicted water levels at both high and low tide. Northern winds produce a set down of the tide while southern winds a set up. Maximum negative surges occur with winds from the NW and maximum positive ones with SW winds (Piccolo et al., 2008).

Salinity

At the head of the bay, there is river discharge entering the ria. This discharge, however, is low and has only limited effect on the ria. Between the head of the bay (mouth of the river) and Ingeniero White Port the partially mixed inner region tends to be vertically homogeneous and salinity patterns in the outer homogeneous region are similar to the adjacent continental shelf (Piccolo et al., 2008).

Considering the salinity and temperature, the Bahia Blanca ria is divided in two areas. The inner one from the ria head where the river is located to Ingeniero White is a partially mixed ria during normal runoff conditions, but during low runoff becomes vertically and sectionally homogeneous. The outer reach is sectionally homogeneous. The boundary is depending on the river discharge (Piccolo et al., 2008). The salinity is generally considered to have a negligible impact.

The mixing regime is characterised by a Richardson number of less than 2, implying strong turbulence. This is especially during maximum ebb and flood conditions, particularly on the northern flank of the ria.

3

Design parameters

As for every design, the design parameters have to be determined. These parameters are split in three categories: (1) the boundary conditions in Section 3.1; (2) the requirements in Section 3.2; and (3) the wishes in Section 3.3. In this chapter, a brief overview is presented of all the parameters. In Appendix A, the background of these parameters is given.

3.1. Boundary conditions

Boundary conditions are limitations for the design in general. These limitations can be caused by the environment, legislation or the allocation of current infrastructure. These boundary conditions are always satisfied for all the designs.

Borders expansion areas – The borders of the expansion area can not be exceeded.

3.2. Requirements

Requirements are the conditions which have to be taken care of in the conceptual designs and cannot be left out. Therefore all alternatives meet these criteria in order to be sufficient.

Area sizes and quaywalls – The terminals have to be designed according to given numbers: Area dimensions, quay length and number of berths. The specific dimensions are given in Table A.2.

Road and rail access – All terminals must have rail and road access.

Clustering of terminals – The terminals have to be clustered by function.

Bulk terminals – Dry Bulk and Agribulk should be separated.

Container terminal – Container terminal and multi-purpose terminal have to be connected to the main channel (not by jetty).

Sewage outlet – The Sewage company must be able to discharge into the ria.

Central Termolèctrica – Central Termolèctrica Luis Piedrabuena must be able to discharge water into the ria.

Design vessel – The design vessel for the port extension is a Suezmax vessel. The current design vessel is a Panamax vessel[1].

Channel Width – The width of the channel has to meet the current requirements according to PIANC (MarCom WG-121, 2014). For the required minimum width one is referred to Appendix L.

3.3. Wishes

This section describes all the criteria which are preferred to be implemented in the conceptual designs, but which are not necessary. Therefore, conceptual designs implementing these conditions score extra points, but if left out is acceptable.

Nuisance by agribulk – Prevent surrounding living areas from influences of the Agribulk terminals (dust, smell etc).

Sediment – A design with the least impact on the morphology is preferred.

Container terminals caissons – Multi-purpose and container terminals have to be built with caissons.

Expansion possibilities – Future expansion possibilities have to be taken into consideration.

---

[1]This vessel size is given as input in this case study, for the motivation of this design vessel one is referred to (Port Consultants Rotterdam, 2017a).

Phase II
Synthesis

4

Conceptual designs

In this chapter the design process of the expansion areas is described. For the south expansion area three conceptual lay-outs are presented and for the east expansion side four conceptual lay-outs are presented. All the designs meet the requirements as stated in Section 3.2, for the required channel width one is referred to Appendix L. Larger maps of the several lay-outs are available in Appendix O.

For the conceptual lay-out the following aspects are considered in the designs and defines the difference between the lay-outs:

- Approach channel lay-out, including turning basin
- Hinterland connections
- Required land (size and type; reclaimed or not)
- Location of terminals and berthing locations
- Expected traffic per terminal

To highlight, e.g., the last point, the container terminal has the least amount of expected traffic and is therefore located furthest upstream.

4.1. East design

In this section the four different alternatives for the east bank are given. An overview of the East expansion area, including the current navigation channel and hinterland connections is given in Figure 4.1.

The different alternatives each have a starting point for the designs; this marks the difference between the main port lay-outs. These different starting points are the following:

Figure 4.1. The expansion area at the east side with the existing roads, railways and navigation channel.

Alternative 1 has the least reclamation as possible, leading to long viaducts.

Alternative 2 is very concentrated towards the current port and is therefore as close as possible to Ingeniero White.

Alternative 3 is based on one of the earlier investigated expansion possibilities done by Munters et al. (2017) and includes a basin.

Alternative 4 is concentrated as much as possible in a long stretch along the channel.

The four different alternatives are displayed in small in Section 4.1 and Figures 4.3 to 4.5; enlarged versions of the figures are available in Appendix O. The main difference between the alternatives are divided in:

- The use of a viaduct vs. reclamation
- Necessity of mooring basin
- Clustering of lay-outs

In the MCA it will be explored whether either of these design elements is an advantage or an disadvantage. Moreover, in Alternative 1 viaducts for transport between the terminal and jetties are designed with a length of more than 2000 m. Currently, the longest viaducts with this purpose in the port only have a length of 750 m.

4.2. South design

In this section the three different expansion alternatives for the south bank are given. The southern location is mostly located opposite of the current port and is characterised by the natural reserve

Figure 4.2. Alternative 1 for the East expansion.

Figure 4.3. Alternative 2 for the East expansion.

Figure 4.4. Alternative 3 for the East expansion.

Figure 4.5. Alternative 4 for the East expansion.

Figure 4.6. General lay-out south position.

in its vicinity. During the 2013 dredging works, as explained in Appendix B, the port authority started with reclamation works at the south bank. An overview of the south expansion is given in Figure 4.6, where the current channel, available area, the current reclamation and tidal channel are indicated.

One of the main challenges is the accessibility of the area as the area has no railways or roads at the moment and construction of these roads will be costly. An overview of all possible hinterland connections for the south bank are presented in Figure 4.7. In respectively red and black the current railways and roads can be seen. The green, blue and yellow lines indicate new possible railways and roads. In previous research done by Weyland (2009), it is found that the blue hinterland connection is the best.

To develop the different alternatives, the following differences are made between the lay-outs:

Alternative 1 is as far as possible to the east.

Alternative 2 is opposite to the current port, Ingeniero White.

Alternative 3 is located as far as possible to the west, utilising the current reclamation as much as possible.

It must be mentioned that the stretch on the south bank is very close to a protected natural reserve. Therefore, the expansion possibilities are limited significantly.

The main distinction between the alternatives are divided in:

- Closure of the tidal channel
- Utilisation of the current reclamation
- Elongation of the current channel to the west.

Figure 4.7. Options for the infrastructural connections to the current port.

In general the channel has to be widened along the port area to allow a two-way channel including mooring on both sides of the channel. The required width is calculated in Appendix L.

The three different alternatives are presented in Figures 4.8 to 4.10. The main differences between the alternatives are the following:

- The use of a viaduct vs. reclamation
- Necessity of mooring basin
- Clustering of lay-outs

In Chapter 9, the different alternatives are simulated to determine the best design.

In the following chapters the designs will be simulated and evaluated. In the simulation process the different quantities of the design are determined, in the evaluation process the best and most feasible design is found.
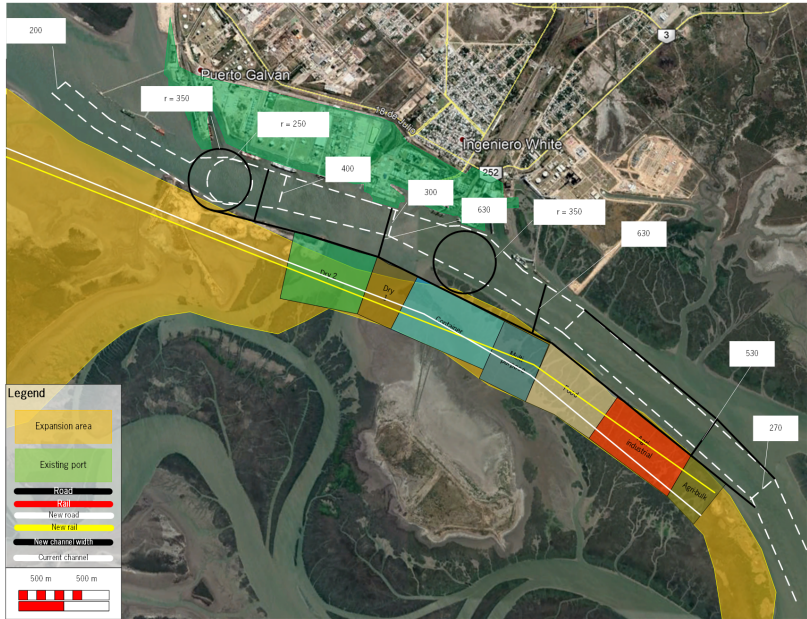
Figure 4.8. Alternative 1 for the South expansion.

Figure 4.9. Alternative 2 for the South expansion.
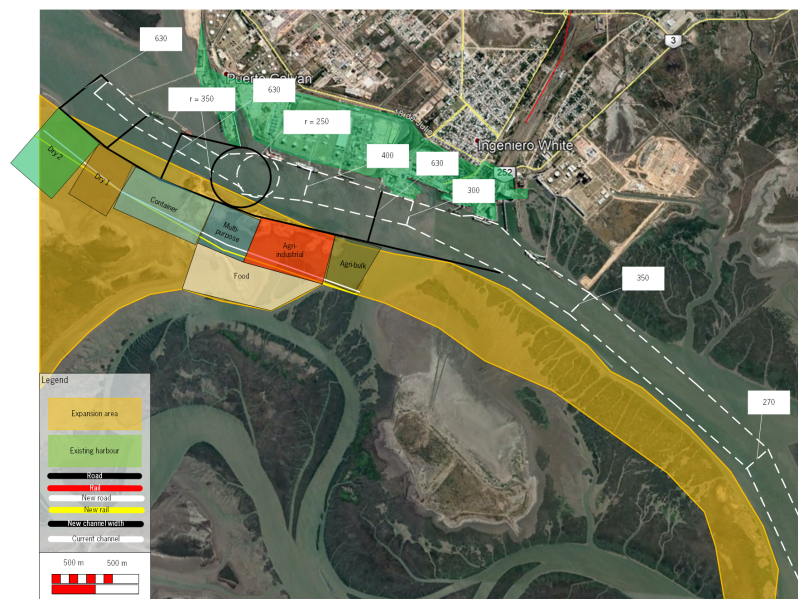
Figure 4.10. Alternative 3 for the South expansion.

5

Ria adaption

First, a rough understanding of the ria and the processes taking place is needed to be able to determine the effects of changes. As mentioned in Chapter 2, a lot of research on the Bahía Blanca ria has been done. This knowledge is used as input for a better understanding of the system.

The chapter starts with a qualitative description of the processes taking place and which of them are taken into account. Next, three points of interest are discussed. Two of these are based on the port expansion alternatives as presented in Chapter 4: (1) the East expansion (Section 5.2); and (2) the South expansion (Section 5.3). The third point of interest is the deepening of the channel along the whole stretch – from the port area to the open ocean – which is discussed in Section 5.4. The choice of the points of interest is also based on the limitations of the available data and model, discussed in Chapter 6.

5.1. Processes

The ria is a complex system of channels and tidal flats which interact with each other. The ria's main forcing is the tide, where during flood the water enters the system through the channels as well as over the tidal flats and during ebb the water drains via the channels back to the ocean (as discussed in Chapter 2).

For the port, three processes are of importance in the port area: (1) the flow velocities; (2) the wind-waves; and (3) the sedimentation rates. The flow velocities are of importance because of the manoeuvrability of the vessels; if the flow velocities are too high, it becomes hard for vessels to moor. Also waves are important for the manoeuvrability of vessels. The sedimentation rate is an important factor from an economic point of view, whereas more sedimentation results in more maintenance

dredging to ensure the draft needed for the vessels. The sedimentation rates are influenced by the flow velocities, which again can be affected by wave action.

Two processes play a role in the driving forces of the flow velocities related to the tide: (1) flow velocity driven by a (tidal) wave entering the system; and (2) flow velocity caused by a flow entering the system. The difference is the dependence of the flow velocity against the depth, amongst other system parameters. In case the flow velocity is based on the wave, the flow velocity increases with depth (Equation 5.1a[1]); in case it is based on the flow, the flow velocity decreases with depth (Equation 5.1b).

$$u = \sqrt{gd} \qquad \text{5.1a} \qquad\qquad u = \frac{Q}{Bd} \qquad \text{5.1b}$$

Because the tide is the dominant forcing on the system due to relatively low river runoffs (e.g. Campuzano et al., 2014), the flow is mainly related to this tidal wave (Equation 5.1a). Nevertheless, due to the huge amount of tidal flats, this wave is strongly distorted and the flats have not yet been completely drained before the next flood wave is already entering the system (Pierini et al., 2013). Therefore, towards the head of the ria, the ebb flow is assumed to be more of a drainage type of flow, hence the flow velocity is more related to the flow (Equation 5.1b) instead of the tidal wave.

Moreover, Pierini et al. (2013) states that the tidal flats are not completely drained yet before the next flood comes in from which can be concluded that the tidal wave is lacking behind at the head of the ria. Due to this fact, it is expected that the flow velocities become more influenced by the flow entering the system – instead of a wave propagating through the system – towards the head of the ria, where the port area is situated.

Beside the tidal wave, also wind-driven waves result in flow velocities. In Section 2.5 the wind-waves in the Bahía Blanca ria are described, where a distinction is made between the waves in the channel area and on the tidal flats. Wind-waves are indirectly important for the sediment transport, whereas their net sediment transport is commonly nihil – especially compared to the influence of the tide – but they stir up the sediment (Bosboom and Stive, 2015). For waves to stir up the sediment at the bottom, the waves must *feel* the bottom.

To determine whether waves reach – and so feel – the bottom, the theory on shallow and deep waters is used as described by Holthuijsen (2010). In this theory, the wavelength (λ) is compared to the depth (d) in which it is travelling: d/λ. If the ratio is smaller than 0.05, it is called that the wave moves through shallow water. Therefore, the wave reaches the bottom and so stirs up the sediment. In case the ratio is greater than 0.5, it is stated that the wave is in deep water at which the wave motion does not reach the bottom and so the sediment is not stirred up by the wave. For $0.05 < d/\lambda < 0.5$, the wave is in an intermediate depth water, which may have some small stirring; depending on its place in the spectrum.

The waves in the channel of the Bahía Blanca ria are stated to have a wavelength of $\lambda = 10 - 30\ m$ (Piccolo et al., 2008). In the port area, a depth of 13.5 metres is maintained, and along the channel depths of 12-13 metres are maintained. The depths are compared to LAT (Lowest Amplitude Tide) and so the average depth in the channel is taken to be $\bar{d} = 13.5\ m$. This means that the ratio becomes $d/\lambda = 1.35 - 0.45$, which means the waves are mainly in deep water. Therefore, the stirring

---

[1]Equation 5.1a is the relation in case of the shallow water approximation. Because a tidal wave is considered, it is fair to state that this relation holds.

effect due to waves in the channel is not taken into account, which is commonly done in sediment modelling due to the large computational efforts to do so (Bosboom and Stive, 2015).

On the tidal flats, the wind-waves have a more significant influence, where the bottom shear stress can reach up to values of $\tau_b = 4\ Nm^{-2}$ (Piccolo et al., 2008), which is also mentioned in Section 2.5. Because the influence of the tidal flats is assumed to be less compared to the channel, this effect of the wind-waves on the sediment transport is neglected.

Leaving the influence of waves on the sediment transport out of scope, only the tidal flow results in sediment transport. There are two ways to relate the flow velocity to the sediment transport: (1) without a threshold velocity (Equation 5.2a); and (2) with a threshold velocity (Equation 5.2b). In both relations, the power n plays a significant role and therefore has to be determined. Based on earlier research about the Bahía Blanca ria performed by Gómez et al. (2010), it becomes clear that $n = 3$[2]. This study advises to use the sediment transport relation as suggested by Bagnold (1963) using a threshold flow velocity (Equation 5.2b). Nevertheless, a critical threshold flow velocity is not taken into account, whereas the influence on the sedimentation rate is negligible ($u_{100,c} = \mathcal{O}(10^{-6}ms^{-1})$, defence in Appendix I).

$$S = mu^n \qquad \text{5.2a} \qquad\qquad S = \beta\left(u_{100}^n - u_{100,c}^n\right) \qquad \text{5.2b}$$

From the sediment transport, the sedimentation rate can be determined. To do so, the gradient in sediment transport has to be computed. Because the Bahía Blanca ria consists of multiple channels, the sediment transport gradients in two directions are needed to calculate the sedimentation rate via the Exner equation (Equation 5.3), which is in essence a mass balance equation.

$$c_b \frac{\partial z_b}{\partial t} + \frac{\partial S_x}{\partial x} + \frac{\partial S_y}{\partial y} = 0 \qquad\qquad \text{5.3}$$

Important to notice in Equation 5.3 is the fact that the gradient in sediment transport – and thus a gradient in the flow velocity – affects the sedimentation rate. Because the sediment transport is related to the flow velocity without a threshold velocity, only the gradients in flow velocity – and thereby in sediment transport – are playing a role in the sedimentation rate. Thereby, a lower flow velocity does not necessarily mean more sedimentation.

To get an understanding of the first response of the system due to the changes in bathymetry, a river engineering method can be applied. This method is used for the short-term response of a river to changes in bathymetry. It starts with determining the specific flow[3] in the area of interest. Based on the specific flow, the equilibrium depth (Equation 5.4) can be determined in which only the relation between the depth and the specific flow is of importance; i.e. all other parameters are assumed to stay constant, are not affected. Because a certain change in the flow and/or the width leads to a certain change in the specific flow, this results in a certain change in the equilibrium depth as well. A certain change in depth would initially result in a certain change in water level, which is physically not possible. Therefore, the water gradually forms to the change in equilibrium depth by forming backwater curves. These backwater curves result in gradients in flow velocity and so in sediment transport. Due to these gradients, the sedimentation rate is affected (Equation 5.3).

---

[2]According to experiments, $n = 3 - 5$ where the value depends on the kind of sediment transport: bed load transport results in lower values, and suspended transport in higher values (e.g. Bosboom and Stive, 2015).

[3]$q = Q/B$; specific discharge/flow is the discharge/flow per metre width.

$$d_e = \left(\frac{c_f}{i_b} \frac{q^2}{g} \right)^{1/3}$$ 5.4

This approach only holds in case the flow velocity is related to the flow in the area of interest; so according to Equation 5.1b. Next to that, some other assumptions have to be true in order to regard the flow as a normal flow. This means (1) that there is a balance of the resistance force and the downstream component of the gravitational force; (2) the water surface must be parallel to the bed surface; and (3) no acceleration or deceleration of the flow. Combining these assumptions, the resulting flow is steady and uniform. However, the flow velocity is not expected to behave according to this approach since the ria is a dynamic system that is highly influenced by the tide. Most of the assumptions can therefore not be applied on this case. However, despite the fact that most assumptions do not hold, this method can still give a good first impression on how the system may initially react to the changes opposed on it. Therefore, this method is used to come up with hypotheses on the points of interest. More details on the method are discussed in Appendix N.3.

5.2. East expansion

East of the existing port a side channel is located which will be (partly) closed off by an expansion of the port to the east. This closure of the side channel will affect the flow conditions in the main channel flowing through the port area. Because the water cannot flow through this side channel anymore, it is expected that the flow velocities in the main channel will increase due to the closure.

Beside the closure of the side channel, the East expansion also gives a widening of the channel. The widening of the channel results in a bigger cross-section through which the water will flow, hence a reduction of the flow velocities is expected.

These two outcomes due to the East expansion counteract each other. Nevertheless, the widening is expected to be of less influence than the closure of the side channel, because the navigation channel needs little widening. Therefore, the hypothesis is that the flow velocities will increase due to the East expansion, which is disadvantageous for the manoeuvrability of the vessels in the port area. Moreover, the increased flow velocities in the affected area result in more sediment transport. Thereby, there will be a larger gradient in the sediment transport at the eastern and western ends of the area. These gradients will result in a decreased sedimentation rate at the eastern end of the area, and these rates will increase at the western end.

5.3. South expansion

Another option is to expand at the southern side of the channel, where there already has been deposited some sand from earlier dredging campaigns. An expansion of the port at the south bank of the main channel will result in a bounded flow through the port area. Furthermore, the flow through the main channel will be (partly) closed off from the tidal flats and another channel south of the main channel (this other channel is clearly visible in Figure 2.3). Therefore, the south expansion limits the interaction between these two channels, and streamlines the flow through the port area.

When the port expansion is placed at the southern side of the main channel, the navigation channel is widened to comply with the needed width of a two way channel in combination with moored vessels at both sides – as mentioned in Appendix L. A widening of the channel results in a reduction of the flow velocity, which can be significant due to the fact that the channel's width must almost be doubled in case of the South expansion.

These two processes counteract each other on the part of the flow velocities. Nevertheless, it is expected that the port area will be more flood dominated because the channel is closed off from tidal flats; hence an increase in the average depth during flood. The change in flow velocity due to the expansion will not influence this change in behaviour. West and east of the port area it is stated to be ebb dominated (Campuzano et al., 2014; Perillo et al., 2001), it is expected that at the western end of the area the sedimentation rate will increase, and at the eastern end, the sedimentation rate will decrease. The change in flow velocity is expected to be of less influence than the increased flood dominance of the area.

The change in flow velocity in the area due to the expansion will have influence on the manoeuvrability of the vessels in the port area; a decrease in flow velocity would be beneficial. Because both processes are of significant importance, it is hard to say beforehand what will be dominant.

5.4. Deepening of the channel

The deepening of the channel – as mentioned – holds for the whole stretch of the navigation channel; from the port area to the open ocean. Nowadays, the port authority works with a tidal window and only the port area is deepened. The reason to investigate the deepening is based on the question whether a deeper channel results in less maintenance dredging besides the possibilities to accommodate larger vessels in the port of Bahía Blanca.

To start, the channel wants sediment that originates from the inner reach and the tidal flats (Perillo and Sequeira, 1989). Thereby, deepening of the channel results in erosion of the inner reach and the tidal flats; so the environmental impact will be significant. Because a larger depth in the channel will increase the sedimentation rate of the channel, deepening will result in more sedimentation and so more dredging maintenance has to be done compared to the initial situation.

On the other hand, deepening of the channel also increases the ebb dominance of Canal Principal; the deepening has relatively more impact on the average depth during ebb than during flood, enhancing the ebb dominance of the channel. This will result in more sediment transport out of Canal Principal, decreasing the sedimentation rate.

That the sedimentation rate will increase is evident, whereas deepening a channel almost always results in more sedimentation. One of the reasons to deepen the channel anyway is due to the fact that a deeper channel results in a larger buffer before it has to be dredged again to ensure the needed draft. Furthermore, part of the dredged material can be used for the land reclamation needed for the port expansion – east or south of the existing port. In this way, costs can be reduced and the dredged material can be used in the most effective way by re-using it for the port expansion instead of disposing the material offshore. Since the dredged material on the upper layer is more muddy, soil improvements will be necessary to be able to use it.

6

Hydrodynamic model

To get an understanding of the Bahía Blanca ria, a hydrodynamic model is used, namely the MOHID-model. Therefore, this chapter starts with an elaboration on this model in Section 6.1. Also the links between the model and the processes as described in Section 5.1 is made. After the introduction on the model, the approach on how the points of interest as introduced in Sections 5.2 to 5.4 are elaborated; starting with a general approach followed up by case specific additions to the road map. The exact model- and computational steps are explained in Appendix E.

6.1. MOHID-model

The MOHID-model is designed by the University of Lisbón. This model has been used in Argentina to obtain hydrodynamic data of the Bahía Blanca ria. The model obtains hydrodynamic data of the ria, and for the purposes in this research, no sedimentation transports are calculated within the model. The hydrodynamic data of the ria is only considered qualitatively due to the complexity of the ria.

A hydrostatic equilibrium and Boussinesq and Reynolds approximations are assumed for this model. These assumptions are frequently made and there is no indication why these would not apply to the Bahía Blanca ria. The MOHID-model is a 2D depth-averaged model (2DH), so only one layer is considered in the z-direction. The momentum balance equations for mean horizontal velocities flow velocities are in a Cartesian frame of reference and shown in Equations 6.1a and 6.1b.

$$\frac{\partial u}{\partial t} + \frac{\partial uu}{\partial x} + \frac{\partial vu}{\partial y} + \frac{\partial wu}{\partial z} - fv + \frac{1}{\rho_0}\frac{\partial p}{\partial x}$$
$$- \frac{\partial}{\partial x}\left((\nu_H + \nu)\frac{\partial u}{\partial x}\right) - \frac{\partial}{\partial y}\left((\nu_H + \nu)\frac{\partial u}{\partial y}\right) - \frac{\partial}{\partial z}\left((\nu_t + \nu)\frac{\partial u}{\partial z}\right) = 0$$

6.1a

$$\frac{\partial v}{\partial t} + \frac{\partial uv}{\partial x} + \frac{\partial vv}{\partial y} + \frac{\partial wv}{\partial z} + fu + \frac{1}{\rho_0}\frac{\partial p}{\partial y}$$
$$- \frac{\partial}{\partial x}\left((\nu_H + \nu)\frac{\partial v}{\partial x}\right) - \frac{\partial}{\partial y}\left((\nu_H + \nu)\frac{\partial v}{\partial y}\right) - \frac{\partial}{\partial z}\left((\nu_t + \nu)\frac{\partial v}{\partial z}\right) = 0$$

6.1b

where u, v and w are the components of the velocity vector in the x-, y-, and z-direction, respectively; f the Coriolis parameter; ν_H and ν_t the turbulent viscosity in the horizontal and vertical directions, respectively; ν is the molecular kinematic viscosity ($\nu = 1.3 \cdot 10^{-6}\ m^2 s^{-1}$); and p is the pressure.

The most important limitations are (1) the grid, which is quite rough with $200 \times 200\ m$; and (2) the fact that the model is not calibrated, whereas this would need field experiments for which no time or money is available at the moment of writing this report. Due to this, only qualitative effects can be investigated. Furthermore, the bathymetry of the ria is not updated by the model; and in this specific case, Coriolis is neglected. Lastly, wind is included in the modelling originating from the south-east direction with a velocity of $10\ ms^{-1}$.

6.2. Approach

The ria is a complex system of channels and tidal flats, which interact with each other. Three points of interest are chosen based on the limitations of the MOHID-model, mentioned in Chapter 5.

The MOHID-model has as output data flow velocities in all three directions, the velocity direction and water levels, where it must be stated that the flow velocities are not calibrated. The locations of these data sets must be placed manually via Virtual Measurement Station (VMS). At every VMS MOHID produces the data files. Choosing the locations correctly, one can create control volumes. The channel is divided into several control volumes to discretise the calculations. Appendix H elaborates further on this topic.

The global roadmap, which holds for all three points of interest, is as follows:

1. Create control volumes in the MOHID-model by setting boundaries in the flow direction and at the tidal flats (Figure H.1).

2. Modify the bathymetry depending on the point of interest.

3. Run MOHID (Output of the MOHID-model: a.o. η, u and v at all VMSs).

4. Create a frame of reference per control volume based on the coordinates (λ, ϕ) of the VMSs in the main channel, whose angles (α) determine the angle between the x, y-axes and the ξ, ψ-axes, as shown in Figure H.2a. (Further elaborated in Appendix F.1.)

5. Determine the sediment transport in x, y-directions via Equation 5.2a: S_x and S_y, respectively.

6. Convert the sediment transport in x, y-directions into the ξ, ψ-directions using geometry, respectively S_ξ, S_ψ:
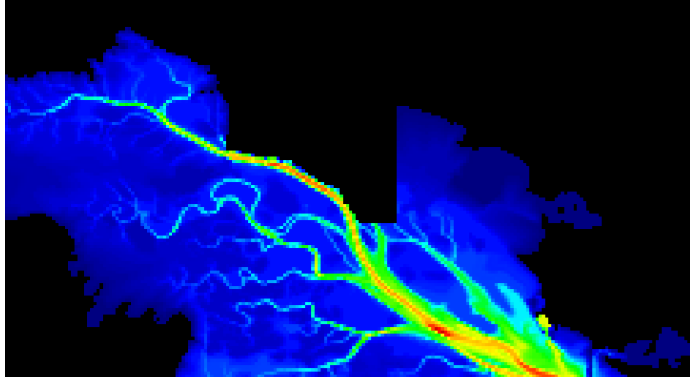
Figure 6.1. East expansion in MOHID.

   (a) $S_\xi = S_x \cos \alpha - S_y \sin \alpha$

   (b) $S_\psi = S_x \sin \alpha + S_y \cos \alpha$

7. Determine the gradient in sediment transport in ξ, ψ-directions, where the length and width of the control volume are determined based on the coordinates (λ, ϕ) of the VMSs (1) in the main channel for the ξ-direction ($\Delta\xi$), and (2) at the tidal flats for the ψ-direction ($\Delta\psi$). (Further elaborated in Appendix F.2.)

8. Determine the sedimentation rate using Exner (Equation 5.3).

East expansion

The East expansion, when large enough, leads to the closure of a side channel of the Canal Principal. In this case, the Canal Principal will need to be deepened or widened for vessels to reach the new port area. Despite this, it is assumed to be of no significant importance when modelling, because the changes on such a small scale in the coarse grid of the MOHID-model is hardly noticeable. The East expansion in the model is set as land points in the model, illustrated in Figure 6.1. The expected effects of the East expansion are further elaborated on in Section 5.2.

The additional step to the global roadmap due to the research on the closure of the side channel is the following:

9. Determine the influence of the East expansion on the flow velocities and sedimentation rates in Canal Principal.

The MOHID-model design of the east expansion is shown in Figure 6.1.

South expansion

For the South expansion, the channel at the port area is set to a depth of 13.5 m and widened for modelling purposes. When the deepening to 13.5 m is not done, there will be a too sudden deepening at the widening. South of the widening the expansion is located as land points, such that water cannot flow in this direction. However, via the tidal flats the water is still able to flow around the expansion. A visualisation of the MOHID-model can be seen in Figure 6.2.
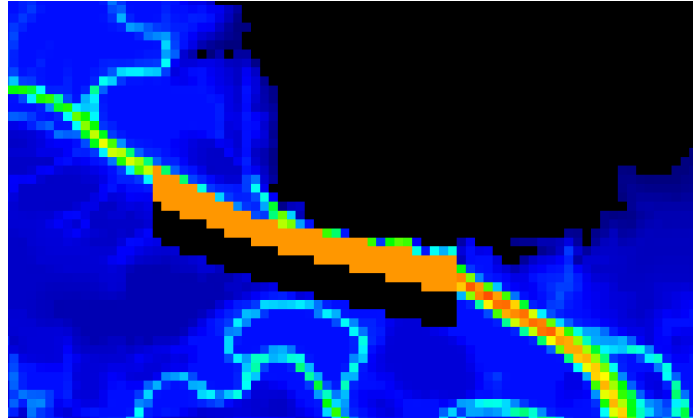
Figure 6.2. South expansion in MOHID.

Furthermore, when the port expansion is placed at the southern bank of the main channel, the navigation channel is widened to comply with the needed width of a two way channel in combination with moored vessels at both sides, as mentioned in Appendix L.

The additional step to the global roadmap due to the research on the south expansion is the following:

9. Determine the influence of the South expansion on the flow velocities and sedimentation rates in Canal Principal.

Deepening of the channel

In the simulation of the deepening, the navigation channel is pointed out manually; looking at the bathymetry and drawing a line on the map where the channel is located (Figure 6.3). This 'channel' is set to eight different minimum depths; $d = 12.0 - 15.5\ m$. This means that the depth of the original bathymetry is compared to this new depth and replaced if the original depth is smaller. An important note is that MOHID uses another datum (LIMB) than the port authorities (LAT), because of a change in datum recently. This correction, which is $0.15\ m$, is taken into account in writing the new bathymetry-files. More detailed information on the deepening and the writing of the files in Appendix C.

The influence of the deepening is reviewed on the flow velocities and the sedimentation rates. Therefore, these two parameters are plotted against the various depths – including d_0, which is the base case – to get a clear understanding of the deepening. The processing of the data is further elaborated in Appendix G.4.

The additional steps to the global roadmap due to the research on the deepening of the channel are the following:

9. Determine the influence of the deepening on the flow velocities and sedimentation rates in Canal Principal.

10. Determine d, u-curves per VMS and the influence the deepening has on the flow velocities in Canal Principal.
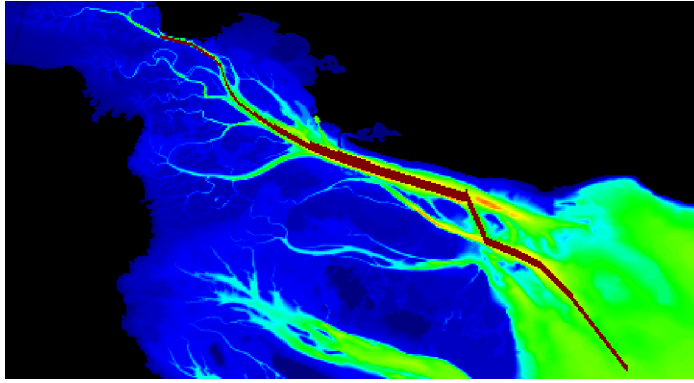
Figure 6.3. Deepening area in MOHID.

11. Determine $d, \dot{z}_b$-curve per control volume and the influence the deepening has on the sedimentation rates in Canal Principal.

7

Caissons

In this chapter the implementation of caisson is described. This follows from the Chapter 4 and Section 3.2. With this input an analysis can be made in order to check the possibility of the use of caissons for the port expansion.

First in Section 7.1 it is explained why the implementation of a caisson is considered for an expansion of the port. Thereafter an elaboration is given on the different kind of phases according to the caisson design method described by Voorendt et al. (2011) and Molenaar and Voorendt (2016). This method consists of the following phases corresponding to various sections in this chapter: (1) preparation (Section 7.2); (2) transport (Section 7.3); (3) immersion (Section 7.4); and (4) finishing (Section 7.5).

The checks, which are done in order to determine the dimensions of the caisson described in Appendix K.1, are based on these stages. Finaly, an estimation of the costs is given in Section 7.6. For this project, however, the maintenance and control phase as well as the final stage are left out of scope.

7.1. Use of caisson

At the container terminal the use of jetties is not advisable (Ligteringen and Velsink, 2012), because it is very convenient to have the storage of the containers as close to the quay wall as possible. Therefore the use of gravity walls, and especially quay walls are preferred when construction a container terminal. An option for the construction of a quay wall is by means of caissons.

The use of caisson is not a common implementation when it comes to constructing quay walls in Argentina, because it was considered to be too expensive in the past. Nowadays, however, due to the development of cheaper construction methods such as the modular construction of caissons, it

41
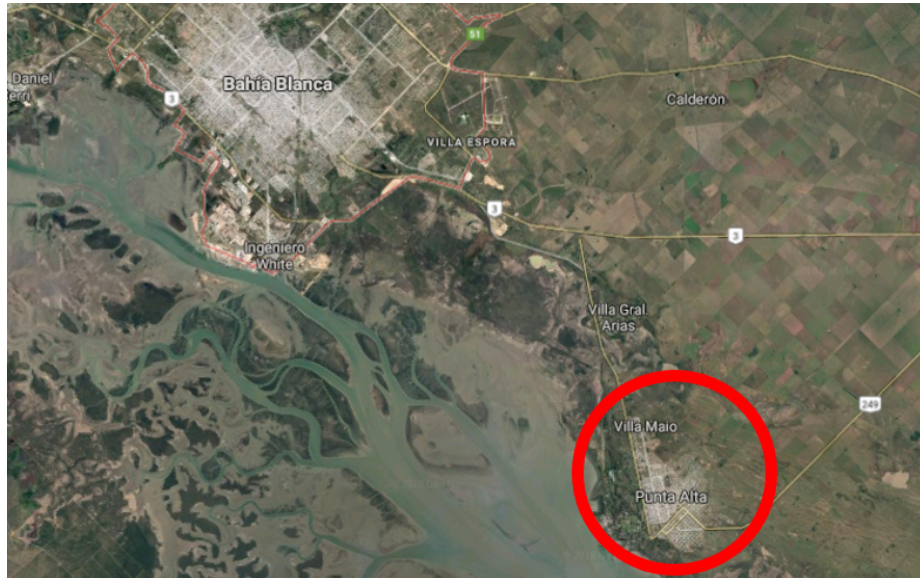
Figure 7.1. Punta Alta as a possible location for the gravingdock.

has become an interesting option to consider. However the modular building of caissons in itself is not described here.

7.2. Preparation

When using caissons in order to construct the quay wall it is common to pre-construct the caisson first. This is often done in a graving dock nearby the final location so the travel distance is as short as possible. In the case of Bahía Blanca, locations downstream (towards the east), could be investigated in order to check whether they are suitable places for a graving dock. Locations nearby Punta Alta (Figure 7.1) could be spots, because they are situated nearby, the port, but also have access roads for the materials to be transported to the building dock.

The cheapest option to pre-construct the caissons is the use of existing graving docks or to create the construction site in the form of a construction pit. However, when there is not enough space to do this, a construction dock with sheet pile walls can also be chosen to be the best option.

It is important to have the right facilities nearby the dry dock. For the construction of caissons, a lot of concrete is needed. Therefore it is convenient to have a concrete batch plant nearby. Other important facilities are:

- Reinforcement bar yard
- Area to assemble and store form work elements
- Storage for materials
- Accommodation for workmen/commissioners
- Storage places for caissons
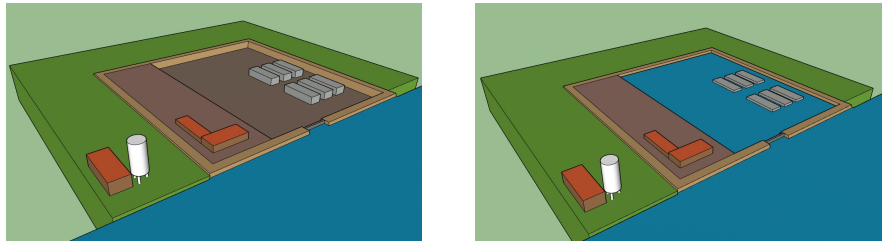
(a)Dry graving dock, during the construction of the caissons.

(b)Inundated graving dock, just before transport of the caissons.

Figure 7.2. Sketch-up impressions of a graving dock.
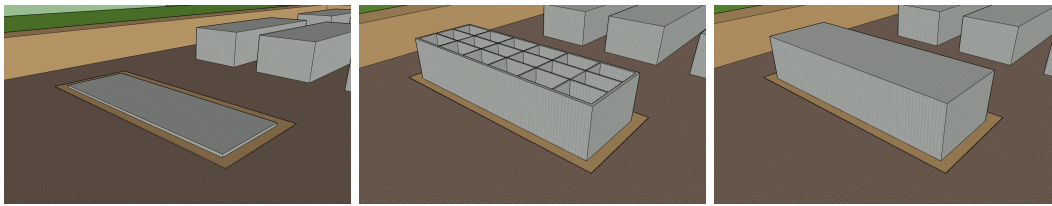
(a)Phase 1.

(b)Phase 2.

(c)Phase 3.

Figure 7.3. Sketch-up impressions of three different building stages.

The caisson

The building of the caisson takes place in a few building stages in order to finish the caisson as soon as possible. Some of the stages are shown in Figure 7.3.

It is important to start with a layer of gravel first before building the bottom of the caisson. The gravel allows the water to get under the caisson more easily. This makes it easier to lift the caisson before transport. On top of this layer of gravel, the bottom, walls and roof can be constructed. This is done by placing the form work and reinforcements first. If these are placed the concrete can be poured.

As stated in Appendix K the dimensions of the caisson have to meet to boundary conditions. Moreover the caisson design will be tested on the following three criteria: (1) draught; (2) shear force resistance; and (3) bending moment resistance. In this case the height of the caisson is set to 22.5 m to meet the depth at the location of container terminal. This means the draught of the caisson would be large as well, while the maximum allowed draught is equal to the water depth. This has been taken into account in the calculations. The elaboration and the results of these tests are given in Appendix K

When the caisson is finished and ready for transport the graving dock will be flooded (Figure 7.2b). Tugboats will then transport the caissons from the dock to the Port of Bahía Blanca, the final location.

During the flooding of the graving dock, it is undesired that the caissons already start floating in an uncontrolled way. Therefore the caissons should be ballasted with water in advance to keep them on the ground (Voorendt et al., 2011).

(a)Transportation by tugboats.　　　　　　　　(b)Immersion of the caissons.
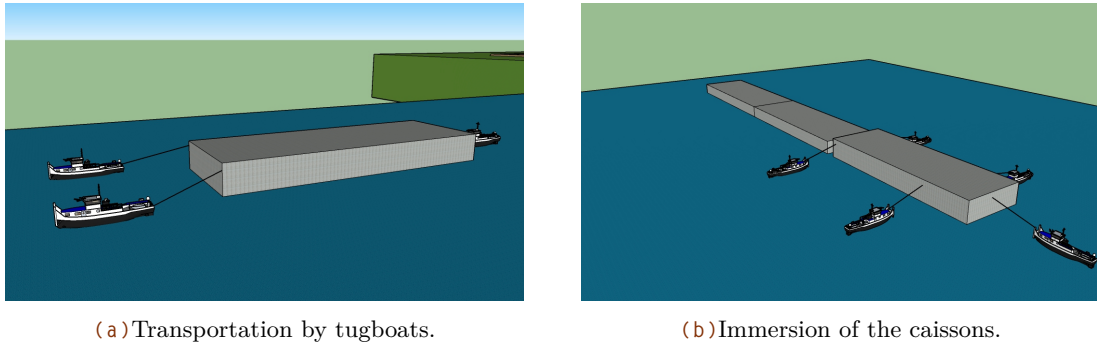
Figure 7.4. Sketch-up impressions of transportation and immersion of the caissons.

In order to do so the caisson are filled with a small amount of water to increase the weight. However, this is not always preferred, because free water ballast causes undesirable water movement, which can cause instability of the caisson. Therefore, the use of ballast tanks are preferred.

7.3. Transport

After the inundation of the graving dock the ballast tanks will be emptied, which means the caissons will start floating. Most of the time tugboats will be used in order to prevent the caissons from floating away. Usually caissons are transported during high water level, because the flow velocities are small.

When transporting the caisson over water some checks have to be preformed in order to ensure its stability. This means the caisson must be tested on two criteria: (1) static stability; and (2) dynamic stability. When both criteria are stable, the caisson can safely be transported over water (Appendix K.5).

7.4. Immersing

Before the arrival of the caissons at the final location, the bed has to be prepared. When this is done, the caissons can be immersed. This must be done during low tide in order to reduce the immersing distance and to minimise the flow velocities of the water, especially since the tidal range at the port is very large. Also the weather plays an important role in the immersing process, since wind and high waves have a big influence. The caissons contain valves to let the water flow into the caisson enabling it to immerse. This has to be done in a controlled way, because the caisson has to be balanced all the time. Especially the use of inner walls has to be taken into account, because it is undesirable that some compartments of the caisson are filled with water and other are not. This could lead to instability of the caisson.

During the immersing phase, the static stability of the caisson has to be checked. Assumed is 10 cm of water in the caisson which increases the weight and therefore decreases the stability. The calculations are elaborated in Appendix K.6.
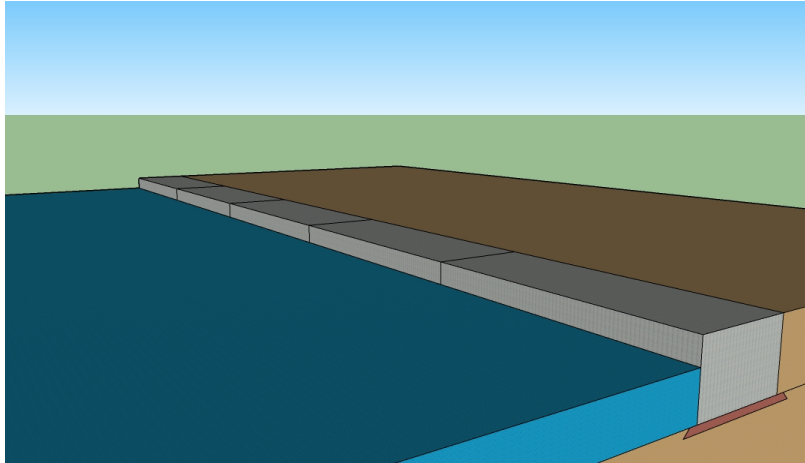
Sketch-up impression of the situation where all the caissons are placed.

After the immersing of the first caisson, the other caissons are placed as well, forming a quay wall. The connection between the caissons is not taken into account in this study.

7.5. Finishing

After the immersing of the caisson the land behind it can be reclaimed. This can be done with sediment from capital dredging or sand from quarries can be used for this. However, the caisson needs to be stable all the time, both before and after the reclamation. Therefore, the caisson is checked for these both situations based on three criteria:

- Shear criterion
- Turnover criterion
- Bearing capacity subsoil

The calculations of these criterion can be found in Appendix K.7.

With the dimensions given in Figure 7.6 the caisson is calculated stable (Figure K.6 in Appendix K), except for the bearing capacity of the subsoil. This means soil improvement is needed.

7.6. Cost estimation

Knowing all the dimensions of the caissons the costs of the quay wall can be calculated. This is an estimation (Buring, 2013), based on the direct costs, such as materials, framework, and the construction of the dry dock. Knowing the direct costs an estimation of the total costs can be made using a factor 1.4: *total costs* = $1.4 \cdot direct\ costs$.

In order to make an estimation for the costs of materials a distinction has to be made between concrete and reinforcement. The amount of concrete used in each caisson is calculated knowing the
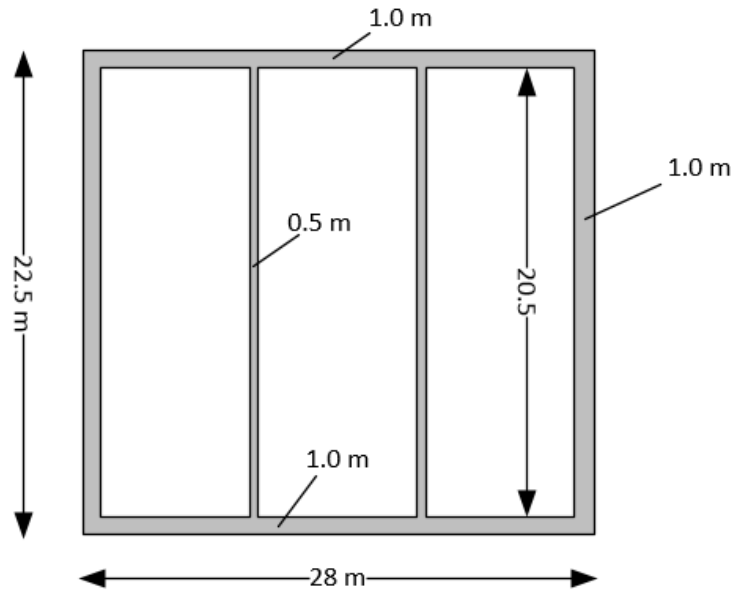
Figure 7.6. The dimensions of the caisson.

dimensions. According to Voorendt et al. (2011), the amount of reinforcement is 1% of the amount of concrete; translated into weight[1] results in almost twelve million kilograms (Table 7.1).

This is based on the assumption that twelve caissons are needed to accomplish the a quay wall of 1000 m. The length of one caisson is set to 84 m, which consequently results in an amount of twelve caissons.

The amount of formwork is determined by means of the surface of the roof and the walls. An assumption is made that the amount of formwork is equal to the surface of the roof and twice at much as the surface of the walls. However in practise, it is useful to put some effort in the building plan of the caisson, because framework can be reused. This will lead to a reduction of the costs. On

---

[1]Density of the reinforcement steel is assumed to be $\rho_{steel} = 7,850$ kg m^3.

	Quantity	Unit price (US$)	Costs (M US$)
Materials			38.8
Concrete	149,190 m^3	170 $/m^3$	22.4
Reinforcement	11,711,415 kg	1.40 $/kg$	16.4
Framework			4.5
Casting top	2,352 m^2	230 $/m^2$	0.5
Other sections	34,496 m^2	115 $/m^2$	4.0
Construction dock		30% of caisson	3.9
Total			50.1

Table 7.1. Estimation of the initial costs.

the other hand, more caissons can be built at the same time, which will lead to an increase of the amount of framework needed. An assumption is made that these two optimisations will cancel each other out.

When the direct costs are determined, an estimation can be made for the total costs of the quay wall: $1.4 \cdot 50.1$ M US\$ $= 70.2$ M US\$. So, the total costs for the caisson method are equal to US\$70.2 million, which is US\$ 70,000 per metre. This is much more than the quay walls, which are used now and costs around US\$ 30,000 per metre (Munters et al., 2017).

Simulation

8

Results of the hydrodynamic model

The outcomes of the MOHID-model have been transformed into figures using MATLAB in order to evaluate them. These outcomes are presented in this chapter and briefly described, starting with the base case in Section 8.1 in which the current port situation is modelled. In this case no adjustments to the port or ria are made. The base case is first elaborated to be able to address the differences in behaviour of the system due to the changes opposed on it. After the base case, the outcomes of the three points of interest are addressed: (1) the East expansion in Section 8.2; (2) the South expansion in Section 8.3; and (3) the deepening of the navigation channel in Section 8.4.

8.1. Base case

In this situation no changes or adaptions are made to the ria. Using the MOHID-model water levels and flow velocities are obtained. With these result the flood and ebb flows are computed and plotted in Figure 8.1. In this figure, the mean velocities are given in case of the ebb, flood and residual flow. The numbers are representing the Virtual Measurement Stations (VMSs) in the channel and the dotted lines represent the port area, also described in Table H.1.

In the base case larger flow velocities are observed near the port area compared to the mouth of the ria. From Figure 8.1 it becomes clear that in the whole navigation channel the ebb velocities are bigger than the flood velocities. From the mouth of the ria towards the head, the flow velocities increase, but experience a jump to higher velocities in the front (east side) of the port area and a reduction of this jump at the entrance of the port area. In the port area, illustrated with the dotted lines, a fall in ebb as well in flood velocities is observed. In the area west of the port the velocities
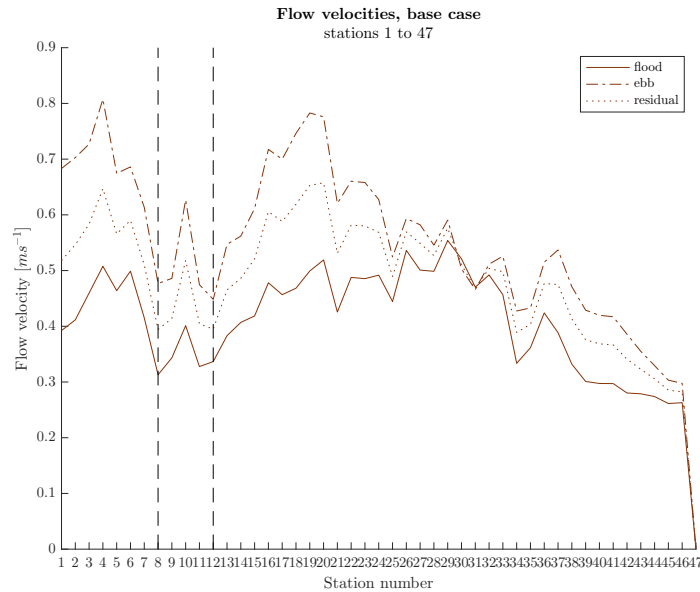
Figure 8.1. Velocity profile channel.

are slightly higher than in the port area itself.

8.2. East expansion

Due to the realisation of the East expansion, a part of the tidal flats east of the port is reclaimed. The expansion replaces a part of the tidal flats, changing the characteristics of the ria. As can be observed from the modelled result, the flow of water through the main channel where the measurement points are located, is affected by the expansion.

The flow velocities in the main channel after the reclamation are compared to the base case and are illustrated in Figure 8.2. The area between the dashed lines represents the area of the channel at the East expansion.

From Figure 8.2 it can be observed that the flow velocities at the east side of the port tend to go down. Both the flood and ebb flow velocities are lower compared to the base case; without expansion. Around VMS 16 however, the flow velocities experience a peak and increase compared to the base case. From this peak further into the port area, the flow velocities are similar to the ones observed in the base case.

Sediment transport is related to flow velocity, thus in case of an increase in flow velocity, there will be an increase in sediment transport as stated in Section 5.1.

However, the estimated sedimentation rates based on the flow characteristics from the MOHID-model do not show much difference compared to the base case. The obtained modelling results are illustrated in Appendix N.4. The control volumes defined in the channel next to the expansion show little to no change of sedimentation compared to the base case. Only at control volume 16 the increased flow velocities lead to an peak of erosion.
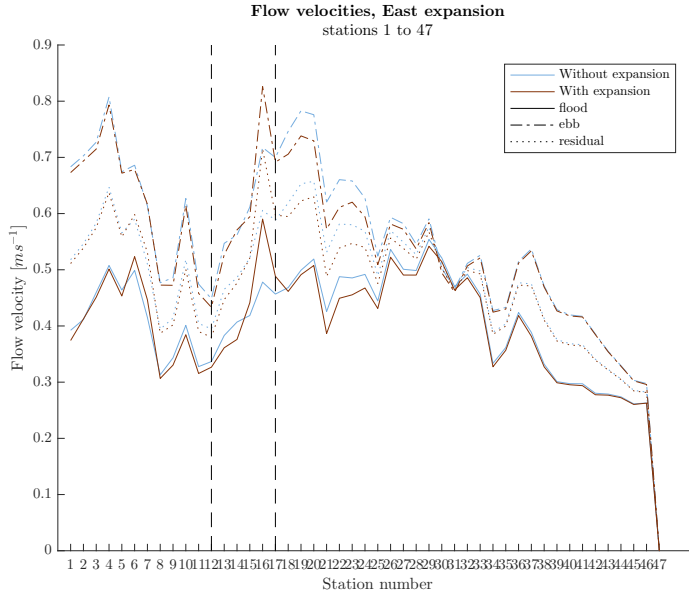
Figure 8.2. Velocity profile East expansion.

8.3. South expansion

The South expansion involves a change in three ways: (1) opposite to the existing port, land is reclaimed which locally cuts off the connection with the tidal flats to the South; (2) the channel will be widened to assure the the possibility for vessels to pass; and (3) the channel is expanded in western direction to serve the expansion. The channel depth in case of the widening is set to $13.5\ m$, similar to the official (current) depth in the port. The expansion of the channel to the west implies a widening and a deepening of this channel section.

There are three main impacts due to the expansion: (1) a blockage of the connection of the channel with the tidal flats; (2) a larger flow area due to the widening; and (3) an equalisation of the channel on $13.5\ m$ depth. The blockage of the flow towards and from the tidal flats acts like a reduction of the tidal flat area at this section.

At the port area, but also at the east and west side of the port the flow velocities change. This is clearly visible in Figure 8.3. The drop in velocity for ebb as well as flood flow at the port area. East of the port there is a small decrease in ebb velocity and a small increase in flood velocity. At the first measurement point the velocities for ebb and flood are exactly the same as before the expansion. Due to the drop in velocities, the residual flow also goes down significantly. Besides the drop in the velocities, the velocities are more equally distributed. The peaks between VMSs as seen before the expansion are mitigated.
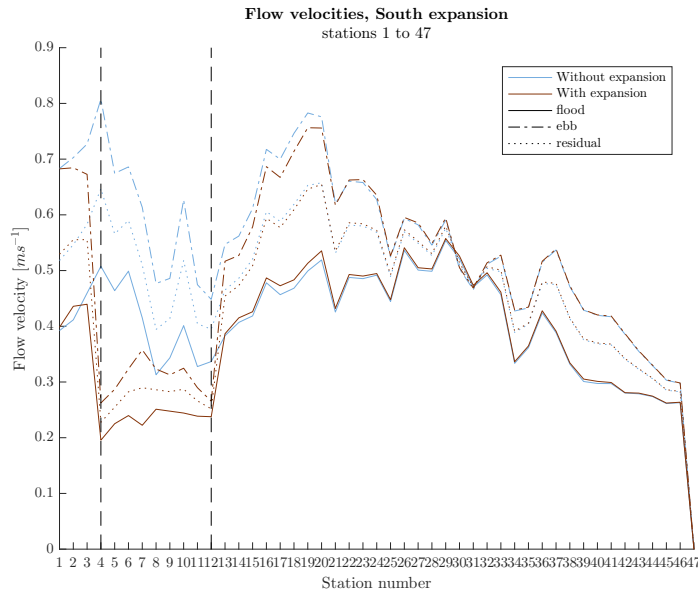
Figure 8.3. Velocity profile South expansion.

8.4. Deepening

The velocities for the various depths over the whole stretch are presented in Figure 8.4, where the influence of the depth on the flow velocity is clearly visible. At the innermost reach – up to VMS 6 – the flow velocities increase with increasing depth; and between VMSs 7–24, the flow velocities decrease with increasing depth. Beyond VMS 24, no clear relation can be set, which can be due to the fact that the flow is more influenced by the tidal wave forcing at the ocean.

From Figure 8.4, it is visible that the gradients in flow velocity do not change much due to the changes in depth. These changes result in changes in gradients of the sediment transport, hence sedimentation rates. That the sedimentation rates are not much affected by the deepening is also visible in Figure 8.5; in most control volumes the sedimentation rates stay relatively constant for the different depths. Noticeable is the initial in-/decline in the sedimentation rates of a couple of control volumes[1] from d_0 to $d = 12.0\ m$, but a rather constant rate from $d = 12.0\ m$ to $d = 15.5\ m$.

---

[1]Control volumes 7–17.
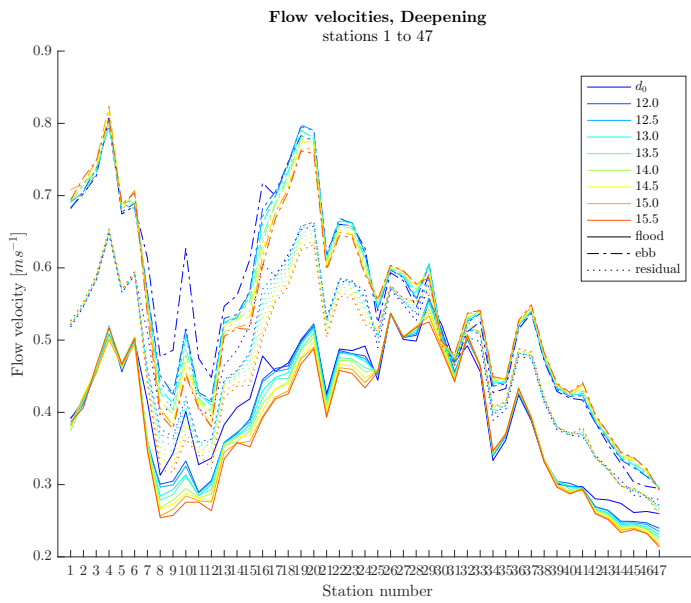
Figure 8.4. Velocity profile deepening.
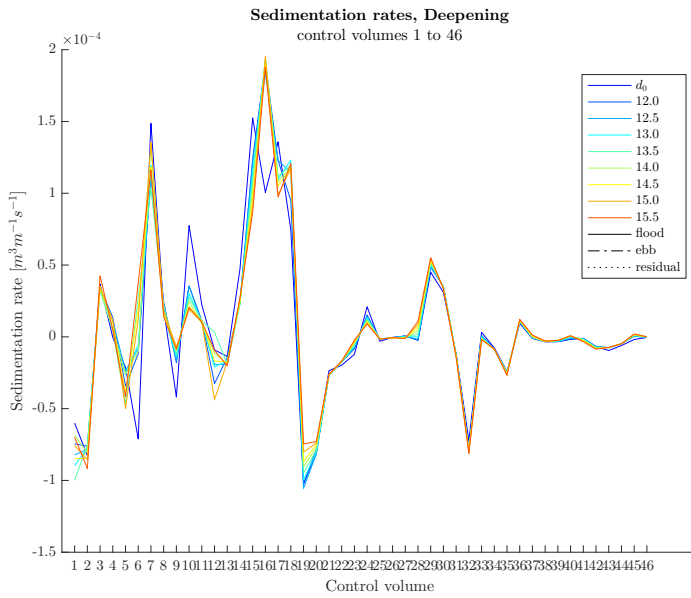
Figure 8.5. Sedimentation profile deepening.

9

Quantifying costs and criteria

In the following chapter the seven different expansion alternatives, which are introduced in Chapter 4, are simulated. Simulation in this report enhances the determination of the scores for the most important criteria. This is required to evaluate the different designs using a formal and transparent procedure. The two most common procedures are: (1) Numerical evaluation; and (2) Monetary evaluation. In the main report the emphasis lies in the methodology. The determination of the exact numbers can be found in Appendix M.

In the numerical evaluation the scores for different aspects are determined, e.g. the environmental impact or safety and the scores are summarised into a MCA. In the monetary evaluation the costs for the different port lay-outs is determined, e.g. the dredging costs of the channel. These criteria and its weight (which is required for the MCA) are composed with the three main parties involved. The criteria are largely adapted from Munters et al. (2017), Ligteringen and Velsink (2012) and updated involving the main stakeholders and experts; being the (Port authority) Consorcio de Gestión del Puerto de Bahía Blanca and Pablo Arecco (supervisor).

In the first section, Section 9.1, the most important criteria for the MCA are described and in the second section the most important cost parameters are described. In Chapter 10, the results of the monetary and numerical evaluation are combined.

9.1. Numerical Evaluation

The main criteria to evaluate the different designs in the numerical evaluation are summarised in this section. For each of the criteria its significance is explained and how its score is determined.

Environmental impact – The environmental impact is a great criterion in the feasibility of the different port lay-outs. As explained in Chapter 1, the port is located in a vulnerable area characterised by large tidal flats and natural reserves. Therefore, it is desirable to have the port as far as possible from the vulnerable areas, reclaim as little land as possible and to change the overall morphology in the ria as less as possible.

- Nuisance to flora and fauna: Proximity of vulnerable environment and amount of reclaimed tidal flats.

- Change in morphology: It is assumed that all changes in morphology are undesired. These changes are determined using the MOHID model. This is thoroughly described in Chapter 5.

Safety – Safety is always of great importance for all designs, not necessarily only because it is a requirement, it is also of great importance to convince stakeholders for a certain design. For a port area, the safety is closely linked to the alignment of the channel, for example a turning basin close to a terminal and the amount or concentration of traffic inside the channel[1].

- Vessel-infrastructure collision: Alignment (Distance to bend) and proximity of turning basin and terminal.

- Vessel-vessel collision: Concentration of traffic in the channel and turning basin in the channel.

Expansion possibilities – In port master planning it is of great importance to allow for future expansion possibilities. In this report the expansion possibilities are scored for both the quantity and quality of the available space. If the port has to expanded in the future it is of great importance to have enough space for new terminals, preferably located close to similar terminals, but also to have enough space available to expand current terminals in the hinterland.

- Space for berthing: Available space along the navigation channel.

- Space hinterland: Available space for the terminals to expand.

- Space for channel expansion: Available space for potential channel expansion.

- Space for clustering: Possibility to clustering for future expansions.

Channel siltation – One of the most important criterion of the port lay-outs is the expected increase of siltation in the port. The expected increase in siltation will lead to higher operation costs as more maintenance dredging is required. The expected increase of siltation in the port is determined using the MOHID-model as described in Chapter 6.

Operational factors – At last, the quality of a port is determined by its operations. Most of the operational factors lie in details outside the scope of this report, (a.o. type of transport system, stacking height, etc.). However, operations are still greatly influenced by the port lay-out. For example, long viaducts between the jetties and terminals will limit operations of the port.

- Connection with port area: The proximity of the current port development to prevent a scattered port lay-out.

- Connection with hinterland: The length of the required hinterland connection and likeliness of bottlenecks.

- Clustering: The amount of clustering of the new development itself .

---

[1]Normally the type of cargo is also considered, but this is assumed to be equal for all designs.

- Nautical access: The easiness to reach the new berthing areas.

- Navigation distance: Total required distance covered by the vessels.

- Length of viaduct: Length of the conveyor belts/viaducts between terminal and jetty.

The most important criteria listed above are (1) the increase in siltation; (2) nuisance to flora and fauna; (3) connection with the hinterland; and (4) vessel-marine infrastructure collision.

9.2. Monetary Evaluation

In the monetary evaluation only the initial costs of the different alternatives are determined. Some expected maintenance costs are included in the in the numerical analysis (e.g. increase in siltation) and hence not included in the monetary evaluation. Also it is assumed that these costs do not substantially differ between different designs. The emphasis in the monetary evaluation is to highlight the difference in costs between the alternatives rather than determining the exact total costs.

The main cost parameters for the monetary evaluation are:

- **Capital dredging**
- **Land reclamation**
  - Quarry material
  - Soil improvement
- **Road and railway connections**
  - Railway
  - Road
  - Viaducts
- **Marine infrastructure**
  - Viaducts (between jetty and terminal)
  - Quay wall
  - Jetties

The costs for the soil improvement are required to use the dredged material as land for the land reclamation. The main cost drivers of the different designs are the costs for land reclamation and the required amount of capital dredging.

Evaluation

10

MCA and CBA

In order to determine the best port lay-out a Multi-Criteria Analysis is performed. The results of the MCA are determined using the methodology as described in Chapter 9 and leads to the best alternative for the port lay-out. When the numerical evaluation (MCA, Section 10.1) and monetary evaluation (Section 9.2) are combined, a Cost-Benefit Analysis Cost-benefit Analysis is performed to determine the most feasible alternative.

In this chapter, first the results of the MCA are evaluated in Section 10.1, then the total costs per lay-out are determined in Section 9.2. As conclusion the most feasible alternative is found in Section 10.3.

10.1. Multicriteria Analysis

In the MCA the total scores of the alternatives are defined based on the methodology described in Section 9.1 combined with the weights given to the different criteria by the client and an expert. The main conclusion of the MCA is summarised below with the best alternatives in descending order (for the full assessment see Appendix M). For the figures of the different alternatives one is reffered to Chapter 4 or Appendix O. For the East expansion the order is as following:

Alternative 2 is characterised by its compact lay-out and viaducts with intermediate length between the terminals and the jetties. This alternative has the highest score, mainly due to the clustered design, good safety and small increase in siltation.

Alternative 1 is characterised by long viaducts between the terminals and the jetties. This alternative has a relative high score due its low impact on the environment. However the disadvantage of the long viaducts between the terminals and jetties is hard to determine.

Alternative 3 is characterised by the in-cooperation of the mooring basin. It is the third best design, mainly due to good future expansion possibilities, good nautical accessibility and its clustered design. The expected siltation of the mooring basin is the main disadvantage of this design.

Alternative 4 is the design being fully aligned with the current channel. Its main disadvantage is the relative large impact on the environment and the small possibilities for future expansions. And therefore this is the least favourable design.

For the South expansion, the alternatives do not have very distinct lay-outs, hence there is only a minor difference in scores between the different designs. Still, the main conclusions are listed below;

Alternative 2 is the design located opposite the current port and utilising the current reclamation on the south side and closing off the channel to the south. Alternative 2 has the highest score, mainly due a slightly smaller impact on the environment and small expected increase in siltation.

Alternative 1 is the design on the south bank being located furthest to the east, not utilising the reclaimed land and closing off the tidal channel to the south. This alternative is the second best design, also due to the small expected increase in siltation. The main disadvantage of this design, although not expressed in MCA, is the fact that the reclaimed land is not utilised.

Alternative 3 is the design located furthest to the west. This alternative enhances the widening of the channel to the west, utilises the current land reclamation and does not close the tidal channel to the south. Nevertheless, this alternative has a relative low score, mainly caused by the large increase of siltation in the port area.

It should be noted though, that in this analysis the expansion of the port west of the current port is neglected. This expansion will require an expansion of the navigation channel and in this way the effect of the widening in Alternative 3 is smaller. Also, the client prefers a design, utilising the current land reclamation. Hence Alternative 2 is preferred.

10.2. Cost Analysis

To determine the most feasible design, the costs have to be determined as well, which is done in this section. An overview on the costs for all the alternatives – for the East expansion as well as the South expansion – are given below. For the complete overview and the determination of the costs, one is referred to Appendix M. For the expansion alternatives for the East expansion holds, from cheapest to most expensive:

Alternative 1 is by far the cheapest option. This is because it requires the least amount of reclamation. This design however requires a long viaduct to the water. This viaduct, however can be designed for low loads, (e.g. just a conveyor belt), since no traffic is expected on these bridges.

Alternative 2 requires some long traffic viaducts and more land reclamation, which makes it more expensive than the first design.

Alternative 3 is quite similar to Alternative 2. However, this alternative requires more dredging, which makes it more expensive.

	Alternative 1	Alternative 2	Alternative 3	Alternative 4
Total score	358.00	375.00	348.00	329.00
Total costs	275	435	433	510
CBA	1.30	0.86	0.80	0.65

Table 10.1. Cost-benefit analysis East expansions.

	Alternative 1	Alternative 2	Alternative 3
Total score	268	272	230
Total costs	1100	990	880
CBA	0.25	0.27	0.26

Table 10.2. Cost-benefit analysis South expansions.

Alternative 4 does not only need the most land reclamation, but also the longest traffic viaduct. This makes it the most expensive alternative in the costliest parts of the design.

For the South expansion the costs are more similar. The differences are shortly explained below, from cheapest to most expensive:

Alternative 3 is closest to the existing infrastructure and fully utilises the already reclaimed land. Making it the cheapest option.

Alternative 2 also fully utilises the already reclaimed land, but needs a slightly longer traffic viaduct, making it a bit more expensive. Especially since the traffic viaduct is a significant part of the total costs.

Alternative 1 needs the longest traffic viaduct, and more land needs to be reclaimed, as none of the already reclaimed land is utilised. Making it the most expensive option.

10.3. Cost-benefit Analysis

To determine the most feasible design, the CBA is performed; balancing the scores with the costs of the designs. In this analysis the total scores for all the alternatives are divided by the costs for the designs. In Table 10.1, the feasibility of the different designs is listed; following this method. As can be concluded from the CBA, Alternative 1 is the most feasible design. This will therefore be presented as the final design for the East expansion.

For the south bank the CBA is given in Table 10.2. The CBA for the South expansion results in almost similar scores for all alternatives. Nevertheless, Alternative 2 is chosen as the most feasible design because of the highest score and the preference of the client.

10.4. Conclusion

In general a few conclusions from the port lay-outs can be drawn. For example, reclamation is the key cost driver determining the costs of a design. Therefore, it can be concluded that designs with

a small amount of required reclaimed land are more feasible. Moreover, as expected, the better designs are more expensive in general. Therefore, the port authority can base their design on the total available budget.

11

Assessment of model results

The results of the three points of interest – as presented in Chapter 8 – are evaluated in this chapter; what do these outcomes of the MOHID-model mean physically. The connection is made between the processes described in Section 5.1 and the hypotheses stated in Sections 5.2 to 5.4 are checked.

In order to assess the influences of the adaptions made, the base case is evaluated first in Section 11.1. Then the alternatives are assessed. The East expansion is discussed first in Section 11.2, followed by the South expansion (Section 11.3), and last the deepening of the channel is assessed in Section 11.4.

11.1. Base case

The channel seems to be ebb-dominant, as can be seen in Section 8.1. The ebb flow velocities are for all observed points in the channel higher than the flood velocities. This is due to the propagation of the flood wave over the tidal flat, whereas the ebb flow only propagates through the channel.

The flood flow thus experiences an increased cross section with a smaller averaged water depth at the place of the tidal flat, therefore bottom resistance increases. The flood flow velocity will decrease and due to this effect the flow velocity is considered to be lower during flood than ebb, implying ebb dominance (Campuzano et al., 2014).

From the mouth to the head of the ria, flow velocities are increasing. This is likely to be due to the geometry of the basin which is funnel shaped. Near the port of Ingiero White there is a reduction of the tidal flats where water can diverge to, such that it remains its velocity.
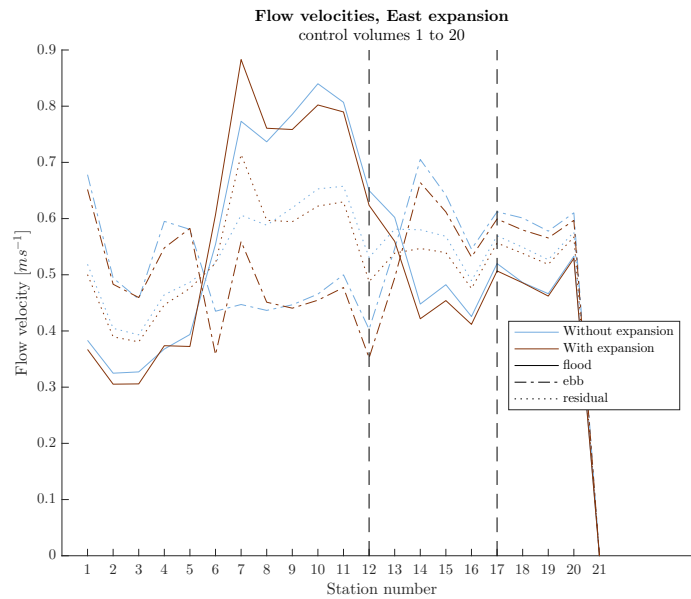
Figure 11.1. Velocity profile East expansion.

11.2. East expansion

As stated in Section 8.2, flow velocities in the channel are lower at the east side of the expansion compared to the base case, as can be seen in Figure 11.1. This is probably because the expansion partially blocks the tidal wave entering the ria from the south-east. The flood flow will pile up against the expansion area and diverge into a flow south of the expansion and a flow to the north-east of the expansion.

The resulting flow south of the expansion will head towards Canal Principal at the port area and the flow at the east side diverges onto the tidal flat. Because of this partial blockage the flood flow velocities go down. Moreover, because of this blockage, less water will flow to the port area, meaning that the returning ebb flow contains less water.

Since the flow velocities are related to sediment transport as described in Chapter 5 the sediment transport is affected by a change in flow velocity. Lower flow velocities mean less sediment transport. However less sediment transport does not mean sedimentation. This depends on the difference in transport rates over a specific control volume.

As illustrated in Chapter 8 the sedimentation rates at the east side of the expansion remain the same, despite the fact that the flow velocities decrease in the area on the east side of the expansion. This is due to the fact that the gradient in the flow velocities does not change.

The sedimentation rates in the control volumes defined in the channel next to the expansion show however some change. In control volume 16 erosion takes place where in the base case sedimentation was observed. This is due to an increase in flow velocity which is the result from a local contraction caused by the expansion area. The expansion causes a narrowing of the channel leading to an increase in flow velocities. Deeper into the port area flow velocities are almost equal to the base case and thus sedimentation rates in this area are equal as well.
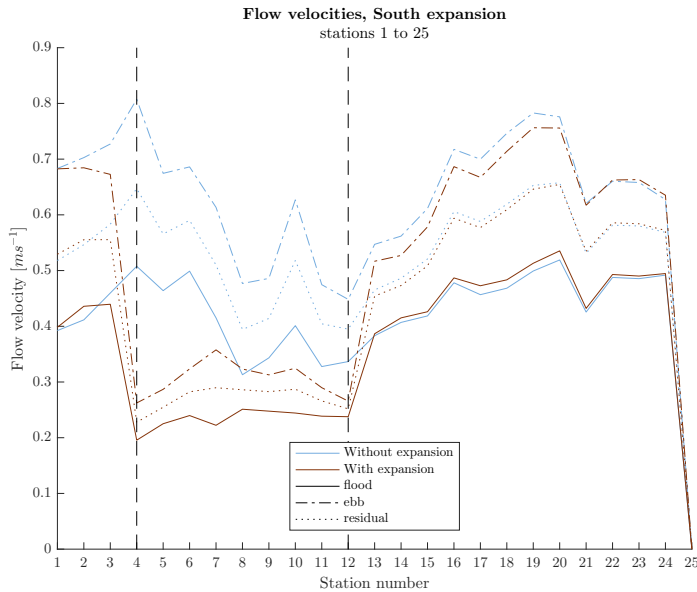
Figure 11.2. Velocity profile South expansion.

To conclude, the East expansion has little effect on sedimentation processes in the navigation channel. Only a local effect of erosion is observed in control volume 16. However this is too local to have a significant impact.

11.3. South expansion

Locally, the widening of the channel has an impact on the flow velocities. A wider channel leads to a lower flow velocity in the port area, as can be seen in Figure 11.2. Considering basic river engineering relationships, it is likely that this will result in sedimentation downstream. Since the residual flow is towards the mouth in the channel (ebb-dominance), the sedimentation starts at the eastern side of the widening. At the western end there will be local erosion.

The drop in velocity at the port area is likely due to the widening of the channel. The velocities go down with a little more or less than half, corresponding to twice the width. This suggests that the widening is more important than the effect of the expansion itself. The expansion was expected to constrain the flow at the port area leading to more discharge through the channel and thus increasing the flow velocities in flood direction. There does seem to be a lower relative decrease at the flood velocities than for the ebb velocities, what may be due to the effect of the reclamation of the expansion area. With the widening, the smoothening of the bed and the expansion as variables, this is hard to say though.

The residual flow is still in east direction as before the expansion, but significantly smaller. With a smaller ebb dominance, it is possible that in the long term, less sediment is transported out of the port area, and thus structural sedimentation can take place.

From the sedimentation rates, it becomes clear that there is a large increase in sedimentation at the

east side of the expansion. From a river engineering approach erosion would have been expected at the east side, and thus is not what would have been expected. This can be due to the fact that there is a tidal motion in the channel, and not a flow in only one direction. At the west only a small change in erosion is observed. The smoothening of the sedimentation rate might also be due to the equalisation of the bottom profile at $13.5m$. The sedimentation will have to be taken into account when dredging activities are planned. The smoothening is not exactly representing reality, so the sedimentation resulting from this will have to be implemented with care.

In general, the main aspects resulting in a difference in velocities and thus having an effect on sedimentation transport are:

- widening lowers the velocity at the port area and this seems to be the dominant response of the system on the expansion

- converging the flood flow between the expansion as a boundary may be diminishing the effect of the widening, but is not dominant

11.4. Deepening

The flow velocities for the various depths, which are outputs of the MOHID-model, show some distinct differences concerning the relation between the flow velocity and the depth, as addressed in Section 8.4 (Figure 11.3). Where the flow decreases with increasing depth, the driving factor can be taken to be the flow as described by Equation 5.1b. This is the case for the inner reach of the system; with the reach west of the current port as exception. The outer reach shows a distorted relation between flow velocities and depth, expected to be due to the influence of the wave as driving force (Equation 5.1a). These findings support the expectation mentioned in Section 5.1, only the influence of the wave-driven flow is less.

Furthermore, the innermost reacht – west of the port – is showing deviations from this behaviour; the flow velocities increase with increasing depth (stations 1–6 in Figure 11.3c). This sudden change cannot be addressed to the fact that the flow is driven by a wave as described by Equation 5.1a, whereas this dampens out towards the head of the ria. Therefore, an other reason has to be found. The increasing flow velocities due to the deepening are probably due to the abrupt change in water depth. Where at first the water is largely stopped by the sudden decrease in depth, it can now flow further into the reach. Due to the absence of a blockage, the flow velocities as inside the port continue further and so the flow velocities – relative to the ones for a depth $d = 12.0 \ m$ – increase.

Eventually, the ria can be devided in three sections based on the influence of the depth on the flow velocities:

- West of the port area (stations 1–6): flow velocity increases with increasing depth;

- Port area up to the naturally deep section of the ria (stations 7–24): flow velocity decreases with increasing depth; and

- Outer reach (stations 25–47): flow velocity neither fully decreases nor fully increases with increasing depth.

As can be seen in Figure 11.3, not all stations exactly follow the description of the sections; mainly the stations in the outer reach, which is due to the fact that there is no clear relation between flow velocity and depth.

(a) Stations 7–24, 30 and 47.

(b) Stations 25:29, 31, 35, 38, 40, 44 and 46.

(c) Stations 1:6, 32:34, 36:37 and 41:43.
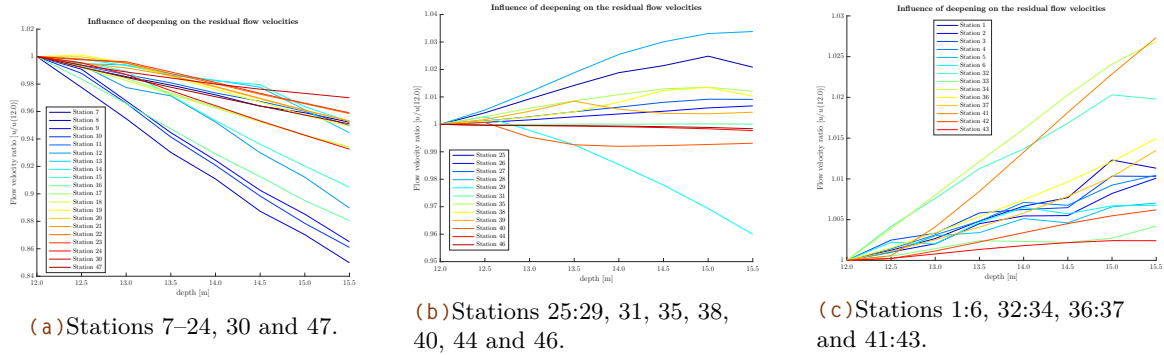
Figure 11.3. Flow velocities per minimum depth for the stations in the channel.

Also mentioned in Section 8.4 is the fact that the larger deviation on the sedimentation rate is seen between the base case (d_0) and the opposed depths; so no significant differences between the different depths. This behaviour can be explained by the method of deepening (Appendix C): the main channel is drawn as a line – varying in width – through the bathymetry. The grid cells of this line are adapted to the new opposed depth, if smaller than the investigated depth. This can result in abrupt changes in bed elevation, which affect the flow velocities. Big changes in velocities can lead to a spatial gradient in the flow velocities and so a change in the sedimentation rate. Therefore, it is more interesting to look at the changes in sedimentation rate between the opposed depths: $d = 12.0 - 15.5\ m$.

The differences in sedimentation rate due to the deepening are small and for most control volumes negligible. There are three possible explanations why: (1) the deviations in depth are too small compared to the initial depth to result in significant changes in the system; (2) there is initially not much sedimentation and erosion, so deviations in depth will not immediately result in sedimentation or erosion; and (3) the depth along the main channel is all set to be at least a certain value with a minimum of twelve metres, bounded by tidal flats.

First, even though the deviations in depth are small compared to the initial depth, they are in the range interesting for the port to dredge to. For future plans, there are not yet clear reasons to deepen the channel except to an overall depth of 13.5 m.

Second, because the initial sedimentation rates are not a lot or even negative (erosion) – vast areas of the navigation channel do not need any dredging to have sufficient depths for the port – a deeper channel is not going to make a significant impact on these small sedimentation rates.

Third, for changes in the sedimentation rates, a gradient in the flow velocities due to the deepening is needed. Because the whole navigation channel is deepened to a certain minimum, there are no expected locations for changes in sedimentation rates. That is also why imposing the rough navigation channel in to the bathymetry firstly resulted in a significant change in the sedimentation rates, whereas the initial bathymetry is much smoother and so the deepening results in a significant change in the bathymetry. Adding another half-a-metre of minimum depth is not going to result in large changes to the bathymetry to result in different sedimentation rates.

Phase V

Conclusion

12

Conclusions

In this chapter the main conclusions of the report are stated. The conclusion of this report consists of four parts, the main findings and final designs for the east bank and for the south bank, the conclusion of the coastal impact and the feasibility of caissons. First the East expansion is elaborated, including the optimisation in Section 12.1; and next the best design for the South expansion is presented in Section 12.2.

12.1. East expansion

For the East expansion an additional optimisation is done. This optimisation is a combination of the first and second alternative. The first alternative being the cheapest and therefore the best from a cost benefit point of view, and the second the best option without taking the costs into account.

This optimisation is executed to tackle the insecurity in the feasibility of the first design. The main question is whether a bridge or conveyor belt of $(2.5\ km)$ is feasible considering operations. Therefore an alternative design with shorter viaducts is proposed. This new "alternative" is a combined design based on Alternative 1, with implementations of Alternative 2. This optimised "alternative" is illustrated in Figure 12.1.

For this alternative also a MCA is done to determine whether this alternative would be better than the previous ones. The summary of this MCA is stated in Appendix M. In order to determine whether the optimised alternative is better compared with the other alternatives a Cost-benefit Analysis is done. The results are illustrated in Table 12.1.

From the multi-criteria analysis the following conclusions can be drawn for this optimised design;

- The design is relative cheap

Figure 12.1. Conceptual design of the optimisation.

	Alternative 1	Alternative 2	Alternative 3	Alternative 4	Optimisation
Total score	358.00	375.00	348.00	329.00	356.00
Total costs	275	435	433	510	376
CBA	1.30	0.86	0.80	0.65	0.95

Table 12.1. Cost-benefit analysis of the East expansions compared with the optimised design.

Conceptual design of the South expansion.

- Little nuisance to flora and fauna
- Little expected increase in siltation
- All terminals can expand

The main disadvantages of this port lay-out are;

- Large viaducts with unknown impact on operational efficiency, (although shorter than in Alternative 1).
- Little space between berthing locations
- Berthing locations aligned with channel.
- Little space available for future expansion of berthing locations

12.2. South expansion

As a result of the MCA (Chapter 10), the best design for the South expansion is chosen to be Alternative 2. An overview of this design is given in Figure 12.2. For this expansion area no optimisation is done, because the best design seems to be suitable from the operational point of view.

The main advantages of this design are;

- Relative small expected increase in siltation
- Possibility to expand to both east and west
- Utilises current reclamation

The main disadvantages of this port lay-out are;

- Concentration of traffic
- Little space available to expand terminals

- Relative large nuisance to flora and fauna
- Long hinterland required

12.3. Coastal impact

The reclamation of the tidal flats in the eastern area does not seem to have a great impact on the hydraulic system, nor on the local conditions. Also on the southern part of the widening seems to have a bigger impact than the reclamation of the tidal flats. For the deepening the effects seem to be positive regarding dredging activities at the port area. Based on these findings, the East expansion, which uses the existing channel, is seen as a favourable expansion area. The deepening is also seen as favourable adaption of the channel since, based on the findings, relatively less sedimentation is expected. Moreover the deepening provides a good possibility to reclaim useful soil material for the expansion and make the port more future proof.

12.4. Caissons

In order to build the quay wall for the container terminal, the caisson method is considered. The use of caissons for the quay wall is possible, but with some difficulties.

For instance, the dimensions are very large since the height is determined to be very large ($22.5\ m$). As a result, the width ($28\ m$) and the length ($84\ m$) of the caisson should be very large too, in order to keep the caisson stable during, for example, immersing. This does not only mean a lot of concrete is needed, but also that it would be more complicated to transport the caissons. However, while having such huge dimensions, it is still possible to use the caissons for the quay wall since the caissons are both statically as dynamically stable.

Because the dimensions are large, the costs are also very high. To build a quay wall the conventional way, it costs around US\$ 30,000 per metre. To build the length same quay wall with caissons, the costs will be around \$ 70,000 per metre. This is more than twice as much.

13

Recommendations

As a first impression of the possibilities for the port of Bahía Blanca to expand, two areas have been investigated: (1) the East expansion; and (2) the South expansion. Furthermore, the possibilities of deepening the navigation channel are researched; this increases the accessibility for larger vessels and hence the future proofing of the port. Moreover, an innovative building method for construction of quay walls is part of the expansion study; by using caissons.

Because this study is the first in its kind, some recommendations to improve the knowledge and optimise the design are inevitable. These recommendations are listed in this chapter and elaborated in more detail, categorised in five subjects: (1) the port lay-out in Section 13.4; (2) the morphology of the ria in Section 13.1; (3) the hydrodynamic model in Section 13.2, including in more detail the East and South expansions and the deepening of the navigation channel in combination with reclamation possibilities; and (4) the design and use of caissons as quay walls in Section 13.3. For clarity, every subject ends with a small summary, which makes it easier to read back.

13.1. Morphology

Since the ria with the fine sediment, large tidal flats and channels is very complicated, more research should be done on the interaction between channels and tidal flats and on the sedimentation itself. Concerning the sediment, it has to be determined how it works; what is possible to happen with the sediment; how does biologic activity effect sedimentation of the bottom profile; and when is sedimentation occurring (e.g. what are the threshold velocities of the sediment types).

- Investigate the interaction between the tidal flats and the channels in the ria of Bahía Blanca in more detail.

- Get more information on the characteristics of the sediments in the ria, to be able to do more detailed studies on the sediment transport.

13.2. Hydrodynamic model

Using a model to represent the reality always presumes some uncertainties. A big part of the uncertainty of the model results is due to the facts that (1) the MOHID-model has not been calibrated; and (2) the roughness of the model, a grid of $200 \times 200 \ m$. Both will have to improve to get more reasonable results. Calibration can be done by introducing a field campaign to measure water levels and flow velocities at the channels (mainly Canal Principal) and the tidal flats. These tidal flats are primarily important because of sediment coming from the tidal flats which ends up in the channel. The mareographic tower measuring the tides is already a good first step to obtain valuable information. Furthermore, Goyenechea (2017) has already done a small field campaign in measuring the flow velocities in the main channel, but the data set is too small; only 35 days with a time step of 15 minutes. Next to this field campaign, other small campaigns have been set up (e.g. Campuzano et al., 2014, 2008) – in which it seems to be about the same data set – is not enough for a complete picture of the ria. Therefore, more has to be done to be able to calibrate the model.

To start with, the flow velocities should be measured across Canal Principal, whereas this is the dominant area of the Bahía Blanca ria. Best would be to have a couple of permanent measurement stations, which are not only in the main channel but also in the branches. Especially, the conjunctions are interesting locations to have such stations.

Next to the flow velocities the wind velocities should be taken into account. For this research the average wind velocity was considered and the assumption was made that the wind had no influence on the sediment transport since the channels where relatively too deep. However at the tidal flats the wind certainly has its influence on the erosion processes of the sediment. Moreover the wind has influence on the set-up and set-up of the waterlevel, thus influencing the tidal range. Therefore it is recommended to have live wind measurements in order to predict the waterlevels more accurately and next to that, to calibrate the hydrodynamic model.

The MOHID-model is a 2D depth-averaged (2DH) model without updated bathymetry. In order to properly observe the results on the long term, an updated bathymetry profile would be preferable. Since the sediment in the ria is very fine and there is a constant suspension in the water column, a 3D model without the simplified depth-averaged water velocity will therefore not be the first priority.

The control volumes of the MOHID-model have been defined as good as possible, within the amount of time available. However, the outcomes might differ too much from reality, especially at the tidal flats where a sediment transport perpendicular to the channel is measured. The process of sediment transport from the tidal flats to the channel can be better researched to understand the relevance and magnitude of this mechanism (Piccolo et al., 2008).

In some cases the placement of the control volumes results in a large depth difference between the Virtual Measurement Stations (VMSs) of one control volume[1]. This difference in depth may distort the results significantly and thereby make it more difficult to derive conclusions from the results.

Moreover, due to the widening and narrowing of the main channel, the widths of two consecutive control volumes might differ. This results in complications at the boundary between these control

---

[1]Two consecutive VMSs in the channel, one at the tidal flat to the north, and one at the tidal flat to the south.

volumes, whereas the width of a control volume is taken constant for the whole control volume. This width is based on the distance between the VMSs of the tidal flats, north and south of the control volume. Because the flow velocity at the VMS between the two control volumes is taken to be the average over the whole width, deviations between outflow of control volume `i` and inflow of control volume `i+1` are expected to influence the computations. This is because the width affects the flow velocity, which is in this manner not fully taken into account. Thereby, the flow velocity represents a smaller flow at control volume `i` than `i+1` in case of a widening, and vice versa. This is especially of importance when the driving force of the flow velocity is the flow, thus described by Equation 5.1b.

Furthermore, due to the bathymetry of the Bahía Blanca ria, the main channel of Canal Principal has many branches. These branches influence the in- and outflow of the main channel significantly. It is worth to check the influence of the various branches on the flow in the main channel of Canal Principal, whereas their influence on the flow conditions in the main channel is not taken into account. Especially for the assumptions made for the control volumes concerning the in- and outflow; flows parallel to the boundary are not taken into account (Section 6.2). Moreover, the assumption that the main flow is through the channel schematise the main channel more like a 1D system instead of a 2D system. When these branches are taken into account, this schematisation no longer holds.

- The MOHID-model is not calibrated, which results in a solely qualitative use of the data. To be able to say more about what happens, calibration of the model is needed. To do so, a couple of permanent measurement stations should be placed in Canal Principal – the main channel and its branches – to be able to have real time water levels and flow velocities along the ria. This data can then be used to calibrate the model results.

- The grid of the model is very rough – namely $200 \times 200\ m$ – which may result in large deviations from reality.

- Morphological processes, hence an updated bathymetry, is recommended to take into account, in order to get a better understanding of the sediment transport in the ria. This includes the effect of the tidal flats on the sediment transport in the channel.

- The locations of the VMSs have to be reconsidered, whereas the depth at the locations used in this report might show significant differences, which affect the flow velocities used for the computations.

- The widening and narrowing of the channel is not fully correct implemented due to the fact that the width of the control volume is taken constant per control volume. A varying width within a control volume would do the job.

- Next to a better calibration, real time validation of a live operating model is also recommended. With live measurements the model can predict the hydrodynamic conditions. With better predictions, the productivity can be optimised.

East expansion

The model results give a first impression of the changes in the ria as a result of the East expansion. Since the flow velocities decrease in the area east of the expansion it is worth to have a deeper investigation about the consequences of the decrease in flow velocity.

Moreover, it is advised to look into the local erosion that appears in control volume 16. There is still uncertainty if this is the only eroding control volume. It is possible that more control volumes next to the expansion will change to eroding channel parts.

At last the influence on the tidal flats at the north-east side of the expansion is researched. The flow that diverges onto the expansion will flow towards this area and can have an impact on the flora and fauna present there.

- Investigate the effect on the system in the long run
- Look into the local erosion at the navigation channel next to the expansion
- Further research to qualify the contribution of each change to the system.

South expansion

It must be recognised that in reality for the South expansion, the depth is not always $13.5\ m$, whereas this is the case for the modelling of the effects. Here a possible improvement can be found.

With the model results, the first response is presented. With a smaller residual flow in ebb direction, it has to be further researched whether this leads to structural sedimentation on the long term. The lower residual flow will in general not impose problems beside this, though the current dredging method, Water Injection Dredging, must not be endangered. Good communication must be maintained with the dredging company to make sure this dredging method is still possible.

To find the separate contributions of each impact, the widening, the expansion and the smoothening, the runs will have to be done separately as well. This way, each effect can be quantified better and it will become easier to correctly adjust the design of the reclamation.

- Investigate the effect on the system in the longer run.
- Do further research to qualify the contribution of each change to the system.

Reclamation & deepening

The reclamation due to the port expansion and the influence of the deepening of the channel have been modelled very roughly. This can already be improved by obtaining a finer grid, but also the sizes and shapes should be reconsidered. The exact size and shape can influence the direction of the flow of water and may lead to a different discharge distribution. Furthermore, the deepening can also be modelled by better representing reality; including the transition from the deepening to its sides instead of a very local deepening as is described in Appendix C. The impact of this robust method of opposing the deepening on the bathymetry is clearly visible in the figures and elaborated in Sections 8.4 and 11.4.

To even further optimise the modelling on the deepening, the exact location of the navigation channel can be used for the shape and location of the deepening. This, again, should include the slopes at the sides of the deepening, whereas a vertical slope at the bottom is an incorrect representation. For the investigation on the deepening of the navigation channel in this report, the location of the channel is determined manually. This implicates errors, which might be of significance.

If morphological processes are taken into account in the modelling, an initial vertical slope at the sides of the deepening will be adjusted to more gentle slopes due to sedimentation processes. Therefore, the input bathymetry can contain the vertical slopes, which might only give a longer spin-up time.

Furthermore, three parts of the navigation channel are being dredged regularly for maintenance: (1) the port basins, by WID; (2) at Canal del Toro; and (3) at the Outer Channel (Bessone, 2017). Because at Canal del Toro, the system is very dynamic as can be seen in Figure N.8g, and as concluded by Perillo and Cuadrado (1991), a reroute of the navigation channel is expected to be interesting to look at. Instead of significant dredging at Canal del Toro, a reroute can result in by-passing this problem. Also other rerouting at the end mouth of the ria can be of interest due to the highly dynamic behaviour of the ria, which has regularly been studied (e.g. Aliotta and Perillo, 1987; Perillo and Cuadrado, 1991; Pierini et al., 2013).

All in all, deepening of the navigation channel is – according to the outcomes of MOHID – of no significant influence on the sedimentation rates of the channel. Therefore, a deepening will only result in advantages for the port of Bahía Blanca, assuming the capital dredging is worth spending. Nevertheless, big questionmarks should be placed at these outcomes, whereas they seem unrealistic. Expected is at least some more sedimentation due to the deepening, but the results do not show such effects. More study has to be done to get better insights in the response of the ria to the deepening of the navigation channel; even though the outcomes of the MOHID-model, which are unrealistic, expected is not a significant increase in maintenance dredging when deepening, because the ria is already in an erosive state (Pierini, 2007).

- The grid is very rough and it is recommended to make it finer to obtain more reasonable data.
- The deepening is imposed locally, without transitions to the surroundings via slopes. Implementing these transitions or making use of a model with an updated bathymetry is recommended to limit the impact of the deepening.
- Further optimisation on the impact of the deepening of the navigation channel should include the exact location of the navigation channel.
- It is worth looking at rerouting the navigation channel due to morphological dynamics at some locations that significantly affect the navigation channel, especially at Canal del Toro.
- Deepening of the navigation channel seems to have little impact on the sedimentation rates and so these should not be taken as limitation concerning the deepening. Nevertheless, more research has to be done on this topic, due to the limitations of the MOHID-model and those outcomes assumed as unrealistically small. Still, due to the erosive state of the ria, deepening the navigation channel is a topic worth spending time on.

13.3. Caissons

Despite the fact that after the first calculations the caisson method can be considered as feasible, there are still some points of concern. First, the shear force acting at the bottom of the caisson is too large compared to the resistance. This means that extra shear reinforcement is needed for the caisson to resist this shear force.

Second, the bearing capacity of the subsoil is insufficient to resist the forces acting on it. This means that soil improvement is needed.

Third, the costs of the caissons are estimated to be US\$ 70,000 per metre. This is rather expensive compared to the conventional quay walls, which are in the order of US\$ 30,000 per metre. However, according to Port Consultants Rotterdam (2017a,b), this does not have to be a problem, since the Port Authority attaches significant value to being innovative. Therefore, it is not all about money, but innovative designs might be implemented even though the costs will increase.

Fourth, the dimensions of the calculated caisson are very large. It is therefore not advisable to use caissons with those dimensions as a quay wall. It is recommended to look into the possibilities of gravity walls; e.g. a block wall, or two caissons on top of each other. Therefore, the caisson method is advised to use when a smaller caisson in combination with an L-wall is considered. However, this needs further investigation.

- The shear resistance of the caisson is not sufficient to resist the forces acting on it. Therefore, it is recommended to implement shear reinforcement and make finer calculations regarding shear force and shear resistance.

- Because the strength of the subsoil is not sufficient, soil improvement is needed. It is recommended to investigate the use of soil improvement.

- It is not advisable to use only caissons as a quay wall, because the dimensions are too large. It is recommended to look at more conventional methods.

13.4. Port lay-out

In the process of developing the different port lay-outs different assumptions are made or some topics are out of scope in general. The most important additional research that is still required concerns the operations inside the port. In the final design for the East expansion, e.g., long viaducts are included between the terminals and jetties, see Figure 12.1). The potential downside of these long viaducts is only addressed as a minor criterion, whereas its impact can be much larger.

Moreover, the hinterland connections required in these conceptual lay-outs are addressed very briefly. Although included in the MCA, more elaboration is required in the possible hinterland connections; whether they are feasible, how they can be optimised, etc.

Another operational aspect that needs more in-depth study is the necessity of an additional turning basin in the East expansion. The necessity of a turning basin is assumed according to the lay-out of the current port, which has a turning basin near Puerto Galván and in front of Ingeniero White.

At last, the quality and costs of the operations of the terminal is closely determined by the facilities, e.g. the type of transport system used.

In the MCA, only the proximity of the areas involved is used as measuring parameter to determine the impact on the environment. In reality the impact on the environment is more complicated than only the proximity of the lay-outs. Also, it is assumed that for the jetties impermeable structures (e.g. caissons) are applied. This means that if permeable structures are applied these scores are invalid.

Also, for the costs a few assumptions are made. First of all, the operational costs are assumed to be alike for the different designs and therefore it is not considered, as this research aims at finding the better design. This assumption, however, can be easily questioned as, e.g., viaducts are more

likely to have higher operational costs than reclaimed land. Moreover, the initial costs are roughly estimated; unit prices are roughly estimated based on comparable operations in the past. Also the dredging and reclamation volumes are a rough estimation using average depths only.

- An in-depth study on the operational costs per port lay-out is needed, whereas it is not taken into account in this report, but can have a significant impact on the optimisation.

- More research must be done on the hinterland connections, which might influence the port lay-out as they are optimised.

- It is recommended to have a closer look on the location and the necessity of an extra turning basin for the East expansion.

- An in-depth study has to be preformed on the environmental impact of the various port lay-outs.

- A more detailed costs calculation is required; in this report only rough estimations have been made

Acknowledgements

First of all, we would like to thank em.prof.ir. T. (Tiedo) Vellinga for supervising and helping us to find a suitable project, which became the expansion possibilities for the port of Bahía Blanca. Via him, we came in contact with Pablo Arecco, who helped us a lot and also was our supervisor in Argentina. Thanks to him we were able to execute the project without any complications because everything was well organised. We could work at his small office, Besna, where we occupied the meeting room when possible. The great team of Besna have taught us a lot about Argentina, and Buenos Aires in special.

Besides em.prof.ir. T. (Tiedo) Vellinga, we also like to thank our supervisors dr.ing. M. (Mark) Voorendt and dr.ir. J.G. (Jarit) de Gijt. They not only helped us at the start of the project in Delft, but also found the time to give feedback very quickly while we were in Argentina.

In building a hydrodynamic model of the Bahía Blanca ria, we came along a lot of papers from J.O. (Jorge) Pierini (IADO[2]) who we asked for help on the hydrodynamic model. Beforehand, we never thought that this request turns out in working with him at his attic for three days; after which he continued working on our model. Due to his efforts, we were able to get way more insight in the processes occurring in the Bahía Blanca ria. Beside Jorge himself, we would also like to thank his family for their openness during our stay at their house as well as Emma (their dog) for her mental support and sharing her knowledge of the MOHID-model.

We also would like to thank the port authority of Bahía Blanca for the opportunity to work on the expansion possibilities of their port. In special we would like to name Gerardo Bessone and Ezequiel Walter for their daily availability, as well as Carlos Ginés, the chief engineer, on his opinions and feedback. Also the openness and the trust of the port towards us, so we were supported in anyway to do what we have done. Of course also all of the port authority for our short stays at their office. Moreover, we cannot be thankful enough to cover the necessary expenses to visit Bahía Blanca for multiple occasions.

Furthermore, we would like to thank R. (Raúl) Escalante and S. (Sebastián) García of the University of Buenso Aires for the possibility to do this project as well as their feedback on our planning and progress of the project; including the feedback on the content as well.

During our stay in Buenos Aires, we came along a couple of challenges for which we could rely on the feedback and knowledge of J. (Jan) van Overeem and R.J. (Robert Jan) Labeur. Their insights helped us to pass hurdles we came across.

We would also like to thank prof.dr.ir. S.G.J. (Stefan) Aarninkhof for his support and believe in our project and getting us in contact with Royal Boskalis Westminster N.V., which is currently active

---

[2]Instituto Argentino de Oceanografía

in the port of Bahía Blanca. Because they are already working in the port for decades, they could help us with insights and data, which helped us with our study. Also Boskalis provided us with great financial support by paying our flight tickets to Argentina.

Moreover, during one of their dredging campaigns we were able to join on board and get a better understanding on the dredging works done. We would like to thank Boskalis for this amazing opportunity.

References

Aliotta, S. and Perillo, G. M. E. (1987). A sand wave field in the entrance of Bahía Blanca estuary, Argentina. *Marine Geology*, 76:1–14.

Bagnold, R. A. (1963). Mechanics of marine sedimentation. In Hill, M. N., editor, *The Sea*, volume 3, page 982. Harvard University Press.

Bessone, G. (2015). Waterways management in Bahía Blanca estuary. *Smart Rivers 2015*.

Bessone, G. (2017). Canal Principal con Zonas de Dragado [map]. (1:250,000) Bahía Blanca: Consorcio de Gestión del Puerto de Bahía Blanca.

Bosboom, J. and Stive, M. J. F. (2015). *Coastal Dynamics I*. Delft Academic Press (VSSD-uitgeverij), Delft, 0.5 edition. Lecture notes CIE4305.

Buring, P. (2013). Flexible quay wall structures for container vessels. Master's thesis, TU Delft.

Campuzano, F. J., Pierini, J. O., and Leitão, P. C. (2008). Hydrodynamics and sediments in Bahía Blanca estuary: Data analysis and modelling. In Neves, R., Baretta, J. W., and Mateus, M., editors, *Perspectives on Integrated Coastal Zone Management in South America*, pages 483–503. IST Press.

Campuzano, F. J., Pierini, J. O., Leitão, P. C., Gómez, E. A., and Neves, R. J. (2014). Characterisation of the Bahía Blanca estuary by data analysis and numerical modelling. *Journal of Marine Systems*, 129:415–424.

Cuardrado, D. G. and Perillo, G. M. E. (1997). Migration of intertidal sandbanks, Bahía Blanca, Argentina. *Journal of Coastal Research*, 13:155–163.

Ginsberg, S. S. and Perillo, G. M. E. (1990). Channel bank recession in Bahia Blanca estuary, Argentina. *Journal of Coastal Research*, 6:999–1010.

Gómez, E. A., Amos, C. L., and Li, M. Z. (2006). Evaluation of sand transport models by in situ observations under unidirectional flow. *Journal of Coastal Research*, SI 39:578–581.

Gómez, E. A., Cuadrado, D. G., and Pierini, J. O. (2010). Sand transport on an estuarine submarine dune field. *Geomorphology*, 121:257–265.

Goyenechea, C. (2017). Estudio de impacto ambiental dragado para la extensión del canal de acceso hasta puerto cuatreros, provincia de buenos aires. Technical report, Serman & Asociados S.A.

Holthuijsen, L. H. (2010). *Waves in Oceanic and Coastal Waters*. Cambridge University Press, 1st edition.

Larrondo, R. (2000a). De Baliza Trípode a Puerto Cuatreros. (1:42,000).

Larrondo, R. (2000b). De Faro Recalda a Faro el Rincón. (1:100,000).

Li, M. Z. and Amos, C. L. (1995). SED-TRANS92: a sediment transport model for

continental shelves. *Computers & Geosciences*, 21:533–554.

Ligteringen, H. and Velsink, H. (2012). *Ports and Terminals.* Delft Academic Press (VSSD-uitgeverij), Delft, 1.0 edition.

MarCom WG-121 (2014). Harbour approach channels design guidelines. Technical report, PIANC, Boulevard Simon Bolivar, Brussels, Belgium.

Molenaar, W. F. and Voorendt, M. Z. (2016). *Manual Hydraulic Structures.* TU Delft.

Munters, A., Stam, B., Van der Wel, T., and Wesstein, R. (2017). Container terminal development for the port of Bahía Blanca. Technical report, Delft University of Technology.

NEDECO (1983). Estudio de dragado del canal de acceso al puerto de Bahía Blanca. Technical report, Consorcio NEDECO - ARCONSULT.

Perillo, G. M. E. and Cuadrado, D. G. (1991). Geomorphologic evolution of E1 Toro channel, Bahia Blanca estuary (Argentina) prior to dredging. *Marine Geology*, 97:405–412.

Perillo, G. M. E. and Piccolo, M. C. (1991). Tidal response in the Bahia Blanca estuary, Argentina. *Journal of Coastal Research*, 7:437–449.

Perillo, G. M. E., Piccolo, M. C., Parodi, E., and Freije, R. H. (2001). The Bahia Blanca estuary, Argentina. *Ecological Studies*, 144.

Perillo, G. M. E. and Sequeira, M. E. (1989). Geomorphologic and sediment transport characteristics of the middle reach of the Bahía Blanca estuary (Argentina). *Journal of Geophysical Research*, 94:14351–14362.

Piccolo, M. C. (2008). Climatological features of the Bahía Blanca estuary. In Neves, R., Baretta, J. W., and Mateus, M., editors, *Perspectives on Integrated Coastal Zone Management in South America*, pages 231–239. IST Press.

Piccolo, M. C., Perillo, G. M. E., and Melo, W. D. (2008). The Bahía Blanca estuary: an integrated overview of its geomorphology and dynamics. In Neves, R., Baretta, J. W., and Mateus, M., editors, *Perspectives on Integrated Coastal Zone Management in South America*, pages 219–229. IST Press.

Pierini, J. O. (2007). *Circulación y transporte en zonas costeras del estuario de Bahía Blanca.* PhD thesis, Universidad de Buenos Aires, Buenos Aires.

Pierini, J. O., Campuzano, F. J., Leitão, P. C., Gomez, E. A., and Neves, R. J. (N.D.). Atmospheric influence over the time residence in the Bahía Blanca estuary, Argentina. Unpublished.

Pierini, J. O., Lovallo, M., Telesca, L., and Gómez, E. A. (2013). Investigating prediction performance of an artificial neural network and a numerical model of the tidal signal at Puerto Belgrano, Bahia Blanca. *Acta Geophysica*, 61:1522–1537.

Pierini, J. O., Marcovecchio, J. E., Campuzano, F., and Perillo, G. M. E. (2008). Evolution of salinity and temperature in Bahía Blanca estuary, Argentina. In Neves, R. J., Baretta, J., and Mateus, M. D., editors, *Perspectives on Integrated Coastal Zone Management in South America*, pages 505–513. IST Press.

Port Consultants Rotterdam (2017a). Port vision 2040. Technical report, PCR.

Port Consultants Rotterdam (2017b). Visión portuaria 2040. Technical report, PCR.

Pratolongo, P. D., Perillo, G. M. E., and Piccolo, M. C. (2010). Combined effects of waves and plants on a mud deposition event at a mudflat-saltmarsh edge in the Bahía Blanca estuary. *Estuarine, Coastal and Shelf Science*, 87:207–212.

Reyes, S. A., Reyes, J. A., Hughes, R., and Darqui, M. R. (2017). Estudio de impacto ambiental para la actualizacion de las operaciones de dragado en el puerto de Bahía

Blanca. Technical report, Reyes & Asociados S.R.L.

unknown (unknown). Informacion base para port scan. Technical report, CGPBB.

Voorendt, M. Z., Molenaar, W. F., and Bezuyen, K. G. (2011). *Hydraulic Structures,* *Caissons, lecture notes.* TU Delft.

Weyland, F. (2009). Estudio sobre el puerto de Bahía Blanca. Master's thesis, Universidad de Buenos Aires, Buenos Aires.

Yalin, M. S. (1977). *Mechanics of sediment transport.* Pergamon Press, 2nd edition.

Appendix

A
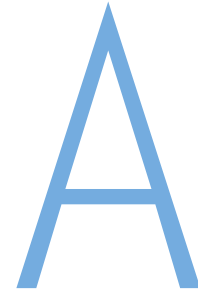
Requirements and boundary conditions

This appendix is an addition to Chapter 3, elaborating the design parameters briefly mentioned in this chapter. This appendix consists of four sections: (1) the boundary conditions (Appendix A.1); (2) the requirements (Appendix A.2); (3) the wishes (Appendix A.3); and (4) the conditions left out of scope (Appendix A.4). These terms are all set by either the Port Authority or literature.

A.1. Boundary conditions

Boundary conditions are requirements regarding the boundary of the area which have to be satisfied at all times.

Borders expansion area – The expansion areas can not exceed the borders of the given areas for both the East as the South expansion.

A.2. Requirements

Requirements are the conditions which have to be taken care of in the conceptual designs. Therefore all alternatives meet these criteria in order to be sufficient.

Area sizes and quay walls – The sizes of the areas of the terminals are given as part of the input parameters Table A.2. The areas are considered to be the minimum and should therefore not

	Current width [m]	required new width [m]
One-way channel	120	180
One-way channel with single mooring	180	280
Two-way channel with single mooring	350	530
Two-way channel with double mooring	410	630
Turning radius	300	350

Table A.1. Required channel width.

be less than these numbers. The same holds for the number of berths and the quay lengths given in this table.

Although the figures of the amount of berths are given, they will not be considered critical since the quay lengths are already known.

Road and rail access – Every terminal needs to have access to both rail and road. Especially the distripark needs good access points, preferred as close to the main road as possible. Since Minerals go mostly by train, rail access is the most important for the dry bulk terminals.

Bulk terminals – For the export of dry bulk mostly jetties are used. The loading of bulk carriers in the export terminal is done by conveyor belts extending right above the ship, from which the material falls freely into the holds at constant and high capacity. As a consequence the export terminal may be more similar to the jetty/platform arrangement for tankers, while the import terminal needs a quay for heavy cranes. Since the terminal of Bahía Blanca is an exporting terminal, these heavy cranes are not required. (Ligteringen and Velsink, 2012)

Container terminal – The storage of containers has to be as close as possible to the berths in order to achieve efficient (un)loading. Moreover, container terminals can not be constructed with jetties due to the high loading of the cranes. Therefore the container terminals have to be close to the waterside (Ligteringen and Velsink, 2012).

Sewage outlet – At the north side of expansion area east a sewage treatment plant is located. This treatment plant discharges waste water into the estuary through a channel. This channel crosses the expansion area, and must be able to discharge water all the time.

Central Termoléctrica – Central Termoléctrica Luis Piedrabuena, which is located at the west side of expansion area East, also has a water outlet. This channel leads the water to the east, where the water will be released. Consequently, the water will find his way down to the ria. When designing the expansion, a solution must be found to lead the water to the ria.

Suezmax – The design vessel for the port of Bahía Blanca will be Suezmax (instead of Panamax right now). Therefore, the channel should be widened inside and outside the port area[1] and the current service level of the port should be maintained. The specifications of the design vessel are given in Appendix L. Also, the service limit of the port should be maintained, therefore the channel inside the port area should be a two-way channel and a one-way channel inside the port area. The resulting widths are given in Table A.1 , and further elaborated in Appendix L.

---

[1]This is given and not further investigated.

	Area (ha)	Number of berths	Quay length (m)	Road and rail connections	Include jetties
Multipurpose terminal	30	2	500	Yes	No
Dry bulk terminal 1	20	1	300	Yes	Yes
Dry bulk terminal 2	40	1	300	Yes	Yes
Agribulk terminal	20	1	300	Yes	
Agri-industrial terminal	50	2	500	Yes	
Food port industrial area	100			Yes	
Distripark	50			Yes	
Container terminal	50	3 to 4	1000	Yes	No
Total	**360**	**10 (11)**	**2900**		

Table A.2. Requirements for each terminal.

A.3. Wishes

This section describes all the criteria which are preferred to be implemented in the conceptual designs, but which are not necessary.

Nuisance by agribulk – The agribulk terminals process a lot of goods, such as grain. These kind of materials produce a lot of nuisance for the surroundings, because of the smell and the generated dust. For this reason the agribulk terminals must be placed as far from the living areas as possible.

Sediment – The port expansion must not result in a lot of sedimentation in the port. Preferred is the least possible amount of sedimentation.

Container terminals caissons – As mentioned in the requirements, the container terminal must be as close to the water as possible. As preferred by the Port Authority, the option for quay walls with caissons is investigated.

Expansion possibilities – The conceptual designs for the expansion areas have to be able to adapt to future expansions. This means that further expansion possibilities have to be taken into consideration designing the port. This does not only include the space needed for such an expansion, but also the function of those spaces. When an extra food terminal is needed in the future it is desirable to build this terminal in the food port and not somewhere else.

A.4. Out of scope

In this section the aspects which are left out of scope are described. These aspects are assumed to be equal for all the alternatives, which means they will not influence the conceptual designs. Examples are economy, legal advice, labour forces and safety engineering. The latter one is considered to be very important, but can be investigated in a later stage of the project.

The logistics inside the terminals were taken out of the scope as well. In the conceptual designs, the area sizes are given as an input value, but the lay-outs of the terminals themselves are not

considered. Also the hinterland connections are not calculated to be sufficient enough, they are just assumed to be there.

B

Dredging activities

When the dredging activities of the port are assessed, the interventions and maintenance campaigns are considered. The main developments can be split into maintenance dredging and capital dredging combined with reclamation.

B.1. Dredging activities

Since the majority of the access channel has at least the required natural depth, maintenance dredging is only required in three stretches of the channel, which are depicted in Figure B.1.

- Interior Channel (km 4 to km 22): the banks of the interior channel are very stable. Only at the major bend at 14 kilometres dredging is required due to migrating sand dunes into the main channel.

- Canal del Toro (km 42 to km 46): the banks of the interior channel tends to move towards the inside of the channel, hence enhancing sedimentation in the channel. The sedimentation is largest between buoy 13 and 14.

- Outdoor channel (km 60 to km 80).

It is interesting to notice that the locations with the highest sedimentation rates are the locations in line with the direction of ebb and flood. Such as the outer channel stretch, which is designed with a general near course in the NW - SE direction, which is practically that of the tidal current. This location decreases the sedimentation of materials within the canal.

The dredging volumes are split into the volumes required for the capital dredging, deepening of the channel and the maintenance dredging to maintain the constructed depth over the years.

Figure B.1. The access channel and the dredged stretches.

B.2. Capital dredging

In 1971 the first dredging in the port enabled a depth of depth 33 ft in the channel; allowing vessels up to 40 ft inside the channel. In 1991, further dredging allowed ships up to 45 ft in 1991 and is further deepened to 50 ft. in 2013. The last capital dredging allows vessels (with 45 ft draught) to sail through the channel regardless of the tide. The newest research for waterways are feasibility studies to continue the deepening of the whole main channel from km 40 until reaching a natural depth 15 metres to Charts Datum. Doing so would permit the traffic of vessels with a draught of 45 ft at all times, and up to 50 ft using the high tide window, thus contributing to maintain the status as Argentina's deepest port (Bessone, 2015).

In Table B.1 an overview of the capital dredging activities is given.

B.3. Maintenance dredging

Since 2005 the dredging strategy for maintenance consists of two periods of dredging per year. These periods last approximately three months; from March to June and from October to December. In total approximately 3,000,000 m^3 sand settles in the channel each year; which logically equals the amount of dredged material each year.

First in 1991, a filling of the area of Cangrejales was made (between Ing. White and Pto Galván) totalling 120 hectares. Of the approximately 11 million cubic meters extracted in the port area, some 7 million were used in the aforementioned landfill, the rest, due to its characteristics, was used to fill sites that would not be affected by infrastructure.

In 2013 another deepening of the outer and inner port area found place. The channel was deepened

---

[1]Total contract value; including five years of maintenance dredging.

Year	Location	Dredged volume ($\times 10^6 m^3$)	Costs (M US\$)	Description
89–91	N/A	50	200	Deepening the main channel to 45 ft; material used as landfill for Cangrejales area.
2009	S1	0.5937		West port of Puerto Galván to -13.50 m.
	S2	0.4888		Antepuerto post of flammable and widening to -12.20 m.
	S3	1.0492		Circle of rotation Galván and channel linking to -13.50m.
	S4	0.7952		Enlarge channel linking White - Galván to -12.20 m.
	S5	0.1413		Rectification manoeuvres area Ing. White at -13.50 m.
	Subtotal	3.0682		Manoeuvring areas and anteports Ing. White and Galván.
	S6	2.6718		Access channel from km. 4 to km. 20 to -13.50 m.
	Total	5.74	90[1]	Deepening of the main channel to allow 45 ft vessels at all times. Material is used as landfill opposite to the current port (south bank).

Table B.1. Capital dredging overview.

Channel	Stretch (km)	Volumes (m^3yr^{-1})	Material
Channel Exterior	60–80	1,800,000	Mixture of fine sand and silt
Channel del Toro	42–45.5	400,000	Medium to fine sand with silt
Channel Interior	16–19	70,000	Gravel
Channel Puerto Rosales	0–1.7	125,000	Silt and fine sand
Channel PNPB	0–4.3	315,000	Very cohesive silt and fine sand
Total		2,710,000	

Table B.2. Yearly maintenance volumes.

to a depth of 13.50 m and a widening found place to improve the operate-ability of the docks in Puerto Galván (in the presence of the Metaneros vessels in Mega). The material dredged from this campaign was selected for a new landfill. The material of high compactness (coarse) was used for the filling of two sites, the so-called Galván Enclosure of 19 Ha. And Sector A located in front of Cangrejales along about 1700 m and with an area of about 44 Ha. In total in the port area, some 3 million cubic meters were extracted, of which some 2.5 million cubic meters were used in the landfills, the rest was deposited in the Eco dump located at km 21 of the Access Channel.

C

Deepening of the main channel

One of the points of interest of the response of the estuary on human interventions is the deepening of the channel. To be able to say something reasonable about it, multiple depths are investigated, whereas the MOHID-model only gives qualitative insights.

C.1. Deepening steps

The deepening of the channel is done via a simple method in which the values between the current channel depth ($d = 13.5\ m$) and the new depth are set to be equal to the new depth. This results in a rectangular deepening, where the slopes on the sides are not taken into account as illustrated in Figure C.1. Beside the fact that this is not completely true, it gives a good understanding of the situation, where the depth of the main channel is leading; the slopes do not have that much impact on what one would expect in the channel.

The location of the deepening is approximated as shown in Figure C.2. Only those locations where the original depth is less than the deepened depth which is aimed for, will be deepened. In practice, the middle reach of the Canal Principal will thus not change because it already has a higher depth than considered.
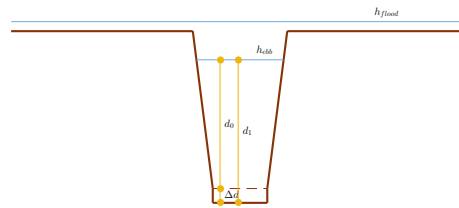
Figure C.1. Schematisation of the deepening of the main channel.
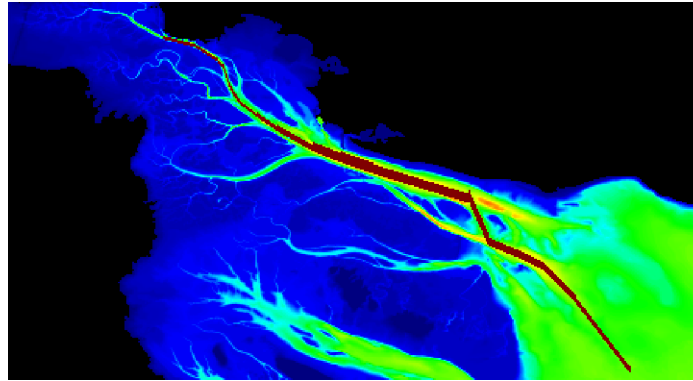
Figure C.2. Locations where the channel is deepened, under the condition that the original depth at these points are less than the deepened depth.

C.2. Elucidation deepening.m

The bathymetry file needed to run MOHID is a `.dat`-file, which consists of one long column. In Script C.1 the MATLAB-file is presented that creates the depth-files for MOHID.

The deepening of the main channel is written as `function` so it can be placed in a `for`-loop for ease. The input parameters are the new depth (`d_new`) up to which level the new channel depth must be, and which data sets has to be load in, stated as `depthnumber`.

The first paragraph – `%% LOADING DEPTH FILE` – loads at first the original bathymetry file, which will be modified[1]. First the location of the x-, y-, and z-values has to be determined, before they can be modified.

Next, these values are assigned to working parameters in `%% ASSIGN DATA TO WORKING-PARAMETERS`. The x- and y-coordinates are directly copied, but the z-values are saved as `NaN` if they represent land ($z \leq -99$). Furthermore, the z-values are also placed in a matrix (Z) to make modification of the depth profile easier.

When all data is well loaded, another file is loaded containing data points of where the main channel is located[2] under paragraph `%% LOADING DEEPENINGS LOCATIONS FILE`. The data points are values of `i` and `j` of the matrix Z that are the beginning of a linear channel section with a certain width; num-

---

[1] `'bblancafilhohighoverlap4b_origineel.dat'`

[2] This file is manually made with care to give the best representation of the navigation channel towards the port; i.e. the locations where deepening is investigated.

ber of data points in the j-direction. These values are specified in the following paragraph, namely `%% SPECIFY THE LOCATIONS OF THE DEEPENING`. This is again, assigning the data to the working parameters, where the subscript `1` indicates the left boundary of the linear section of the main channel, and `2` the right boundary. The linear sections are such shaped that its western and eastern boundary – in x-direction – are always parallel to the y-direction. The northern and southern boundaries of the channel section can be placed under an angle. In this manner, only the `i,j`-coordinates of the south-west and south-east boundary of the channel section needs to be specified in combination with the width of the section – which is completely directed to the north.

With the `i,j`-coordinates of the boundaries set, all `i,j`-coordinates in between has to be determined. Script C.2 computes these data points. Because `i,j` have to be integers, `j` is rounded down. The output of Script C.2 is an array of `i`-coordinates and a matrix of `j`-coordinates, where the number of rows is specified by the width of the channel section.

The `i,j`-indices of the matrix Z are modified to the new depth in the paragraph `%% DEEPEN THE CHANNEL` after which the matrix Z is written as one column again to be written on to the `.dat`-file. Before the data is written to the file, the values of Z that equal `NaN` are set to -999 – representing land.

The writing of the file starts with a couple of rows that are standard for the bathymetry-file of MOHID. Followed up by the x-, y-, and z-values, which are started and ended with the suiting commands.

Script C.1. Create various depths of the main channel.

```
1   function deepening(d_new,depthnumber)
2   % %%   INPUT PARAMETERS
3   % d_new=30;        % metres
4   % depthnumber=1;   % deepening stage
5
6   %%   LOADING DEPTH FILE
7   filename='bblancafilhohighoverlap4b_origineel.dat';
8   fileID=fopen(filename);
9   file=textscan(fileID,'%s %s %s');
10  fclose(fileID);
11  % find locations of the x-data (between <BeginXX> and <EndXX>)
12  BeginXX=find(strcmp(file{1,1},'<BeginXX>'));
13  EndXX=find(strcmp(file{1,1},'<EndXX>'));
14  % find locations of the y-data (between <BeginYY> and <EndYY>)
15  BeginYY=find(strcmp(file{1,1},'<BeginYY>'));
16  EndYY=find(strcmp(file{1,1},'<EndYY>'));
17  % find locations of the z-data (between <BeginGridData2D> and <EndGridData2D>)
18  BeginZZ=find(strcmp(file{1,1},'<BeginGridData2D>'));
19  EndZZ=find(strcmp(file{1,1},'<EndGridData2D>'));
20
21  %%   ASSIGN DATA TO WORKING-PARAMETERS
22  x=zeros(EndXX-BeginXX-1,1);
23  for i=1:EndXX-BeginXX-1
24      x(i)=str2double(file{1,1}{BeginXX+i,1});
25  end
26  y=zeros(EndYY-BeginYY-1,1);
27  for i=1:EndYY-BeginYY-1
28      y(i)=str2double(file{1,1}{BeginYY+i,1});
29  end
30  z=zeros(EndZZ-BeginZZ-1,1);
31  Z=zeros(length(x)-1,length(y)-1);
32  for i=1:EndZZ-BeginZZ-1
```

```matlab
33        z(i)=str2double(file{1,1}{BeginZZ+i,1});
34        if z(i)<=-99
35            Z(i)=NaN;
36        else
37            Z(i)=z(i);
38        end
39    end
40
41    %%  LOADING DEEPENINGS LOCATIONS FILE
42    filename='punten_MOHID_matlab.csv';
43    fileID=fopen(filename);
44    file2=textscan(fileID,'%s %s %s %s %s',...
45        'Delimiter',';');
46    fclose(fileID);
47
48    %%  SPECIFY THE LOCATIONS OF THE DEEPENING
49    i1=str2double(file2{1,1});i1=i1(2:end);
50    j1=str2double(file2{1,2});j1=j1(2:end);
51    i2=str2double(file2{1,3});i2=i2(2:end);
52    j2=str2double(file2{1,4});j2=j2(2:end);
53    w=str2double(file2{1,5});w=w(2:end);
54
55    %%  DEEPEN THE CHANNEL
56    d_new=d_new+.15;    % calibrate from LAT to LIMB
57    for l=1:length(w)
58        [i_line,j_line]=j_calc(i1(l),j1(l),i2(l),j2(l),w(l));
59        for xx=1:length(i_line)
60            for yy=1:w(l)
61                if Z(i_line(xx),j_line(yy,xx))<d_new
62                    Z(i_line(xx),j_line(yy,xx))=d_new;
63                end
64            end
65        end
66    end
67
68    % %%  FIGURE
69    % figure;hold on;
70    % imagesc(Z.');
71    % hold off;
72
73    %%  FORMATTING NEW DEPTH
74    z_new=zeros(length(z),1);
75    for zi=1:length(z)
76        if isnan(Z(zi))
77            z_new(zi)=-999;
78        else
79            z_new(zi)=Z(zi);
80        end
81    end
82
83    %%  WRITING THE FILE
84    [fid,msg] = fopen(sprintf('channeldepth_%g.dat',depthnumber),'wt');
85    assert(fid>=3,msg)
86    fprintf(fid,'FILL_VALUE                : -999\n');
87    fprintf(fid,'ILB_IUB                   : 1  340\n');
88    fprintf(fid,'JLB_JUB                   : 1  580\n');
89    fprintf(fid,'ORIGIN                    : -62.57 -39.38\n');
90    fprintf(fid,'GRID_ANGLE                : 0\n');
91    fprintf(fid,'COORD_TIP                 : 4\n');
92    fprintf(fid,'LATITUDE                  : 42\n');
```

```
93  fprintf(fid,'LONGITUDE                      : -8\n');
94  fprintf(fid,'<BeginXX>\n');
95  fprintf(fid,'%g\n',x);
96  fprintf(fid,'<EndXX>\n');
97  fprintf(fid,'<BeginYY>\n');
98  fprintf(fid,'%g\n',y);
99  fprintf(fid,'<EndYY>\n');
100 fprintf(fid,'<BeginGridData2D>\n');
101 fprintf(fid,'%g\n',z_new);
102 fprintf(fid,'<EndGridData2D>');
103 fclose(fid);
104 end
```

Script C.2. Create various depths of the main channel.

```
1   function [i_new,j_new] = j_calc(i1,j1,i2,j2,width)
2   % (i1,j1)    :    left boundary
3   % (i2,j2)    :    right boundary
4   % width      :    width of the deepened channel north of the defined line
5   % i1=135;j1=298;
6   % i2=154;j2=293;
7   % width=10;
8
9   i_new=i1:1:i2;
10  j_l=j1:1:j1+width-1;
11  j_r=j2:1:j2+width-1;
12  j_new=zeros(width,length(i_new));
13  for k=1:width
14      j_new(k,:)=-(j_r(k)-j_l(k))/(i2-i1)*(i1-i_new)+j_l(k);
15  end
16  j_new=floor(j_new);
17  end
18
19  % i_new=i1:1:i2;
20  % j_new=-(j2-j1)/(i2-i1)*(i1-i_new)+j1;
21  % j_new=floor(j_new);
```

D
Reading MOHID output files

The output of a run in MOHID results in a `.srh`-file, which has to be read to present the results. The output file is a time series of two days long with time steps of ten minutes consisting of fourteen parameters (`j=1:14`). At the bottom of the file, the residual values for all fourteen 'virtually measured' parameters are listed.

Script D.1 reads the `.srh`-files as `for`-loop to give a clear structure as output; here called `loc`. The length of the `for`-loop depends on the number of files at the specified location: e.g. five adjacent data files of the Virtual Measurement Stations (VMSs) in the channel, from the fourth to the eighth VMS.

Because every output file of MOHID has the same format – every run simulates two days with a time step of ten minutes – the length is predetermined. Thereby, it does not depend on that many parameters; only the location of the files and the range of VMSs. Due to the fact that every file is equal in formatting, the number of rows is predefined (`R=304`) as well as the range of rows that have to be assigned to the parameters (`k=11:299`) and the residual values (data on row 302).

The location of the `.srh`-files is set by defining to maps: (1) `map1` is the point of interest in consideration; and (2) `map2` is the option in consideration. The option is with or without expansion in case of the East and South expansion, and is the minimum depth in case of the deepening. The range of VMSs that have to be read with Script D.1 is defined by a starting point (`Nbegin`) and an ending point (`Nend`). This results in a length of the range of `N=Nend-Nbegin+1`.

Script D.1. Reading MOHID output file.

```matlab
function loc=MOHID_data(map1,map2,location,Nbegin,Nend)
R=304;
for i=Nbegin:Nend
    filename=fullfile(map1,map2,'results',[location,num2str(i),'_macro.srh']);
    fileID = fopen(filename);
    X = textscan(fileID,'%s %s %s %s %s %s %s %s %s %s %s %s %s %s',R);
    fclose(fileID);
    M(i-Nbegin+1).X=X;
    for j=1:14
        for k=11:299
            loc(i-Nbegin+1).var(j).data(k-10,1)=str2double(M(i-Nbegin+1).X{1,j}{k,1});
            loc(i-Nbegin+1).var(j).Name=M(i-Nbegin+1).X{1,j}{9,1};
        end
        loc(i-Nbegin+1).res(j).data=str2double(M(i-Nbegin+1).X{1,j}{302,1});
        loc(i-Nbegin+1).res(j).Name=M(i-Nbegin+1).X{1,j}{9,1};
    end
end
end
```

E
Sediment transport and sedimentation rates

Because the MOHID-model does not take sediment transport into account, this is derived from the flow velocities – which are part of the output of MOHID. Based on the sediment transport, the sedimentation rates can be determined. The relations used for the computations – done with MATLAB – are elaborated in Section 5.1. For readability, the relevant equations are given again below: (1) the sediment transport relation (Equation E.1a, Equation 5.2a in Section 5.1); and (2) the sedimentation relation, also known as the Exner equation (Equation E.1b, Equation 5.3 in Section 5.1).

$$S = mu^n \qquad \text{E.1a} \qquad\qquad \frac{\partial z_b}{\partial t} + \frac{\partial S_x}{\partial x} + \frac{\partial S_y}{\partial y} = 0 \qquad \text{E.1b}$$

As input of Script E.1 are the output files of MOHID (`.srh`-files) and the control volumes under consideration; between `Nbegin` and `Nend`. The number of control volumes considered (N) in the sediment transport function is the difference between the first and the last control volume specified, plus one.

For the computations, two consecutive data sets from the channel Virtual Measurement Stations (VMSs) are needed, one data set from the Northern tidal flat VMS, and one data set from the Southern tidal flat VMS are needed. There are $N + 1$ VMSs in the channel needed to compute the sedimentation rates in N control volumes, where there are N VMSs on the tidal flats needed, both North and South of the control volume. The data sets are loaded using `MOHID_data` (elaborated in Appendix D).

Next, the $\Delta \xi$ and $\Delta \psi$ of the control volumes under consideration are determined using `txt2metres`

(Appendix F.2). As last loaded data are the angles of the control volumes using `txt2angles` (Appendix F.1).

All data loaded, the flow velocities in x- and y-direction (u, v) are used to compute the sediment transport in these directions using Equation E.1a: S_x and S_y, respectively. In this way, two new timeseries are created so the effect of the power n in the sediment transport relation (Equation E.1a) is taken into account correctly. Using the residual flow to compute the sediment transport results in an underestimation of the influence of differences in flow velocity; this power becomes more important for larger deviations between the flow velocities.

Once the sediment transport computed in the original frame of reference (x, y), the sediment transport in the new frame of reference are computed: S_ξ and S_ψ. This transformation from the x, y-axes to the ξ, ψ-axes is done using simple geometry, using the determined angle (α) between the two frames of reference.

For the sediment transport in ξ-direction, only the data sets obtained by the VMSs in the channel are used, and the sediment transport in ψ-direction is solely based on the data from the VMSs at the tidal flats. This, because the orientation of the ξ- and ψ-direction are such defined that they are perpendicular to the channel boundaries of the control volume and the tidal flats boundaries, respectively. The flows parallel to the boundaries are assumed to result in no sediment transport in or out of the control volume.

Therefore, the net sediment transport in ξ-direction is the difference in sediment transport between two consecutive channel boundaries; and the net sediment transport in ψ-direction is the difference in sediment transport between Northern and Southern boundary. These net sediment transport per control volume devided by the distance between the boundaries ($\Delta\xi$ and $\Delta\psi$) results in the sedimentation rate (Equation E.1b[1]).

Script E.1. Sediment transport.

```
1   function [dzb,s]=sediment4(map1,map2,Nbegin,Nend)
2   % map1, map2: mapping structure
3   % Nbegin: begin control volume of area of interest
4   % Nend: end control volume of area of interest
5   %
6   % map1='Deepening';map2='depth0';
7   % Nbegin=1;
8   % Nend=37;
9   N=Nend-Nbegin+1;
10
11  % power in the sedimentation relation: s=mu^n
12  n=3;
13
14  % load data of the channel (ch), northern tidal flats (tfn), and the
15  % southern tidal flats (tfs)
16  ch=MOHID_data(map1,map2,'Channel',Nbegin,Nend+1);
17  tfn=MOHID_data(map1,map2,'TFN',Nbegin,Nend);
18  tfs=MOHID_data(map1,map2,'TFS',Nbegin,Nend);
19
20  % determine the distance between following virtual measturement stations in
21  % the main channel (dxi), and the distance between the virtual measurement
22  % stations on the northern and southern tidal flats (dpsi), based on the
23  % coordinates
24  [dxi,dpsi]=txt2metres('delftstations_channel.txt',...
```

---

[1] Replace x by ξ, and y by ψ.

```matlab
25      'delftstations_TFN.txt',...
26      'delftstations_TFS.txt',...
27      Nbegin,Nend);
28
29  % determine the orientation of the frame of reference per control volume
30  % based on the virtual measurement stations in the main channel; including
31  % virtual points before the first and after the last control volume, which
32  % are the same as the first and last angle, resp.
33  a(2:N+1)=txt2angles('delftstations_channel.txt',Nbegin,Nend);
34  a(1)=a(2);a(N+2)=a(N+1);
35
36  % load the data for the x,y-directions (u,v) and converting them to the
37  % sediment transport in xi,psi-directions using geometry and the angle of
38  % the FoR, where the orientation of the velicity vectors at the inter-
39  % channel boundaries are based on the average angles of the control volumes
40  % where they are in between
41  sxc=zeros(N+1,1);sxn=zeros(N,1);sxs=zeros(N,1);
42  syc=zeros(N+1,1);syn=zeros(N,1);sys=zeros(N,1);
43  for i=1:N+1
44      % channel
45      sxc(i)=mean(ch(i).var(8).data.^n);
46      syc(i)=mean(ch(i).var(9).data.^n);
47      s.xic(i)=sxc(i)*cos(mean([a(i) a(i+1)]))...
48          -syc(i)*sin(mean([a(i) a(i+1)]));
49      if i<N+1
50          % northern tidal flat
51          sxn(i)=mean(tfn(i).var(8).data.^n);
52          syn(i)=mean(tfn(i).var(9).data.^n);
53          s.psin(i)=sxn(i)*sin(a(i))+syn(i)*cos(a(i));
54          % southern tidal flat
55          sxs(i)=mean(tfs(i).var(8).data.^n);
56          sys(i)=mean(tfs(i).var(9).data.^n);
57          s.psis(i)=sxs(i)*sin(a(i))+sys(i)*cos(a(i));
58      end
59  end
60
61  % determine the net sediment transport over the control volume in
62  % xi,psi-directions
63  for i=1:N
64      s.xi(i)=s.xic(i+1)-s.xic(i);
65  end
66  s.psi=s.psin-s.psis;
67
68  % determine the sedimentation rate
69  dzb=-s.xi./dxi -s.psi./dpsi;
70  end
```

Angles and distances

The orientation of the frame of reference per control volume is based on the angle between two Virtual Measurement Stations (VMSs). Moreover, the distance between two VMSs determines the length and width of the control volume; distance between two VMSs in the channel the length, and between the VMS at the northern tidal flat and the VMS at the southern tidal flat the width. For the determination of these three parameters – the angle, α; the length, $\Delta\xi$; and the width, $\Delta\psi$ – a couple of MATLAB-scripts are written. To start with, Script F.1 calculatates the angle between two VMSs. Next, Script F.2 determines the length and width of the control volumes.

F.1. Elucidation txt2angles.m

The orientation of the frame of reference is determined by the angle between two VMSs in the channel. This angle is calculated based on the difference in latitude and longitude; $\Delta\lambda$ and $\Delta\phi$, respectively. Because the MOHID-model does not take the curvature of the Earth's surface into account due to the relatively small area of interest. Therefore, the angle can be determined using a simple tangent (Equation F.1). This angle is determined per control volume.

$$\tan\alpha = \frac{\Delta\lambda}{\Delta\phi} \qquad\qquad \text{F.1}$$

Script F.1 uses a file with the coordinates of the VMSs as input. Because N is the amount of control volumes, there are N+1 VMSs. The file is read up to line N+2 (line 4), because the file contains headings as well. This is also why lines 9–10 assigns data point i+1 of the file to data point i of the arrays with the coordinates. Line 15 is the equivalent of Equation F.1, per control volume.

Script F.1. Determination of the orientation of the frame of reference of the control volumes.

```
1  function a=txt2angles(fileID,Nbegin,Nend)
2  N=Nend-Nbegin+1;
3
4  fileID = fopen(fileID);
5  A=textscan(fileID,'%s %s %s %s'); % ,N+2
6  fclose(fileID);
7
8  lon=zeros(N+1,1);lat=zeros(N+1,1);
9  for i=1:N+1
10     lon(i)=str2double(A{1,1}{i+Nbegin,1});
11     lat(i)=str2double(A{1,2}{i+Nbegin,1});
12 end
13
14 a=zeros(1,N);
15 for i=1:N
16     a(i)=atan((lat(i+1)-lat(i))./(lon(i+1)-lon(i)));
17 end
18 end
```

F.2. Elucidation txt2metres.m

The length and width of the control volume are based on the distance between two following VMSs in the channel, and the distance between the northern and southern boundary – respectively. Therefore, the coordinates of all three VMSs-arrays needs to be loaded (lines 6–16 in Script F.2). First the length ($\Delta\xi$) is determined, solely based on the coordinates of the VMSs in the channel (lines 19–26). To determine the distance in metres based on the coordinates, the haversine formula is used (Equation F.2), which can be written as Equation F.3[1] – for computational purposes. The latter equation is scripted in Script F.3. Next, the width is determined; distance between the northern VMS and southern VMS of the control volume (lines 28–39) in the same manner as the length (according to Equation F.3, Script F.3).

$$\mathrm{hav}\,(\Theta) = \mathrm{hav}\,(\phi_1 - \phi_2) + \cos\,(\phi_1)\cos\,(\phi_2)\mathrm{hav}\,(\lambda_1 - \lambda_2) \quad \text{in which} \quad \Theta = \frac{d}{r} \qquad \text{F.2}$$

where

ϕ_i : latitudinal coordinate of point i;
λ_i : longitudinal coordinate of point i;
d : distance between two points;
r : radius of the sphere, i.e. radius of the Earth (R).

$$d = 2R \arctan 2\left(\sqrt{a}, \sqrt{1-a}\right) \qquad \text{F.3a}$$

in which

$$a = \sin^2\left(\frac{\Delta\phi}{2}\right) + \cos\phi_1 \cos\phi_2 \sin^2\left(\frac{\Delta\lambda}{2}\right) \qquad \text{F.3b}$$

In Script F.2, the difference between the various locations of the VMSs is presented as (1) c for the channel; (2) n for the northern tidal flat; and (3) s for the southern tidal flat.

---

[1]By definition: $\mathrm{hav}\,(\theta) = \sin^2\left(\frac{\theta}{2}\right) = \frac{1-\cos\theta}{2}$.

Determination of the distance length and width of the control volumes.

```matlab
function [dxi,dpsi] = txt2metres(fileIDc,fileIDn,fileIDs,Nbegin,Nend)
% Nbegin=1;
% Nend=37;
% fileIDc='delftstations_channel.txt';
% fileIDn='delftstations_TFN.txt';
% fileIDs='delftstations_TFS.txt';

N=Nend-Nbegin+1; % number of control volumes

fileID = fopen(fileIDc);
c=textscan(fileID,'%s %s %s %s'); % ,N+2
fclose(fileID);

fileID = fopen(fileIDn);
n=textscan(fileID,'%s %s %s %s'); % ,N+1
fclose(fileID);

fileID = fopen(fileIDs);
s=textscan(fileID,'%s %s %s %s'); % ,N+1
fclose(fileID);

lonc=zeros(N+1,1);latc=zeros(N+1,1);
dxi=zeros(1,N);
for i=1:N+1
    lonc(i)=str2double(c{1,1}{i+Nbegin,1});
    latc(i)=str2double(c{1,2}{i+Nbegin,1});
end
for i=1:N
    dxi(i)=coor2metres(latc(i),lonc(i),latc(i+1),lonc(i+1));
end

lonn=zeros(N,1);latn=zeros(N,1);
lons=zeros(N,1);lats=zeros(N,1);
dpsi=zeros(1,N);
for i=1:N
    lonn(i)=str2double(n{1,1}{i+Nbegin,1});
    latn(i)=str2double(n{1,2}{i+Nbegin,1});
    lons(i)=str2double(s{1,1}{i+Nbegin,1});
    lats(i)=str2double(s{1,2}{i+Nbegin,1});
end
for i=1:N
    dpsi(i)=coor2metres(lats(i),lons(i),latn(i),lonn(i));
end
end
```

Determination of metres based on the coordinates (λ, ϕ) of two locations.

```matlab
function d = coor2metres(lat1,lon1,lat2,lon2)
R=6378.137; % kilometres
dlat=deg2rad(lat2-lat1);
dlon=deg2rad(lon2-lon1);
a=(sin(dlat./2)).^2+cos(deg2rad(lat1)).*cos(deg2rad(lat2)).*(sin(dlon./2)).^2;
c=2.*atan2(sqrt(a),sqrt(1-a));
d=1000.*R.*c; % metres
end
```

Data processing

The MOHID-model has a.o. as output the flow velocities in all three directions and the water levels. Especially the flow velocities in x- and y-directions – u and v, respectively – are used for further computations. The processing is done using MATLAB and for all the cases they are rather similar: (1) base case; (2) East expansion; (3) South expansion; and (4) deepening.

Because of these similarities, the common part is elaborated in Appendix G.1 after which the base case, the East and South expansion, and the deepening are briefly discussed in Appendices G.2 to G.4, respectively. Because the processing of the East and South expansion is the same in general, they are elaborated together. Furthermore, the part of the MATLAB-code in which the figures are drawn is left out, because it consists of many lines, which are irrelevant for this report.

G.1. Common processing

The common part starts with the determination of which data has to be loaded, depending on the point of interest (`PoI`; lines 2–17). Next, the number of control volumes is determined based on first and last control volumes (`Nbegin` and `Nend`, respectively; line 18).

Under the heading `%% Data`, the data of the point of interest (or the base case) is loaded. This data consists of (1) the sedimentation rates; (2) the sediment transport; and (3) the flow velocities, which the raw data.

Next the computations are performed, where the common part includes (1) the determination of the flood, ebb, and residual flow per Virtual Measurement Station (VMS) (lines 32–61); and (2) the sedimentation rate per control volume (lines 69–75). The flood and ebb flow are determined based on the fact if the water level is rising (line 42); flood is defined by a rising water level, and ebb by a sinking water level. Based on this criterion, the flow velocities are assigned to the flood flow and the

ebb flow (lines 52–58) after which the mean per VMS is taken. The residual flow is given as output by the MOHID-model, and this data is used.

The sedimentation rates per control volume are directly taken from the computations performed in the function `sediment4`, which is elaborated in Appendix E. For plotting purposes, the data is reassigned (lines 69–75).

In all four cases, at least two figures are drawn: (1) the velocity profile, making the distinction between flood, ebb, and residual flow; and (2) the sedimentation rate profile (which is not elaborated on).

G.2. Processing base case

The base case is the simplest of the four and fully discussed in Appendix G.1. In its processing only the location of the existing port is added to the figures, by setting the left and right boundaries: `left=8` and `right=12`, respectively.

G.3. Processing East and South expansion

In case of the East and South expansion, one extra computation is performed: the differences in flow velocities for the flood, ebb, and residual flow (lines 62-66). The `if`-statement is written as such, so it can also be used for the deepening (Appendix G.4).

G.4. Processing deepening

The processing of the deepening includes all the computations and figures mentioned in Appendices G.1 and G.3, and three more figures are drawn: (1) the relation between the depth and the sedimentation rate; (2) the total sedimentation of the whole navigation channel; and (3) the velocity ratio relative to the minimum depth. The total sedimentation and the velocity ratio relative to the depth also includes two extra computations, which are elaborated below.

First, the total sedimentation due to the deepening is determined by multiplying the sedimentation rate of the control volume `i` by the length ($\Delta\xi_i$) and the width ($\Delta\psi_i$) of that control volume (lines 78–92). Therefore, the length and width of every control volume has to be determined, which is done with the function `txt2metres`, which is elaborated in Appendix F.2 (lines 79–82).

Second and last, the velocity ratios give a clear overview of the effect of the depth on the flow velocity per VMS. The figure on this determination is such, that various VMSs can be taken out; which are comparable to each other via the input parameter `stations`. The velocity ratios are compared to $d = 12.0\ m$, instead of the base case (d_0)[1], because of large deviations in the velocity profiles after opposing a new bathymetry. This is further elaborated in Section 11.4. Moreover, only the residual flow is taken into account in this computation for clarity of the figures.

---

[1]Therefore, `dmin=2;` (line 96) is added: $d = 12.0\ m$ is at the second place of the depth-matrix.

```matlab
1   function processing(PoI,Nbegin,Nend,left,right,stations)
2   if strcmp(PoI,'basecase')
3       map1='Base_case';map2='Base_case';
4       runs=1;
5   elseif strcmp(PoI,'east')
6       map1='East_Exp';map2='option';
7       runs=2;
8       pname={'Without expansion','With expansion'};
9   elseif strcmp(PoI,'south')
10      map1='South_Exp';map2='option';
11      runs=2;
12      pname={'Without expansion','With expansion'};
13  elseif strcmp(PoI,'deepening')
14      map1='Deepening';map2='depth';
15      runs=9;
16      pname={'$d_{0}$','12.0','12.5','13.0','13.5','14.0','14.5','15.0','15.5'};
17  end
18  N=Nend-Nbegin+1;     % number of control volumes
19
20  %%  Data
21  if strcmp(PoI,'basecase')
22      [data.zb,data.s]=sediment4(map1,map2,Nbegin,Nend);
23      data.loc=MOHID_data(map1,map2,'Channel',Nbegin,Nend+1);
24  else
25      for i=1:runs
26          [data(i).zb,data(i).s]=sediment4(map1,[map2,num2str(i-1)],Nbegin,Nend);
27          data(i).loc=MOHID_data(map1,[map2,num2str(i-1)],'Channel',Nbegin,Nend+1);
28      end
29  end
30
31  %%  Computations
32  % % % determine the velocity characteristics
33  res=zeros(runs,N+1);dres=zeros(runs-1,N+1);
34  mean_flood=zeros(runs,N+1);dflood=zeros(runs-1,N+1);
35  mean_ebb=zeros(runs,N+1);debb=zeros(runs-1,N+1);
36  for i=1:runs
37      for j=1:N+1
38          res(i,j)=(data(i).loc(j).res(11).data);
39          ifflood=zeros(length(data(1).loc(1).var(1).data),1);
40          for k=1:length(data(1).loc(1).var(1).data)
41              if k<length(data(1).loc(1).var(1).data)
42                  if data(i).loc(j).var(13).data(k)<data(i).loc(j).var(13).data(k+1)
43                      ifflood(k)=1;
44                  else
45                      ifflood(k)=0;
46                  end
47              else
48                  ifflood(k)=ifflood(k-1);
49              end
50          end
51          ebb=zeros(length(ifflood),1);flood=zeros(length(ifflood),1);
52          for k=1:length(ifflood)
53              if ifflood(k)
54                  flood(k)=data(i).loc(j).var(11).data(k);
55              else
56                  ebb(k)=data(i).loc(j).var(11).data(k);
57              end
58          end
59          mean_flood(i,j)=mean(flood(flood>0));
```

```matlab
60          mean_ebb(i,j)=mean(ebb(ebb>0));
61      end
62      if i>1
63          dres(i-1,:)=res(i,:)-res(1,:);
64          dflood(i-1,:)=mean_flood(i,:)-mean_flood(1,:);
65          debb(i-1,:)=mean_ebb(i,:)-mean_ebb(1,:);
66      end
67  end
68
69  % % % determine sedimentation rate per control volume
70  zb=zeros(N,runs);
71  for i=1:N
72      for j=1:runs
73          zb(i,j)=data(j).zb(i);
74      end
75  end
76
77  if strcmp(PoI,'deepening')
78      % % % determine the total sedimentation
79      [dxi,dpsi]=txt2metres('delftstations_channel.txt',...
80          'delftstations_TFN.txt',...
81          'delftstations_TFS.txt',...
82          Nbegin,Nend);
83      vol=zeros(runs,N);
84      tot_vol=zeros(runs,1);
85      ratio_vol=zeros(runs,1);
86      for i=1:runs
87          vol(i,:)=data(i).zb.*dxi.*dpsi;
88          tot_vol(i)=sum(vol(i,:),2);
89      end
90      for i=1:runs
91          ratio_vol(i)=tot_vol(i)./tot_vol(1);
92      end
93
94      % % % determine velocity ratio
95      res_ratio=zeros(runs,N+1);
96      dmin=2;
97      for i=1:runs
98          res_ratio(i,:)=res(i,:)./res(dmin,:);
99      end
100 end
```
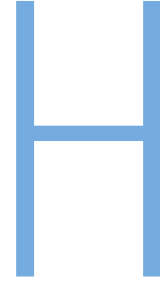
H
Control volumes

To determine the sedimentation rate, the channel is divided into N control volumes (Figure H.1) by determining the net sediment transport at the boundaries of these locations in both x- and y-direction. Each control volume is the area between two Virtual Measurement Stations (VMSs) in the channel and perpendicular to this direction two VMSs at the tidal flats (Figure H.2b). The location of certain channel sections and the control volumes are summarised in Table H.1.

For every control volume, the frame of reference is rewritten in such a way that the axes are parallel and perpendicular to the flood-ebb directions; the ξ-axis is parallel to the main flow direction in the channel, and the ψ-axis is perpendicular to this. The angle the frame of reference of the control volumes make to the Cartesian frame of reference (x, y-axes) is determined using the VMSs in the channel (Appendix F.1). Moreover, the in- and outflow at the channel boundaries are rewritten to a frame of reference specific to that boundary, where the ξ-axis is perpendicular, and the ψ-axis is parallel to the boundary (Figure H.2b).

VMSs	Control volumes	Section name of the channel
1–7	1–6	West of the current port area
8–12	7–11	Current port area
13–16	12–15	Possible expansion area (East)
17–20	16–19	Channel section in north-south direction
21–24	20–23	Natural widening of the main channel
25–29	24–28	Natural deeper section of Canal Principal
30–31	29–31	Canal del Toro
32–47	32–46	Outer Channel

Table H.1. Noticeable sections of the navigation channel.
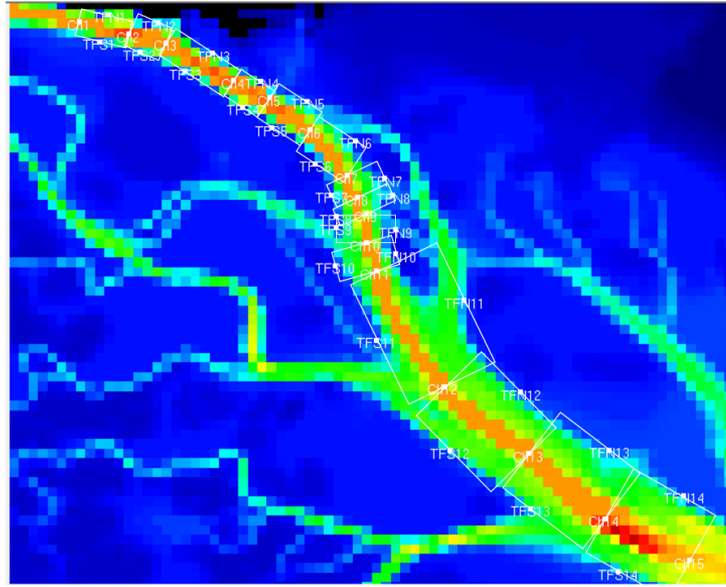
Figure H.1. Control volumes along the main channel in the port area.

From the sediment transport through the borders of the control volumes, the sedimentation rate of the control volumes can be determined according to the Exner equation (Equation 5.3), which is a mass balance equation. Because of the orientation of the control volumes, the sediment transport through the border between two control volumes – hence channel-to-channel sediment transport – is determined solely based on the sediment transport in ξ-direction[1]. For the sediment transport between the control volume and the surrounding tidal flats holds that it is solely determined on the sediment transport in ψ-direction[2].

Because the MOHID-model itself is not calibrated, the constants in the equations do not have to be calibrated either. To still be able to tell something about the processes and the outcomes of the model, all results are compared to the initial state; the current situation[3].

---

[1]Sediment transport at the channel boundary in ψ-direction is not taken into account due to the fact that it is parallel to the control volume's boundary, by definition.

[2]Sediment transport at the tidal flats boundary in ξ-direction is not taken into account due to the fact that it is parallel to the control volume's boundary, by definition.

[3]So the calibration constants m in Equation 5.2a and c_b in Equation 5.3 are not determined.
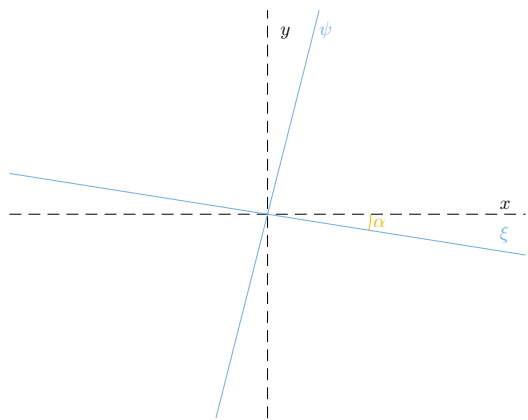
(a) Conversion from x, y-axes to ξ, ψ-axes.
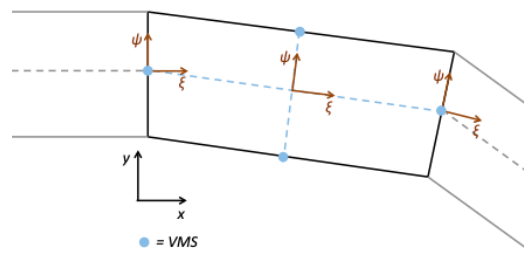
(b) ξ, ψ-axes for a control volume.

Figure H.2. Changing frame of reference.

Sediment transport relation

The sedimentation relation as proposed by Gómez et al. (2010) is based on the assumption that sediments do not move until a certain velocity; the critical velocity. This mainly holds for coarser sediments, which indeed are stable under lower flow conditions. First of all, the sediments in the Bahía Blanca estuary are mainly fines, and so easily transported – especially with the high flow velocities in the Bahía Blanca estuary.

Nevertheless, Gómez et al. (2010) used this method and thereby it is interesting to see what the impact of using a threshold flow velocity is on the sediment transport, keeping in mind the accuracy of the flow velocities obtained with the MOHID-model. To do so, some small calculations are performed using orders of magnitude of the input parameters. To start with, the sediment transport relation (Equation 5.2b) as described by Bagnold (1963) is again stated in Equation I.1 for convenience.

$$s = \beta \left(u_{100}^3 - u_{100,c}^3 \right) \qquad\qquad \text{I.1}$$

The next step is to determine β, which is a function of D_{50} (Equation I.2 as suggested by Gómez et al. (2006)). Because D_{50} is very small – hence the sediments are fines, $\mathcal{O}(10^{-4}\ m)$ – its influence on β is negligible: $\beta \approx 3.547$.

$$\beta = -4.057 D_{50} + 3.547 \qquad\qquad \text{I.2}$$

Following up, the flow velocities have to be determined. First the flow velocity one metre above the bed (u_{100}) is determined, using the law of wall (Equation I.3), where is assumed that the depth-averaged velocity – the output of MOHID – is located half way the total depth.

$$\frac{u_i}{\ln \left(z_i / z_0 \right)} = \frac{u_j}{\ln \left(z_j / z_0 \right)} \qquad\qquad \text{I.3}$$

Furthermore, z_0 is taken as 1% of the total depth for this estimation. The maximum depth-averaged flow velocities are stated by e.g. Campuzano et al. (2014) to be $\bar{u} = \mathcal{O}(1\ ms^{-1})$. With a depth of 13.5 metres, the flow velocity at one metre above the bed is given by $u_{100} \approx 0.43\ ms^{-1}$.

Last, the critical flow velocity ($u_{100,c}$) is determined with the critical shear stress (τ_c^*) using the relation described by Yalin (1977), which is given by Equation I.4b. With this critical shear stress, the critical flow velocity can be determined according to Li and Amos (1995) as shown in Equation I.4a.

$$u_{100,c} = \sqrt{\frac{\tau_c^*}{\frac{1}{2}\rho_w}} \qquad\qquad \text{I.4a}$$

in which

$$\tau_c^* = \theta(\rho_s - \rho_w)gD_{50} \qquad\qquad \text{I.4b}$$

For $\rho_s = 2620\ kgm^{-3}$, $\rho_w = 1020\ kgm^{-3}$[1], $D_{50} = 800\ \mu m^2$[2], $g = 9.81\ ms^{-2}$, and $\theta \approx 0.035$ (Shields parameter) holds that $u_{100,c} \approx 0.023\ ms^{-1}$.

Furthermore, the smaller the D_{50} becomes, the smaller its influence on the critical flow velocity. Therefore, a multiple layer system does not make a difference, whereas the smaller grain sizes will have even less impact on the critical flow velocity. A distinction between e.g. clay, silt, and fine sand in their sediment transport relations will not result in significant differences and so is negligible.

Due to the power n in Equation I.1, which equals 3, the influence of the critical flow velocity relative to the flow velocity at one metre above the bed becomes negligible: the difference between taking a threshold flow velocity or not is $\mathcal{O}(10^{-2}\ \%)$ on the sediment transport. Due to the fact that the MOHID-model does not meet such an accuracy, an easier sediment transport relation is used for the computations of the output data (Equation 5.2a): $s = mu^n$.

In addition, even though the critical velocity can be determined with the available input, the MOHID-model is not calibrated and so does not produce quantitative usable depth-averaged velocities. Thereby, these velocities cannot be compared to the critical velocities. All in all, enough reason to use the more simple sediment transport relation given by Equation 5.2a.

---

[1]Salt water has a slightly higher density than fresh water; $\rho_w = 1000\ kgm^{-3}$.
[2]Based on Table 2.1 in which it is the biggest D_{50}.

J
Residence time

An important parameter in terms of hydrodynamic regimes characterisation and subsequently for water quality is the residence time i.e. the length of time required to evacuate water from the estuary and to replace it with new water (Pierini et al., ND). The residence time is the time for a substance to flow trough a volume. The time scales related to the exchange of water between the ria and the ocean depends on freshwater runoff, tidal range, bathymetry and the wind regimes. Using the residence time of a part of an estuary or ria, sediment transport or ecological processes can be assessed. This property indicates the length of time that the compounds carried by the water are subject to the ecological processes within the estuary. Studies where performed to investigate the overall particle residence time in the Bahia Blanca Ria.

In the research of Pierini et al. (ND) obtained for each of the defined boxes in the estuary range from 12 to 77 days for every season of the year and wind forcing combinations. As was described by Pierini (2007), at the head of the Principal Channel, net transport in deeper areas is seawards while in shallower waters is landwards. especially in the most inside area of the ria. This is the area on the west side of the port which has, as assessed in Pierini et al. (ND), has a long residence time. In this area the sediment is almost trapped in the ria. So sedimentation is likely to occur, especially in case of dredging a channel in this area.

K
Caisson calculations

To ensure the caisson is stable and has sufficient strength, calculations are made. These calculations are done with the help of MATLAB, so the dimensions can be easily changed during the process. The MATLAB-script can be found in Script K.1. In this appendix the calculations in MATLAB are explained step by step. The results are found in Figure K.6.

Different stages of the caisson are taken into consideration. These steps are based on the design method described by Voorendt et al. (2011).

K.1. Dimensions of the caisson

The dimensions of the caisson were changed all the time during the design phase. The final dimensions of the conceptual design of the caisson are illustrated in Figure K.1.

The determination of the length of the caisson is based on a design assumption given by Voorendt et al. (2011), which states that the length of a caisson can be assumed to be three times its width. In this case the length of the caisson is assumed to be 84 metres. The amount of inner walls in the longitudinal direction is considered to be equal to six.

All the input values can be found in Script K.1 (lines 4-45). These values are based on estimations and optimisation in the design process.

K.2. Draught

The maximum allowable draught can be calculated by setting the mass of the caisson equal to the mass of the displaced water. However, in order to calculate the draught of the caisson the depth
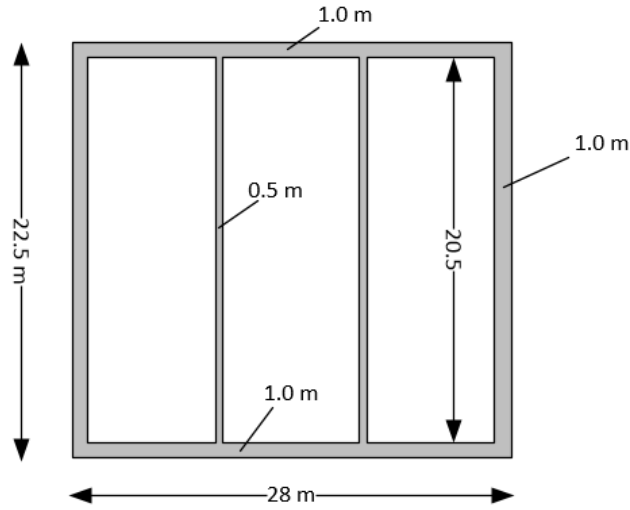
Figure K.1. The dimensions of the caisson.

of the channel has to be taken into consideration. Because the draught of the caisson is limited by this depth and a required keel clearance, the mass of the displaced water (buoyancy force F_b (Equation K.1a)) needs to be large enough to manage the mass of the caisson, but also needs to be small enough in order to meet the boundary condition: the depth of the ria.

In other words, the caisson cannot be too heavy or otherwise the channel would become too narrow. However, by adjusting the width (b) of the caisson the mass of the displaced water can be increased, which will result in a smaller draught.

Because the assumption is made that the length of the caisson is three times its width, Equation K.1a can be simplified to Equation K.1b.

$$F_b = bld\rho_w \qquad \text{K.1a} \qquad\qquad F_b = 3b^2 d\rho_w \qquad \text{K.1b}$$

The weight of the caisson is calculated with Equation K.2. Notice that the volume of the inner walls are depended on the number of inner walls and their width. A calculation of the volume and the volume of the inner walls can be found in Script K.1, lines 31-53.

$$F_w = (lbh - (l - 2t_w)(b - 2t_w)(h - t_f - t_t) + V_{innerwalls})\rho_c \qquad \text{K.2}$$

By combining Equations K.1b and K.2 the width can be calculated, because all other parameters are known. Taking into account the maximum depth of the channel with the keel clearance, the maximum draught can be set at 14.5 m (Script K.1 lines 56-57).

Knowing the draught of the caisson it is possible to calculate the p_{max}. This value gives the maximum pressure by the water at the caisson, which engages at the bottom of the caisson.

$$p_{max} = \rho_w d \qquad \text{K.3}$$

In this formula the draught is given by d, and ρ_w is the density of water.

K.3. Shear

Knowing the draught of the caisson it is possible to check the shear force criterion. This check is needed to ensure the floor and walls to be of sufficient thickness in order to resist the shear forces. First the forces due to the water pressure are calculated, which is done with Equation K.4a. The shear forces are dependent on the draught of the caisson, which is equal to 13.2 m in this case (Appendix K.2).

To calculate the maximum shear force of the floor of the caisson, the weight of the walls and of the roof have to be calculated (Equation K.4b).

$$F_{shear,wall} = 0.5\rho_w d^2 \qquad \text{K.4a} \qquad\qquad F_{shear,floor}t_w h_w \rho_c + 0.5bt_t\rho_c \qquad \text{K.4b}$$

Following the design method, it should be noticed that half of the roof is taken into account for the maximum shear force, because only half of the roof will contribute to the maximum shear force of the floor at the left bottom corner.

An overview of the numbers of the maximum shear forces are illustrated in Figure K.2a. These numbers are checked by the Dutch standard TGB 1990 to determine the shear stress criterion (Voorendt et al., 2011). Assumed is that in this case the Dutch standard is sufficient enough for Argentina.

$$\tau = \frac{3F_{shear}}{2bt} \leq \tau_1, \quad \text{where} \quad \tau_1 = 0.4f_b + 0.15\sigma_{bmd} \qquad \text{K.5}$$

- F_{shear} = shearforce
- b = Useful concrete thickness (0.9 m)
- t = thickness of floor or wall (both 1.0 m)
- f_b = design tensile strength (1.47 MPa)
- σ_{bmd} = calculation value of concrete pressure stress

The value of f_b can be found with help of Table K.1 using concrete class C35/45. The characteristic axial tensile strength divided by 1.5 gives the value of the design tensile strength. Furthermore, σ_{bmd} is found using Equation K.6.

$$\sigma_{bmd} = \frac{F_{normal}}{1000b} \qquad \text{K.6}$$

Script K.1 (lines 62-79) calculates whether all the requirements are met. For the shear stress the requirements are not met (Figure K.6). Therefore, extra measures are needed, e.g. the use of shear reinforcement.

K.4. Moments

In order to check whether the caisson can resist the moments, the moments first have to be calculated. This check has to be done at the critical places, which are at the bottom corners of the caisson and in the middle.

Concrete class (old)	$f_{ck,cil}$ [MPa]	f_{ck} [MPa]	f_{cm} [MPa]	f_{ctm} [MPa]	$f_{ctk,0.05}$ [MPa]	$f_{ctk,0.95}$ [MPa]	E_{cm} [GPa]
C12/15 (B15)	12	15	20	1.6	1.1	2.0	27
C20/25 (B25)	20	25	28	2.2	1.5	2.9	30
C30/37 (B35)	30	35	38	2.9	2.0	3.8	33
C35/45 (B45)	35	45	43	3.2	2.2	4.2	34
C45/55 (B55)	45	55	53	3.8	2.7	4.9	36
C55/67 (B65)	55	67	63	4.2	3.0	5.5	38

Table K.1. Characteristics of concrete (Voorendt et al., 2011).

(a)Shear forces in the caisson.

(b)Moments in the caisson.
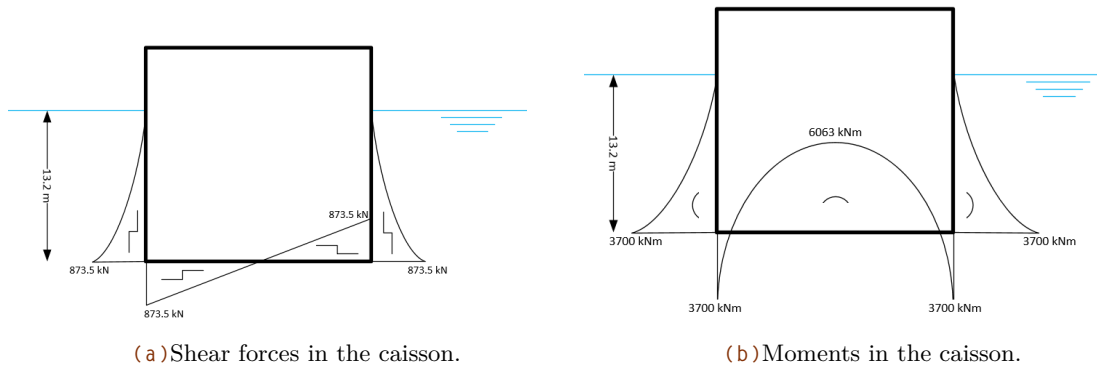
Figure K.2. Forces in the caisson.

PoDeA

The moments in the bottom corner can be found with the shear force acting on the walls; the distance from this shear force to the middle of the bottom plate is equal to the arm of the moment resulting from this shear force. Using Equation K.7a, which results in Equation K.7b, the moment in the middle of the bottom of the caisson can be calculated.

$$M = \frac{1}{8}ql^2 \qquad \text{K.7a} \qquad\qquad M = \frac{1}{8}q(b - t_w)^2 \qquad \text{K.7b}$$

It must be noticed that q is equal to the water pressure p_{max} as calculated in Appendix K.3 (Equation K.3) minus the concrete density. Distance l is the same as the width of the caisson minus the wall thickness.

An overview of all the moments is given in Figure K.2b. The water pressure acting at the bottom of the caisson results in a negative bending moment. However, in practice, the inner walls can contribute as reduction of the maximum negative bending moment. This has to be investigated in a later stage since it is left out of the scope.

When the bending moments are determined, the thicknesses of the bottom plate and the side walls can be calculated. In Equation K.8 the equation is illustrated which is used to this.

$$t = \sqrt{\frac{M_d}{150bf_b}} \qquad\qquad \text{K.8}$$

The thicknesses calculated in this formula are compared with the actual thickness in order to check whether the thicknesses comply with the requirements. This is illustrated in Figure K.6, and the calculations are found in Script K.1 (lines 82-87).

K.5. Stability

In this section all the failure mechanisms during transport of the caissons are checked. The stability of floating elements depends on vertical forces, moments and dimensions of the caisson. The caisson is considered stable, when it is statically and dynamically stable.

Vertical forces

In order to establish an equilibrium, the sum of the vertical forces must be equal to zero. This means that the buoyant force has to be equal to the weight of the displaced volume of fluid; here water. A vertical equilibrium is usually reached if the element is floating, or resting on the bottom of the water body. The sum of the vertical forces is used to calculate the draught of the caisson (lines 91-92).

Equilibrium of moments

To assure the elements do not tilt in an unacceptable degree during the floating transport or the immersing procedure, elements must be designed or equipped in such a way that a rotation, caused by external factors, is corrected by a righting moment that will return the element to its original position.
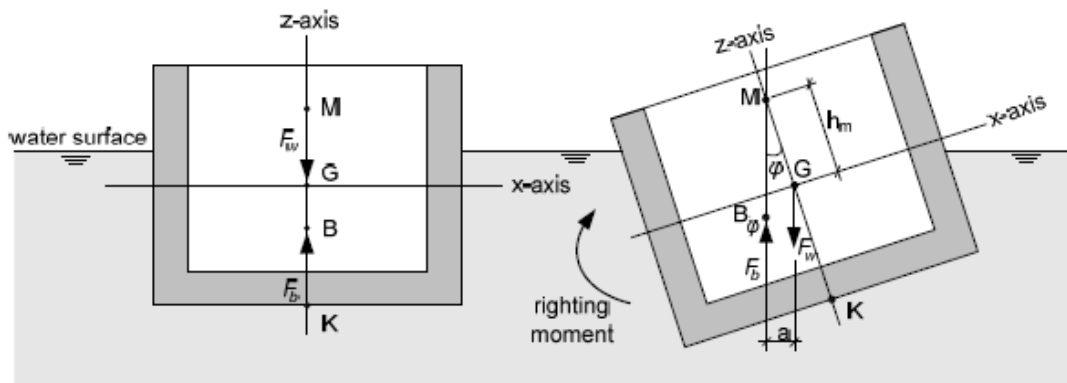
Figure K.3. Static stability (Molenaar and Voorendt, 2016).

Static stability

In the case of a caisson floating in still water, a check of moments can be sufficient. However, in this case, the static stability has to be calculated in order to say something about the stability of the floating element. Therefore, four points have to be defined:

- The centre of buoyancy: B
- The centre of gravity: G
- The metacentre: M
- Bottom of the caisson: K

The centre of buoyancy is the defined by Molenaar and Voorendt (2016) as:

> '...the point of application of the buoyant force F_b in state of equilibrium (the state in which the axis of symmetry of the element is vertical). B is therefore the centre of gravity of the displaced water.'

The centre of gravity is equal to the centre of mass of a volume; and the metacentre is defined by Molenaar and Voorendt (2016) as:

> '...the point of intersection of the axis of symmetry, the z-axis, and the action line of the buoyant force in tilted position.'

Lastly, the bottom of the caisson is the lowest point of the bottom plate.

In Figure K.3 an overview with all the different points of interest is given. In order to conclude that a caisson is statically stable, the distances between the points have to be determined. With help of Equation K.9 the distance between the centre of gravity and the metacentre can be calculated. As a criterion holds that the metacentre of a caisson has to be at least 0.5 m above the centre of gravity to be stable.

$$h_m = GM = KB + BM - KG \qquad \text{K.9}$$

The calculations done in order to determine whether the caisson is statically stable or not are presented at lines 90–102 in Script K.1.

Dynamic stability

Because during transport the caisson can be effected by wind or swell waves. It is therefore important for the caisson not to have the same natural oscillation as these waves or swell. If the caisson has the same natural oscillation this could lead to resonance and instability of the caisson.

$$T_0 = \frac{2\pi j}{\sqrt{h_m g}} \quad \text{in which} \quad j = \sqrt{\frac{I_{polar}}{A}} \tag{K.10}$$

In this formula I_{polar} is equal to the sum of I_{zz} and I_{xx}, and A is the surface in the vertical cross-section.

During these calculation no attention was paid to the inner walls, because they lead to a higher I_{polar}, and therefore a larger T_0. A high value of T_0 would increase the dynamic stability the calculation without these is sufficient enough. The MATLAB-script can be found in Script K.1 (lines 103-111).

K.6. Stability during immersing

Also the static stability during the immersing of the caisson has to be checked. The situation is slightly different than the situation during transport, because some extra ballast (water at the bottom of the caisson) will increase the draught of the caisson. However, the moment of inertia will be decreased considerably, which means a lower value of BM. This results in a smaller value of GM and therefore the caisson will be less stable. The calculations for static stability during immersing are illustrated in Script K.1 (lines 113 - 129). To do this calculation only 10 cm of water inside the caisson is considered.

K.7. Finishing

When the caisson has been transported to its final location, two different calculations on the stability have to be done. One when it just hits the ground, with water on both side and the second with water on one side, and soil on the other side. Three different types of possible failure will be checked. First the horizontal stability so the caisson doesn't move in this direction. When the stability on that front is confirmed. The moment equilibrium is checked for both situations. Last but not least, the bearing capacity of the subsoil needs to be checked. This is equal for both situations. We assume the groundwater level to be two meters below surface.

Shear criterion

In the first situation water is on both sides, and no soil is present on either side. The difference between the forces on either side of the caisson should not exceed the vertical forces multiplied with a friction coefficient.

$$\sum H < f \cdot \sum V \tag{K.11}$$
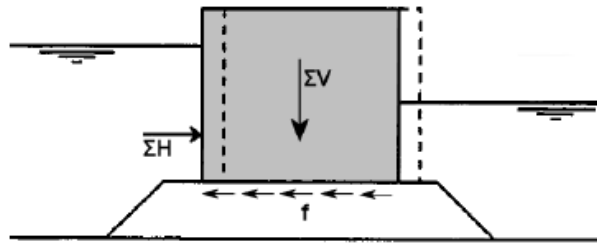
Figure K.4. Shear criterion.

For the first situation, this leads to:

$$H_L = \frac{1}{2} \cdot \rho_w \cdot h^2 = \frac{1}{2} \cdot 10 \cdot 22.5^2 = -2595 \; kN \qquad \text{K.12}$$

$$H_R = \frac{1}{2} \cdot \rho_w \cdot h^2 = \frac{1}{2} \cdot 10 \cdot 20.5^2 = 2153 \; kN \qquad \text{K.13}$$

The coefficient factor is assumed to be 0.5 (Voorendt et al., 2011). Since $\sum H = 1120 \; kN$ and by adding Equation K.12 and Equation K.13 it is shown that $\sum V = 422 \; kN$, we know that $\sum H < f \cdot \sum V$. So the caisson will not be pushed off in any direction.

In the end situation, more forces act on the caisson. In lines 139–144 of the MATLAB code, these forces are calculated. The final force on the structure is calculated in line 146. In the function "weightcheck", defined in line 237, the actual check is done. The structure has sufficient weight to withstand the horizontal forces. Also in the end phase.

Turnover criterion

The turnover criterion considers the moment equilibrium of the caisson, see Figure K.5. According to this criterion rotational stability is achieved if the following condition is met:

$$\frac{\sum M}{\sum V} \leq \frac{1}{6} \cdot b \qquad \text{K.14}$$

In which $\sum M$ is the total moment on the caisson, $\sum V$ is the total of the vertical forces acting on the caisson and b is the width of the structure. In lines 139–144 all these forces are defined. In line 150 these forces are multiplied by there distance from the bottom. The function "rotationcheck", defined in line 245, checks if the condition Equation K.14 is met.

In the first situation the sum of the moments is calculated in line 149. In line 165 the function is called using this as one of the parameters. For the final situation the sum of the moments is calculated in line 150. For both situations the MATLAB-script calculated the condition Equation K.14 to have been met.
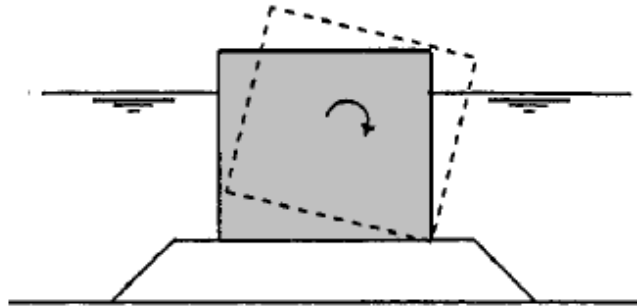
Rotational stability.

Bearing capacity subsoil

The soil is not strong enough to withstand the forces on the caisson. The soil underneath the caisson needs improvement. This is not within the scope of our design, so this would need further investigation.

K.8. Outcomes

The outcomes of the MATLAB-script are illustrated in Figure K.6.

```
The moment in the corners is 3700.6771
The moment in the middle is -6063.2001
The draught is 13.2148
The clearance is 2.2852 m
The walls thickness is sufficient 0.9559
The floor thickness is sufficient 0+1.2236i
ERROR, Shear is too much 1.4553 < 0.73175 N/mm2
ERROR, Shear is too much 1.4375 < 0.73353 N/mm2
Static stable 1.6926
Dynamic stable 21.7128
During immerging: Static stable 1.3852
This is stable in the end phase  0.11572
This is stable in the building phase  -0.38374
This is rotary stable in the end phase  -0.093976
This is rotary stable in the building phase  -4.1281
```

Figure K.6. Results of the MATLAB-script.

Script K.1. Designing the caisson.

```
1  clc;
2  clear all;
3
```

```matlab
4  % % % % % % % % % Parameters
5  global maxdepth;
6  global maxwallt;
7  global b;
8  maxdepth = 15.5 - 1;
9  maxwallt = 0.5;
10 %thickness
11 tw = 1.0;
12 tt = 1.0;
13 tb = 1.0;
14
15 %Basic layout
16 h = 22.5;
17 hw = h-tb-tt;
18 b = 28;
19 l = 3*b;
20
21 %Rho
22 rhoC = 25;
23 rhoW = 10;
24 rhoS = 20;
25 rhoSd = 18;
26
27 %Other
28 g = 9.81;
29 waterincaisson = 0.1;
30
31 % Inner walls (Longitudinal)
32 a = 2;
33 lt = l-2*tw;
34 ht = hw;
35 t = 0.5;
36
37 Vt = t*lt*ht;
38
39 % Inner walls (transverse)
40 c=6;
41 lt2 = b-2*tw-a*t;
42 ht2 = hw;
43 t2 = 0.5;
44
45 Vt2 = t2*lt2*ht2;
46
47 %Volume
48 Vvol = l*b*h;
49 Vleeg = (l-2*tw)*(b-2*tw)*(hw);
50 Vc = Vvol-Vleeg + a*Vt + c*Vt2;
51
52 Weight = ((Vc*rhoC)+(Vvol-Vc)*rhoS)/1000;
53 MaxFh = 0.5*Weight;
54
55
56 % % % % % % % % Draught check
57 depth = ((Vc*rhoC)/(rhoW*b*l));
58 Pmax = depth*rhoW;
59
60
61 % % % % % % % % Moments at the bottom
62 % Force left
63 Fl = 0.5 * depth^2 *rhoW;
```

```matlab
64   % Force beneath
65   FO = tw*hw*rhoC + b*tt*0.5*rhoC;
66
67   % % % % % % % % Shear forces
68   fb = 1.47;
69   sigma1 = FO/(0.9*1000);
70   sigma2 = Fl/(0.9*1000);
71
72   % Walls
73   tauw = 3*Fl/(2*0.9*tw*1000);
74   tau1 = 0.4*fb + 0.15*sigma1;
75
76   % Bottom
77   taub = 3*FO/(2*0.9*tb*1000);
78   tau2 = 0.4*fb + 0.15*sigma2;
79
80
81
82   % Calculating moments
83   Arm = (depth - 0.5*tb)/3;
84   Moment1 = Arm*Fl;
85   fprintf("The moment in the corners is " + num2str(Moment1) + "\n")
86   Moment2 = Moment1 - 1/8*(depth*rhoW-rhoC)*(b-tw)^2;
87   fprintf("The moment in the middle is " + num2str(Moment2) + "\n")
88
89
90   % % % % % % % % Static stability
91   Fw = Vc * rhoC;
92   depth = ((Vc*rhoC)/(rhoW*b*l));
93
94   KG =((Vvol*0.5*h) -(Vleeg*((0.5*hw)+tb))+Vt*a*(0.5*ht+tb))/Vc;
95   KB = 0.5*depth;
96
97   Iyy = l*b^(3)/12;
98   Vuw = l*b*depth;
99   BM = Iyy/Vuw;
100
101  GM = KB+BM-KG;
102
103  % % % % % % % % Dynamic stability
104  Ixx = (tb*b^(3)/12)+(tt*b^(3)/12) + 2*(hw*tw^3/12 + hw*tw*(0.5*b-0.5*tw)^2);
105  Izz = b*tb^3/12 + b*tt^3/12 + b*tb*(KG-0.5*tb)^2 + b*tt*((h-KG)-0.5*tt)^2 ...
106      + 2*(tw*hw^3/12+ hw*tw*(tb+0.5*hw-KG)^2);
107
108  Ip = Ixx+Izz;
109  Ac = b*h-(b-2*tw)*hw;
110  j = sqrt(Ip/Ac);
111  T0 = 2*pi*j/(sqrt(GM*g));
112
113  % % % % % % % %  Static stability during immersing
114  Vw = waterincaisson*(l-2*tw)*(b-2*tw);
115  Fw = Vc * rhoC + Vw *rhoW;
116  depthi = ((Fw)/(rhoW*b*l));
117
118  KGi =((Vvol*0.5*h)*rhoC -(Vleeg*((0.5*hw)+tb)*rhoC)+Vt*a*(0.5*ht+tb)*rhoC ...
119      +((tb+0.5*waterincaisson)*Vw*rhoW))/(Vc*rhoC+Vw*rhoW);
120  KBi = 0.5*depthi;
121
122  Icaisson = l*b^(3)/12;
123  Icomp = lt*((b-2*tw-a*t)/(a+1))^3/12;
```

```
124  Iyyi = Icaisson -(a+1)*Icomp;
125  Vuwi = l*b*depthi;
126  BMi = Iyyi/Vuwi;
127
128  GMi = KBi+BMi-KGi;
129
130
131  %%%%%%%%Horizontal forces
132  % Soil pressure
133
134  q = 22;
135  ka = 1/3;
136  x = 2.0;
137
138  %Pressures at +7.00 m
139  H2 = -1/2*rhoW*h^2;
140  H3 = q*ka+0.5*ka*rhoSd*x^2;
141  H4 = q*ka;
142  H5 = ka*rhoS*(h-x);
143  H6 = H3*(h-x);
144  H7 = 1/2*rhoW*(h-x)^2;
145  %Calculate the sum of the pressures
146  phe = H2+H3+H4+H5+H6+H7;
147  phb = H2+H7;
148  % Calculate the moments acting on the caisson
149  sm1 = H2*1/3*h + H7*1/3*(h-x);
150  sm2 = H2*1/3*h-H3*(h-2/3*x)-H4*(h-1/2*x)+H5*(1/3*h)+H6*1/2*(h-x)+H7*1/3*(h-x);
151
152
153
154
155  % % % % % % % % checks
156  depthcheck(depth)
157  walltcheck(tw, Moment1, 150, 27)
158  floortcheck(tb, Moment2, 150, 27)
159  shearwall(tauw,tau1)
160  shearbottom(taub,tau2)
161  staticstability (GM)
162  dynamic(T0)
163  staticstabilityimmerging (GMi)
164  weightcheck(phe, Weight, 'end');
165  weightcheck(phb, Weight, 'building');
166  rotationcheck(Weight, sm2, 'end');
167  rotationcheck(Weight, sm1, 'building');
168
169
170  function y = staticstability (x);
171  if  x < 0.5
172     fprintf("ERROR,Static unstable " + x + "\n")
173  else
174     fprintf("Static stable " + x + "\n")
175  end
176  end
177  function y =dynamic (x);
178  if x < 4
179     fprintf("ERROR, Resonance " + x +"\n")
180  else
181     fprintf("Dynamic stable " + x + "\n")
182  end
183  end
```

```matlab
184
185  function y = staticstabilityimmerging (x);
186  if   x < 0.5
187      fprintf("ERROR,During immerging: Static unstable " + x + "\n")
188  else
189      fprintf("During immerging: Static stable " + x + "\n")
190  end
191  end
192
193  function y = shearwall(tauw,tau1)
194  if (tauw > tau1)
195      fprintf("ERROR, Shear is too much " + tauw +" < "+ tau1 + ' N/mm2\n')
196  else
197      fprintf("The sheaar criterion is; " + tauw +' kN\n')
198  end
199  end
200  function y = shearbottom(taub,tau2)
201  if (taub > tau2)
202      fprintf("ERROR, Shear is too much " + taub +" < "+ tau2 + ' N/mm2\n')
203  else
204      fprintf("The sheaar criterion is; " + taub +' kN\n')
205  end
206  end
207
208  function y = walltcheck(wallt, Moment1, ConPara, fb)
209  q = sqrt(Moment1/(1.0*ConPara*fb));
210  if q > wallt
211      fprintf("ERROR, The wall thickness is too thin " + num2str(q) + '\n')
212  else
213      fprintf("The walls thickness is sufficient " + num2str(q) + "\n")
214  end
215  end
216
217  function y = floortcheck(floort, Moment2, ConPara, fb)
218  q = sqrt(Moment2/(1.0*ConPara*fb));
219  if q > floort
220      fprintf("ERROR, The floor thickness is too small " + num2str(q) + '\n')
221  else
222      fprintf("The floor thickness is sufficient " + num2str(q) + "\n")
223  end
224  end
225
226  function y = depthcheck(x)
227  global maxdepth
228  if x > maxdepth
229      fprintf("ERROR, the draught is to big " + x + "\n")
230  else
231      fprintf("The draught is " + x + "\n")
232  end
233  draught = maxdepth + 1 - x;
234  fprintf("The clearance is " + draught + " m\n")
235  end
236
237  function y = weightcheck(a, b, fase)
238  if(abs(a/b)>0.5)
239      fprintf("ERROR: This is not stable in the  " + fase + "phase " + a/b + '\n')
240  else
241      fprintf("This is stable in the " + fase + " phase  " + a/b + '\n')
242  end
243  end
```

```
244
245  function y = rotationcheck(a, c, fase)
246  global b;
247  if(abs(c/a)> (1/6*b))
248      fprintf("ERROR: This is not rotary stable in the " + fase + c/a + '\n')
249  else
250      fprintf("This is rotary stable in the " + fase + " phase  " + c/a + '\n')
251  end
252  end
```

L
Channel lay-out

In order to have a correct port lay-out, several nautical aspects have to be checked. One of the main nautical aspects is the lay-out of the approach channel, which has to meet several criteria. In the new situation the approach channel has to be widened to allow larger vessels to enter the port; Suezmax instead of Panamax. The most important characteristics of both vessels are given in table Table L.1. All formulas and values are derived from the most recent guideline for the design of approach channels: Harbour Approach Channels Design Guidelines (MarCom WG-121, 2014).

To calculate the required width of the channel, MarCom WG-121 (2014) is used. The total width is made up of four components for the main part of the channel and some additional width in the

---

[1] In general the largest vessels in the port are dry bulk carriers
[2] In general the largest vessels in the port are dry bulk carriers
[3] 60,000 -- 80,000 DWT
[4] 120,000 -- 180,000 DWT
[5] This draught will depend on the conditions in the channel

	Current design vessel (Panamax)	New design vessel (Suezmax)
Freight type	Dry Bulk / Container [1]	Dry Bulk / Container [2]
Tonnage	52,500 DWT [3]	160,000 DWT[4]
Capacity	5,000 TEU	10 000 - 15 000 TEU
Length	294.1 m	350 m
Draft	12.0 m	20.1 m (66 ft) (max) [5]
Beam (B_s)	32.3 m	50 m

Table L.1. Main characteristics of current and new design vessel.

port area. The total formula is given by Equations L.1a and L.1b.

$$W = W_{BM} + \sum W_i + W_{BR} + W_{BG} \qquad \text{L.1a}$$

$$W = 2W_{BM} + 2\sum W_i + W_{BR} + W_{BG} + \sum W_p \qquad \text{L.1b}$$

In which W_{BM} equals the basic width, W_i is the additional width, W_{BR} the bank clearance and W_P the required separation width for a two-way channel.

In Tables L.2 to L.4 an overview of the required dimensions is given. In the following subsections the values of the dimensions are explained. The channel is characterised as an inner channel in the port area.

L.1. Basic Width (W_{BM})

The basic width of a channel is determined by the manoeuvrability of the vessel. In general, bulk carriers have a poor manoeuvrability and container vessels have a moderate manoeuvrability. Therefore, a larger channel width is required for a bulk carrier of $1.8B_s$, and a smaller basic width for a container vessel of $1.5B_s$.

L.2. Additional Width (ΣW_i)

The additional required width is determined by several environmental and other navigation factors, which are explained in the following sections.

Vessel speed – The velocity of the vessel inside the port area is below 12 kn. Therefore no additional width is required to account for the velocity.

Prevailing winds – The average wind speed is 12 kn, with 50% coming from the fourth quadrant (W-NW-N). Therefore, no additional width is required to account for the wind (unknown, nown).

Currents – Most of the currents are caused by the tide and are therefore directed along the channel, instead of crossing the channel. The highest current velocity in the port is 1.27 ms^{-1} which is caused by the ebb current. This equals 2.47 kn, therefore the additional width required for the long-currents is $0.1B_s$ and $0.2B_s$ for the cross-currents (NEDECO, 1983).

Aids to navigation – Since VTS is available, the aids to navigation is considered to be good and therefore no additional width is required.

Bed characteristics – The bed material is soft everywhere along the channel. Therefore an additional width of $0.1B_s$ is required.

Significant waves – The waves, taking into account the frequency and intensity of the winds, do not reach more than 0.65 metres and a period of 3.0 seconds (unknown, nown). Therefore no additional width is required.

Depth of the waterway – The depth of the waterway near the port is smaller than 1.15 times the draught. Therefore the required additional width equals $0.4B_S$.

Cargo hazard – The cargo visiting the port mainly exists of containers and dry bulk having a low hazard. Therefore no additional width is required.

L.3. Bank clearance (W_{BR})

The width required for the bank clearance depends on the speed of the vessel and the edge of the channel. The vessels have a moderate velocity and the edges of the channel are steeper than 1:10, so the required bank clearance is $0.5B_s$. Since there are two banks, a total of $1.0B_s$, is required for the channel.

L.4. Passing distance (W_P)

The passing distance is the distance required between two passing vessels in case of a two-way channel. Since the vessels have a moderate speed, the additional distance would be $1.4B_s$.

L.5. Other distances

Clearance for moored ships – Since the vessels are moored along the channel, instead of a separate basin, additional width is required between the sailing vessels and the moored vessels. The velocity of the ships inside the port area has to be limited to $4kn$, to have a separation distance of $2.0B_s$.

Turning area – As a large proportion of the vessels will call the port area close to the entrance, it could be beneficial to add an additional turning basin or relocate the current basin. In conceptual lay-outs the required radius of the turning basin equals LOA; $r = LOA$.

Basin – As alternative, a mooring basin can be included in the design. As a rule of thumb, the width of a basin equals $4 - 5B_s + 100\ m$. For the Suezmax this would equal 300 to 350m. In case of long basins, it is desirable for ships to be turned in the basin. This would lead to a basin width of $L_s + B_s + 50\ m$. For the Panamax this would lead to approximately $380\ m$.

L.6. Summarized

All values above are summarised in Table L.2. The values of the current channel are checked with the values of the current channel.

It can be concluded that the current channel in the port area behind buoy 31 is wide enough for the expansion on the east side. In case of a Suezmax vessel and a single-way channel the required width equals $280\ m$, with a mooring vessel on one side of the channel.

Moreover, for the south expansion it should be noted that for a single-way channel with double mooring a total width of 380m is required. It should be noted that the LNG tanker should be removed in this scenario, or the channel should be widened. This is mainly because the LNG tanker does not have a zero risk.

One way channel	Formula		Panamax		Suezmax	
	Container	Dry bulk	Container	Dry bulk	Container	Dry bulk
Length			294.1	294.1	285	285
Beam			32.3	32.3	50	50
Basic width	1.5	1.8	48.45	58.14	75	90
Additional width						
Vessel speed	0	0	0	0	0	0
Prevailing winds	0	0	0	0	0	0
Prevailing cross current	0.2	0.2	6.5	6.5	10	10
Prevaling long current	0.1	0.1	3.2	3.2	5	5
Aids to navigation	0	0	0	0	0	0
Bed characteristics	0.1	0.1	3.2	3.2	5	5
Significant waves	0	0	0	0	0	0
Depth of the waterway	0.4	0.4	13	13	20	20
Hazard	0	0	0	0	0	0
Bank clearance (green)	0.5	0.5	16	16	25	25
Bank clearance (red)	0.5	0.5	16	16	25	25
Total	3.3	3.6	**107**	**116**	**165**	**180**
Mooring clearance	2	2	65	65	100	100
Total with single mooring	5.3	5.6	**172**	**180**	**265**	**280**
Double mooring	2	2	65	65	100	100
Total with double mooring	7.3	7.6	**235**	**245**	**365**	**380**

Table L.2. Total widths for different options for one-way channel.

Two way channel	Formula		Panamax		Suezmax	
	Container	Dry bulk	Container	Dry Bulk	Container	Dry Bulk
Length			294.1	294.1	285	285
Beam			32.3	32.3	50	50
Seperation distance	1.4	1.4	45	45	70	70
Total			**258**	**278**	**400**	**430**
Mooring clearance	2	2	65	65	100	100
Total with single mooring			**325**	**345**	**500**	**530**
Double mooring	2	2	64	65	100	100
Total with double mooring			**390**	**410**	**600**	**630**

Table L.3. Total width for two-way channel for different lay-outs.

Other dimensions	Formula		Panamax		Suezmax	
	Container	Dry bulk	Container	Dry bulk	Container	Dry bulk
Length			294.1	294.1	285	285
Beam			32.3	32.3	50	50
Turning basin radius	LOA		294	294	285	285
Mooring basin width	$4B_s + 100 \ m$		229	229	300	300
Mooring basin width	$B_s + LOA + 50 \ m$		376	376	385	385

Table L.4. Summary of additional dimensions.

In Tables L.3 and L.4 the required dimensions for a two-way channel are given. As can be seen in Table L.3 the width of the channel should almost be doubled, which – according to the current freight projections – is not feasible.

For the design of the port expansion it can be beneficial to add or relocate the current turning basin. Moreover, in some of the designs it is verified whether is feasible to add a mooring basin instead of jetties. The dimensions used in these designs are derived from these tables.

At last, it should be determined whether the channel in the port area should be a one-way or two-way channel. According to the current width ($\pm 350 \ m$) the channel inside the port is designed for a two way Panamax vessel with single mooring clearance. This would mean that the channel inside the port should have the same service level and therefore have a two channel width up to the turning basin. In case of a Suezmax vessel, this would mean a width of 630 m.

M

Multicriteria
Analysis

In the following chapter of the appendix the background of the MCA is given. The MCA is used to define the best design in a neutral way. At first, the weights of the different criteria are determined (Appendix M.1), followed by the scores of all the criteria for both expansion areas in Appendix M.2. This combination gives the MCA determining the best design.

Moreover, the costs have to be found to determine the feasibility of the design, as the combination of the score and the costs are summarised in the cost/benefit analysis in Appendix M.3, determining the most feasible design; this chapter ends with the optimisation (Appendix M.4).

M.1. Weight determination

These criteria are a combination of insights of the following parties; PoDeA, Pablo Arecco (UBA) and Gerardo Bessone (CGPBB). The results of these insights are presented in Table M.1.

M.2. Determination of scores

In the following subsections the scores for the different criteria for the MCA are determined.

Criteria	Weights			
	Pablo Arecco	PoDeA	Gerardo Bessone	Rounded
Environmental impact	15	15	20	17
Nuisance to flora and fauna	12	10	13	12
Change in morphology	3	5	7	5
Safety (vessel collision)	15	20	10	15
Quay–vessel	10	15	5	10
Vessel–vessel	5	5	5	5
Expansion possibilities	15	15	15	15
Space for berthing	4	6	5	5
Space hinterland	5	3	5	4
Space for channel expansion	3	2	3	3
Space for clustering	3	4	2	3
Channel siltation	20	20	15	18
Operational factors	35	30	40	35
Connection with port area	5	6	10	7
Connection with hinterland	15	7	10	11
Clustering	10	5	10	8
Nautical access	5	5	3	5
Total Navigation distance	0	2	2	1
Length of viaduct	0	5	5	3
Total	100	100	100	100

Table M.1. Determination of the weights for the MCA.

East expansion

In the following subsection the scores for the east alternatives are determined and explained.

Environmental impact

Nuisance to flora and fauna The vulnerable natural reserve is located at the south-west of the port, hence this reserve is not directly affected. However, the more tidal flats are reclaimed the lower the score. Since it is assumed that these tidal flats are still of great importance to the flora and fauna (although not necessarily protected). Also, the larger the change in the environment, the lower the score.

Change in morphology As stated previously, it is assumed that all changes in morphology are undesired. The largest changes in morphology tend to occur in the designs cutting off the side channel. In the designs it is assumed that the quay structures are impermeable and therefore divert the flow.

Safety

Vessel-infrastructure collision In all the alternatives at the east bank, apart from the third alternative, the marine infrastructure is in line with the approach channel, increasing the risk of a collision between a vessel and jetty.

	Alternative 1	Alternative 2	Alternative 3	Alternative 4
Turning basin terminal	5	5	5	3
Berthing aligned	1	1	5	1

Vessel-vessel collision It is assumed that a turning basin inside the channel increases the chances of a vessel-vessel collision. Also the concentration of the traffic increases the risk of a vessel-vessel collision.

	Alternative 1	Alternative 2	Alternative 3	Alternative 4
Turning basin	5	5	3	3
Traffic concentration	5	5	5	5

Expansion possibilities

Space for berthing The space for berthing is determined by the available remaining space along the channel. Due to the presence of the basin, alternative 3 has a lot of remaining space for berthing locations. Whereas the other alternatives utilise most of the available space along the approach channel.

Space hinterland It is determined how many elements have space to expand. For example, in alternative 1, all terminals have space available in the hinterland to expand the terminals in the future, leading to the highest score; 5/5.

Space for channel expansion All the alternatives have space left on the west bank for future widening of the channel, if required. Therefore all the alternatives obtain the full score.

Space for clustering The space for clustering is determined by the space in between different terminals to prevent future scattering of terminals.

Increase in siltation

In general, it is expected that a lot of sedimentation occurs close to the parts of the port lay-out which are not aligned with the channel. Therefore, it is expected that only alternative 3 will have a large increase in sedimentation rates; i.e. maintenance dredging. Unfortunately, due to the coarse grid of the MOHID-model its application is limited.

Operational factors

Connection with port area In general the better the connection with the current port, the higher the efficiency of the total port as services can be shared for example.

Connection with hinterland The quality of the hinterland connection is determined by the the required length of the connection and likeliness of bottlenecks. The lowest scores are given to the designs with only a link to the current port, as there is a higher risk of bottlenecks.

Clustering The more clustered the total port lay-out the better it is. For example to share services.

Nautical access The nautical access is a measure to determine the easiness for ships to moor at the different jetties and quay walls. In general it is assumed to be more difficult for the alternatives without a turning basin in its vicinity. Moreover, the proximity of the sharp bend reduces the score.

Navigation distance Although of minor importance, the total navigation distance can be reduced with 5% of the total distance in the port by adding a turning basin halfway.

Length of viaduct It is assumed that these conveyor belts cause a large inconvenience to the efficiency of the port and hence lead to a low score.

In the following table the full score of the MCA is shown. As can be seen alternative 2 has the highest score and is therefore the best design, neglecting the costs.

As can be seen in Table M.2 the main differences between the alternatives are:

- Nuisance to flora and fauna
- Quay - vessel safety
- Siltation
- Clustering of the alternatives

Moreover, it is obvious from this MCA that Alternative 2 is the best design.

South expansion

In the following subsection the scores for the south alternatives are determined and explained.

Criteria	Weight	Alternative 1 Score	W x S	Alternative 2 Score	W x S	Alternative 3 Score	W x S	Alternative 4 Score	W x S
Environmental impact	17								
Nuisance to flora and fauna	12	5	60	4	48	3	36	2	24
Change in morphology	5	2	10	2	10	3	15	1	5
Safety (vessel collision)	15								
Quay – vessel	10	3	30	3	30	5	50	2	20
Vessel – vessel	5	5	25	5	25	4	20	4	20
Expansion possibilities	15								
Space for berthing	5	3	15	3	15	5	25	2	10
Space hinterland	4	5	20	3	12	3	12	4	16
Space for channel expansion	3	5	15	5	15	5	15	5	15
Space for clustering	3	3	9	2	6	3	9	2	6
Siltation	18	5	90	5	90	1	18	5	90
Operational factors	35								
Connection with port area	7	3	21	4	28	4	28	3	21
Connection with hinterland	11	3	33	3	33	4	44	4	44
Clustering	8	2	16	5	40	4	32	3	24
Nautical access	5	2	10	2	10	5	25	3	15
Total Navigation distance	1	1	1	1	1	4	4	4	4
Length of viaduct	3	1	3	4	12	5	15	5	15
Total	100		358		375		348		329

Table M.2. The full MCA for the East expansion.

Environmental impact

Nuisance to flora and fauna Although all alternatives are located outside the national reserve, the designs still have an impact on the environment. Since alternative 1 has the longest border with the national reserve its impact is considered to be the largest and therefore the lowest score.

Change in morphology For all the alternatives the channel is widened, which is assumed to give the same effects for the alternatives. In general, the widening leads to much lower velocities, both flood and ebb velocities, and therefore the gradient in flow velocity in general is less. Nevertheless, this is assumed to have a neutral impact on the environment. The elongation of the channel (as in alternative 3) has a large impact on the sedimentation rates more to the west. Therefore the elongation is assumed to have a bad environmental impact. In alternative 1 and 2, the alternatives close the entrance channel to the southern part of the tidal flats. This is assumed to have a large impact on the environment. In this study, the negative effect of the closure and elongation are assumed to be equal.

	Alternative 1	Alternative 2	Alternative 3
Elongation	3	3	1
Closure	1	1	3

Safety

Vessel-infrastructure collision The safety is based on the likelihood of a collision between a vessel and a jetty or quay wall. For the south expansion none of the mooring places is in line with the channel, so a collision between a vessel and the wall is unlikely. However, the proximity of a turning basin to a terminal increases the risk.

	Alternative 1	Alternative 2	Alternative 3
Turning basin terminal	3	3	1
Berthing aligned	5	5	5

Vessel-vessel collision It is assumed that a turning basin inside the channel and a possible concentration of traffic in the channel increases the chances of a vessel-vessel collision. For the south expansion,

	Alternative 1	Alternative 2	Alternative 3
Turning basin	3	3	3
Traffic concentration	3	1	1

Expansion possibilities

Space for berthing The space for berthing is determined by the available remaining space along the channel. In general it is stated that the alternatives with possibilities in both directions have the higher score. Moreover, alternative 1 requires the least additional measures to utilise the remaining part to the west.

Space hinterland It is determined how many elements have space to expand. As expected this is the main disadvantage of the design on the south side, as the narrow stretch limits future expansion possibilities.

Space for channel expansion All the alternatives require a widening of the channel, however alternative 1 has for example space for future widening of the channel towards the east, whereas the other designs are very limited to widen the channel in the future.

Space for clustering The space for clustering is determined by the space available to expand certain clusters of the port. For example, in design two, two-third of the clusters (dry bulk and food cluster) can expand its clusters.

Increase in siltation

In general it is expected that a lot of sedimentation occurs close to the parts of the port lay-out which are not aligned with the channel. In this case, however, all the expansion elements are aligned with the current channel. Moreover, it is tried to determine the siltation rates using the MOHID-model. According to the model the following can be concluded:

- The widening of the channel itself will not lead to higher sedimentation rates
- The elongation of the channel will lead to very high sedimentation rates in the elongated part of the channel

Operational factors

Connection with port area In general the better the connection with the current port, the higher the efficiency of the total port as services can be shared for example. Since the south development is isolated from the current port, all alternatives obtain the lowest score.

Connection with hinterland The quality of the hinterland connection is determined by the the required length of the connection and likeliness of bottlenecks. Since the hinterland connection is the same for all the designs, based on the study performed by Weyland (2009).

Clustering The more clustered the total port lay-out the better it is. For example to share services. The measure of clustering is determined by measuring the total spread of the terminals.

Nautical access The nautical access is a measure to determine the easiness for ships to moor at the different jetties and quay walls. In alternative 3 it is questionable how easy the ships can moor at the end of the navigation channel.

Navigation distance Although of minor importance, the total navigation distance can be reduced with 5% of the total distance in the port by adding a turning basin halfway.

Length of viaduct None of the alternatives has a viaduct incorporated so this is not applicable.

In the following table the full score of the MCA is shown. As can be seen alternative 2 has the highest score and is therefore the best design, neglecting the costs.

The main differences between the alternatives, according to the MCA, is caused by:

- Nuisance to flora and fauna

Criteria	Weight	Alternative 1		Alternative 2		Alternative 3	
		Score	W x S	Score	W x S	Score	W x S
Environmental impact	17						
Nuisance to flora and fauna	12	1	12	2	24	3	36
Change in morphology	5	2	10	2	10	2	10
Safety (vessel collision)	15						
Quay – vessel	10	5	50	5	50	5	50
Vessel – vessel	5	3	15	2	10	3	15
Expansion possibilities	15						
Space for berthing	5	5	25	3	15	2	10
Space hinterland	4	1	4	2	8	3	12
Space for channel expansion	3	3	9	1	3	1	3
Space for clustering	3	3	9	3	9	1	3
Siltation	18	3	54	3	54	1	18
Operational factors	35						
Connection with port area	7	1	7	1	7	1	7
Connection with hinterland	11	1	11	1	11	1	11
Clustering	8	3	24	4	32	4	32
Nautical access	5	4	20	4	20	1	5
Total Navigation distance	1	3	3	4	4	3	3
Length of viaduct	3	5	15	5	15	5	15
Total	100		268		272		230

Table M.3. The full MCA for the south expansion.

- Siltation

M.3. Cost analysis

The costs of the design are determined based on the following parameters:

- **Land reclamation**
  - Quarry material
  - Soil improvement, required for disposed dredged material
- **Capital dredging**
- **Road and railway connections**
  - Railway
  - Road
  - Viaducts
- **Marine infrastructure**
  - Viaducts
  - Quay wall
  - Jetties
  - Caisson

Again these costs are specified per expansion area, in the following sections.

Costs

Capital dredging

To determine the costs for the required capital dredging, two parameters have to be determined: (1) the volume in m^3; and (2) the price in \$ per m^3. The price per m^3 varies between 10 US\$ for large volumes ($> 6 \cdot 10^6 m^3$) and 15 US\$ for small volumes ($\pm 1 \cdot 10^6 m^3$). The volumes for the East expansion are given in Table M.4 in which the following sections are used:

Part 1 The required widening of the channel from 170 m to 270 m.

Part 2 The required widening of the channel from $270 - 350$ m to 530 m.

Turning basin The required turning basin halfway the channel for Alternative 3.

Mooring basin The mooring basin for Alternative 3.

For the South expansion, the following sections are used and the volumes are presented in Table M.5:

Part 1 The required widening of the channel from 350 m to 530 m (Alternative 1) which is required for all the alternatives or from 350 m to 630 m (Alternative 2).

Part 2 The required widening or elongation of the channel from 230 m to 630 m.

Turning basin The required turning basin halfway the channel for Alternative 3.

To calculate the required volume it is assumed that the average current depth is 4 m and has to be excavated to 9.5 m. This is derived from the bathymetry given, where it can be seen that the banks are very steep.

	Width [m]	Length [m]	Depth [m]	Volume [$\times 10^6 \ m^3$]
Alternative 1				9
Part 1	100	3,000	9.5	2.85
Part 2	220	3,000	9.5	6.27
Turning basin	-	-	-	-
Mooring basin	-	-	-	-
Alternative 2				9
Part 1	100	3,000	9.5	2.85
Part 2	220	3,000	9.5	6.27
Turning basin	-	-	-	-
Mooring basin	-	-	-	-
Alternative 3				22
Part 1	100	2,000	9.5	1.9
Part 2	260	4,500	9.5	11.11
Turning basin	192,422	-	9.5	1.82
Mooring basin	400	1,300	13.5	7.02
Alternative 4				10
Part 1	100	3,000	9.5	2.9
Part 2	260	3,000	9.5	7.41
Turning basin	-	-	-	-
Mooring basin	-	-	-	-

Table M.4. Total volumes capital dredging east (rounded to whole numbers).

	Width [m]	Length [m]	Depth [m]	Volume [$\times 10^6 \ m^3$]
Alternative 1				25
Part 1	180	4333	9.5	7.4
Part 2	280	6667	9.5	17.7
Turning basin	-	-	-	-
Alternative 2				22
Part 1	280	7500	9.5	20
Part 2	-	-	-	-
Turning basin	188.5	1	9.5	1.8
Alternative 3				24
Part 1	280	4000	9.5	10.6
Part 2	400	3000	9.5	11.4
Turning basin	188.5	1	9.5	1.8

Table M.5. Total volumes capital dredging south (rounded to whole numbers).

	Quantity [$\times 10^6\ m^3$]	Unit price [US$]	Costs [M US$]
Alternative 1	8.26		97
Quarry material	3.7	20.–	74
Soil improvement	4.6	5.–	22.8
Alternative 2	18		288
Quarry material	13.3	20.–	265.1
Soil improvement	4.6	5.–	22.8
Alternative 3	14.6		128
Quarry material	3.7	20.–	73.5
Soil improvement	10.9	5.–	54.7
Alternative 4	18.3		289
Quarry material	13.2	20.–	263
Soil improvement	5.1	5.–	25.7

Table M.6. Quantity and costs of the reclamation material for the East expansion.

	Area [m^2]	Elevation [m]	Volume [m^3]
Alternative 1	1,180,000	7	8,260,000
Alternative 2	2,545,000	7	17,815,000
Alternative 3	2,087,000	7	14609000
Alternative 4	2,611,455	7	18,280,185

Table M.7. Quantity of material needed for the East expansion.

Land reclamation

To obtain the required land for the land reclamation there are two options: use quarry material for 20 US$ per m^3; and/or use dredged material, of which it is assumed 50% can be used, requiring additional soil improvement, of 5 US$ per m^3.

In Table M.6 the total volume of reclamation material needed and the accompanying costs per alternative of the East expansion are shown. These are calculated using the areas of each design that needs reclamation, and the current height of that area.

For most of the designs, this is the most expensive aspect. The south expansion areas all differ very little in the amount of reclamation needed. These are calculated in the same way. On the south side some reclamation has already been done. The designs mostly differ in the use of this part of land. Besides this, all areas on the south need reclamation.

For the South expansion, the same can be done; the differences between these quantities is the use of the already reclaimed land. Tables M.8 and M.9 show the results of the determinations of the volumes and the costs.

Road and railway connections

The different designs differ significantly in the amount of road and railway connections that is needed. This is substantial part of the total costs, mostly because viaducts have to be build for the

	Area $[m^2]$	Elevation $[m]$	Volume $[m^3]$
Alternative 1	2,925,800	7	20,480,900
Alternative 2	2,816,700	7	19,716,900
Alternative 3	2,816,700	7	19,716,900

Table M.8. Quantity of material needed for the South expansion.

	Quantity $[\times 10^6]$	Unit price [US\$]	Costs [M US\$]
Alternative 1	20.5		225
Quarry material	8	20.–	160
Soil improvement	12.5	5.–	65
Alternative 2	20		235
Quarry material	9	20.–	180
Soil improvement	11	5.–	55
Alternative 3	20		220
Quarry material	8	20.–	160
Soil improvement	12	5.–	60

Table M.9. Quantity and Costs of the reclamation material for the South expansion.

connection with land. Especially in the south expansion this is an important part. For each of the designs the total amount of viaduct, road and railway to be constructed is calculated (Table M.10).

In case of the South expansion, this is one of the main costs, because the viaducts to the mainland are very long. For each of the alternatives, this is more or less the same and presented in Table M.11.

Marine infrastructure

For marine infrastructures only the viaducts to the possible jetties are taken into account, cost-wise. This is shown in Table M.12 for the East expansion. The South expansion does not have any marine infrastructure, and so no extra costs due to this.

Total costs

The total costs for the different alternatives for the East and South expansions are displayed in Appendices M.3 and M.3, respectively. As can be seen in the tables, the costs are very similar for each of the designs, especially when the costs of the hinterland connections are neglected.

M.4. Optimisation

In this section the Multi Criteria Analysis is done for the optimised design at the East expansion. First the scores are determined, after that the costs are calculated.

	Length [m]	Costs [M US$]
Alternative 1		19.6
Rail	9,130	12.8
Road	9,000	6.8
Viaduct	-	-
Alternative 2		52.1
Rail	11,750	16.5
Road	10,200	7.1
Viaduct	800	28.8
Alternative 3		86.2
Rail	15,500	21.7
Road	14,930	10.5
Viaduct	1,500	54
Alternative 4		118.3
Rail	13,890	19.4
Road	12,750	8.9
Viaduct	2,500	90

Table M.10. Coast of the road and railway connections for the alternatives of the East expansion.

	Length [m]	Costs [M US$]
Alternative 1		100.9
Rail	20,700	28.8
Road	20,700	14.5
Viaduct	16,000	57.6
Alternative 2		89.4
Rail	18,550	26
Road	18,550	13
Viaduct	14,000	50.4
Alternative 3		73.2
Rail	16,000	22.4
Road	16,000	11.2
Viaduct	11,000	39.6

Table M.11. Coast of the road and railway connections.

	Length [m]	Costs [M US$]
Alternative 1		67.5
Viaduct	3,750	67.5
Alternative 2		3.6
Viaduct	200	3.6
Alternative 3		-
Viaduct	-	-
Alternative 4		1.8
Viaduct	100	1.8

Table M.12. Costs of the marine infrastructure.

Operation	Unit price [US$]	Alternative 1 Quantity	Costs [M US$]	Alternative 2 Quantity	Costs [M US$]	Alternative 3 Quantity	Costs [M US$]	Alternative 4 Quantity	Costs [M US$]
Land reclamation[i]		8	97	18	287	15	135	18	290
Quarry material	20	3.5	74	13.5	265	4	80	13	265
Soil improvement	5	4.5	23	4.5	22	11	55	5	25
Capital dredging[i]	10–15	9	90	9	90	22	220	10	100
Road & rail connections[ii]			19.1		52.6		86.2		118.4
Rail track	1,400	9,130	12.8	11,750	16.5	15,500	21.7	13,890	19.5
Road	700	9,000	6.3	10,200	7.1	14,930	10.5	12,750	8.9
Viaducts	36,000	-	-	800	29	1,500	54	2,500	90
Marine infrastructure[ii]			67.5		3.6		-		1.8
Viaducts	18,000	3,750	67.5	200	3.6	-	-	100	1.8
Quay length	30,000	-	-	-	-	-	-	-	-
Jetties	22,000	-	-	-	-	-	-	-	-
Total			275		435		433		510

[i] Quantities in $\times 10^6 \ m^3$;   [ii] Quantities in m.

Table M.13. Total costs for the alternatives of the East expansion.

Operation	Unit price [US$]	Alternative 1		Alternative 2		Alternative 3	
		Quantity	Costs [M US$]	Quantity	Costs [M US$]	Quantity	Costs [M US$]
Land reclamation[i]		20.5	222.5	20	235	20	220
Quarry material	20	8	160	9	180	8	160
Soil improvement	5	12.5	62.5	11	55	12	60
Capital dredging[i]	10–15	25	250	22	220	24	240
Road & rail connections[ii]			619.5		543		429
Rail track	1,400	20,700	29	18,550	26	16,000	22
Road	700	20,700	14.5	18,550	13	16,000	11
Viaducts	36,000	16,000	576	14,000	504	11,000	396
Marine infrastructure[ii]			-		-		-
Viaducts	18,000		-		-		-
Quay length	30,000		-		-		-
Jetties	22,000		-		-		-
Total			1100		990		880
Subtotal[iii]			515		490		490

[i] Quantities in $\times 10^6$ m^3; [ii] Quantities in m; [iii] Total costs excluding hinterland connection.

Table M.14. Total costs for the alternatives of the South expansion.

Explanation MCA

The optimised alternative – Alternative I – is mostly based on Alternative 1 and Alternative 2, which means a lot of the same design aspects can be found. For this reason, a lot of numbers in the MCA are the same, especially for the nautical part of the design. In this section only the differences between the Alternative I and the other two alternatives (1 and 2) are explained.

Nuisance to flora and fauna Because the vulnerable natural reserve is located at the south-west of the port, this expansion will not affect this reserve directly. However, this alternative will have a small influence on the tidal flats, like the Alternative 2.

Space for berthing Because the quays of the optimisation is the same as the Alternative 2, these scores are considered to be equal.

Space for clustering The space for clustering is determined by the space available to expand certain clusters of the port. The optimisation is able to expand the dry bulk and food cluster easily, while it is hard to expand the container terminals. An other location for a possible expansion of the container terminal has to be found when expansion is needed.

Connection with the port area The connection with the port area can be compared with Alternative 1, where the connection with the port area is made with two roads. Because the roads both are situated at the north of Termolèctrica Luis Piedrabuena, it is scored lower than Alternative 2 (which has a road at the south of Termolèctrica Luis Piedrabuena).

Clustering The more clustered the total port lay-out, the better it is. Alternative I is more clustered than Alternative 1, but not as much as Alternative 2.

Length of viaduct The biggest difference between Alternative I and Alternative 1 is the length of the viaducts, which are reduced with at least 50%.

In Table M.15 the full score of the MCA is shown. As can be seen, Alternative I scores slightly worse than Alternative 1.

Costs

The costs of Alternative I can be found in Table M.16, which shows that the total costs for the Alternative I are 376 million US$. This is more than the costs for Alternative 1, but less than Alternative 2.

Criteria	Weight	Optimised design Score	Optimised design W × S
Environmental impact	17		58
Nuisance to flora and fauna	12	4	48
Change of morphology	5	2	10
Safety (vessel collision)	15		55
Quay - vessel	10	3	30
Vessel - vessel	5	5	25
Expansion possibilities	15		55
Space for berthing	5	3	15
Space hinterland	4	4	16
Space for channel expansion	3	5	15
Space for clustering	3	3	9
Siltation	18	5	90
Operational factors	35		98
Connection with port area	7	3	21
Connection with hinterland	11	3	33
Clustering	8	3	24
Nautical access	5	2	10
Total navigation distance	1	1	1
Length of viaduct	3	3	9
Total	100		356

Table M.15. MCA of Alternative I (East expansion).

Operation	Optimised design Quantity	Optimised design Costs [M US$]
Land reclamation		302.8
Quarry material	$9.44 \times 10^6 \ m^3$	188.8
Soil improvement	$4.56 \times 10^6 \ m^3$	22.8
Capital dredging	$9.12 \times 10^6 \ m^3$	91.2
Road and railway connections		
Rail track	$13,740 \ m$	19.2
Road	$7,710 \ m$	5.4
Viaducts	-	-
Marine infrastructure		
Viaducts	$2,700 \ m$	48.6
Total		376

Table M.16. Costs of Alternative I.

N

Plots and figures

In this appendix, the figures obtained from the hydrodynamic model MOHID are depicted. These figures are used to asses the modelled points of interest and their influence on the ria. Next to these figures, other figures of added value to the reader are presented in this appendix. These are for extra clarification of the content of the report.

N.1. Overview sediment measurements

In this section the overview of the sediment measurement locations is given, as described in Chapter 2 (Figure N.1).

Figure N.1. Locations of the sediment measurements.

N.2. Overview MOHID bathymetry

In this section an overview of the model bathymetry is given as described in Chapter 6. This bathymetry is the original bathymetry used by Campuzano et al. (2014). For this project this bathymetry is used to assess the base case and to investigate the influence of the expansion by changing this bathymetry.

N.3. River approximation

In this section the river cases as described in Chapter 5 are illustrated in the following figures. In this way a clearly image of the influence of an adaption per channel section is given if the method as used in river engineering is applicable.

For the widening case, the depth remain the same, but the width of the channel changes. Therefore the specific discharge lowers. Initially this results in higher flow velocities upstream of the widening and lower flow velocities at the place of the widening. Resulting in related sediment transport and local erosion or sedimentation as illustrated in Figure N.3.

The same but completely opposite happens in case the discharge increases at a river section, where the width stays the same. This would lead to an increase in the specific discharge, and all the graphs in Figure N.3 flip; and so the locations of the hump and pit as well.

In case of deepening, the specific discharge and the width remain the same, but the depth of the channel changes. Initially this results in higher flow velocities upstream of the deepening and decreasing flow velocities towards the downstream end of the deepening. The related sediment transport and local erosion or sedimentation are illustrated in Figure N.4

N.4. Sedimentation rates

In this section the sediment rates as described in Chapter 8 and Chapter 11 are plotted for each point of interest. Furthermore, a plot per channel section – as stated in Table H.1 – is added for the deepening of the navigation channel, to clearly present the influence of the deepening per channel section.
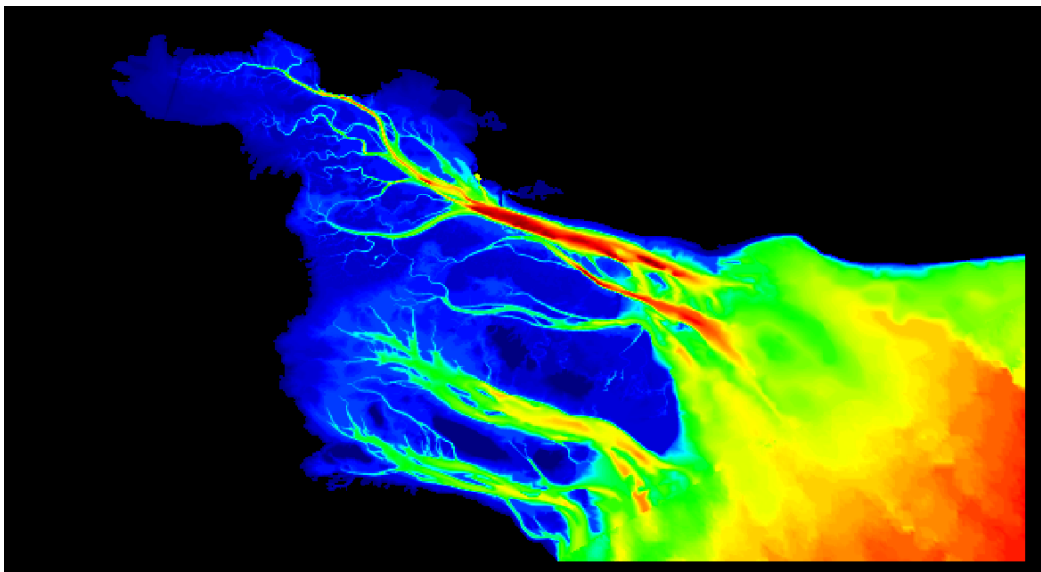
Figure N.2. overview MOHID bathymetry.

PoDeA
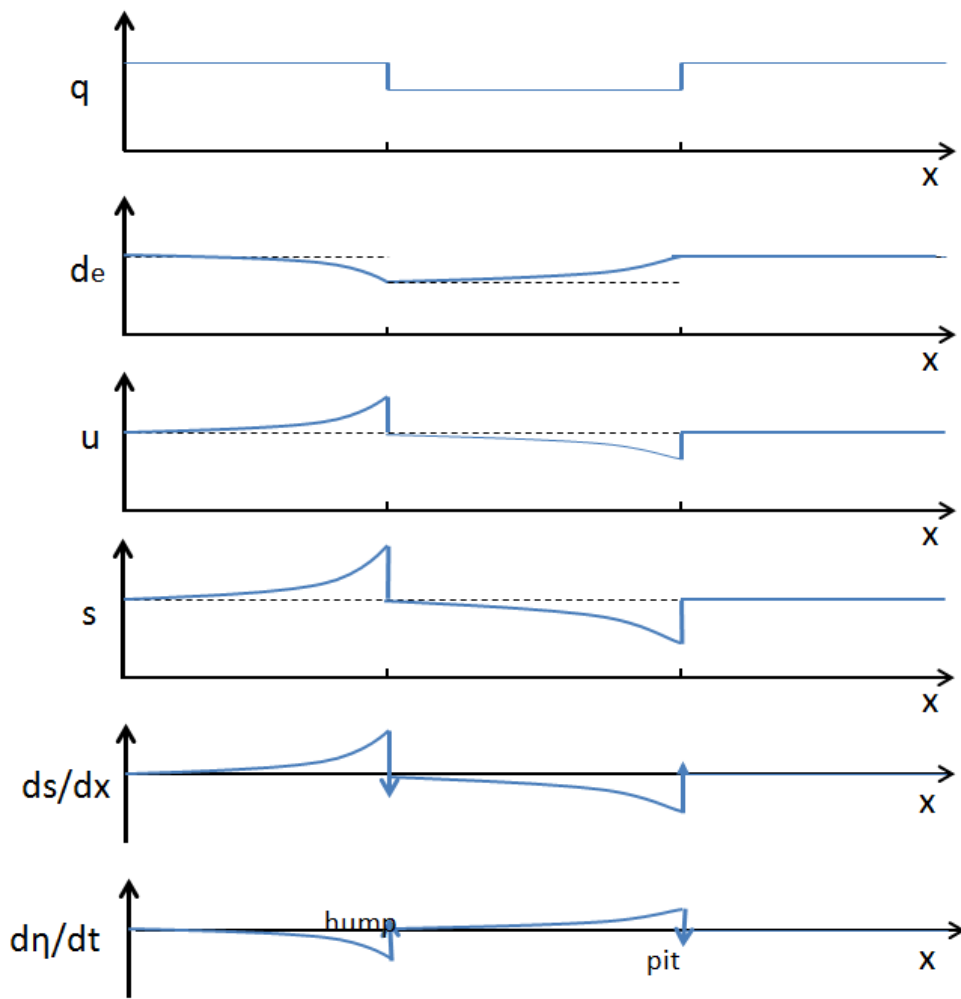
Figure N.3. Overview river case widening.
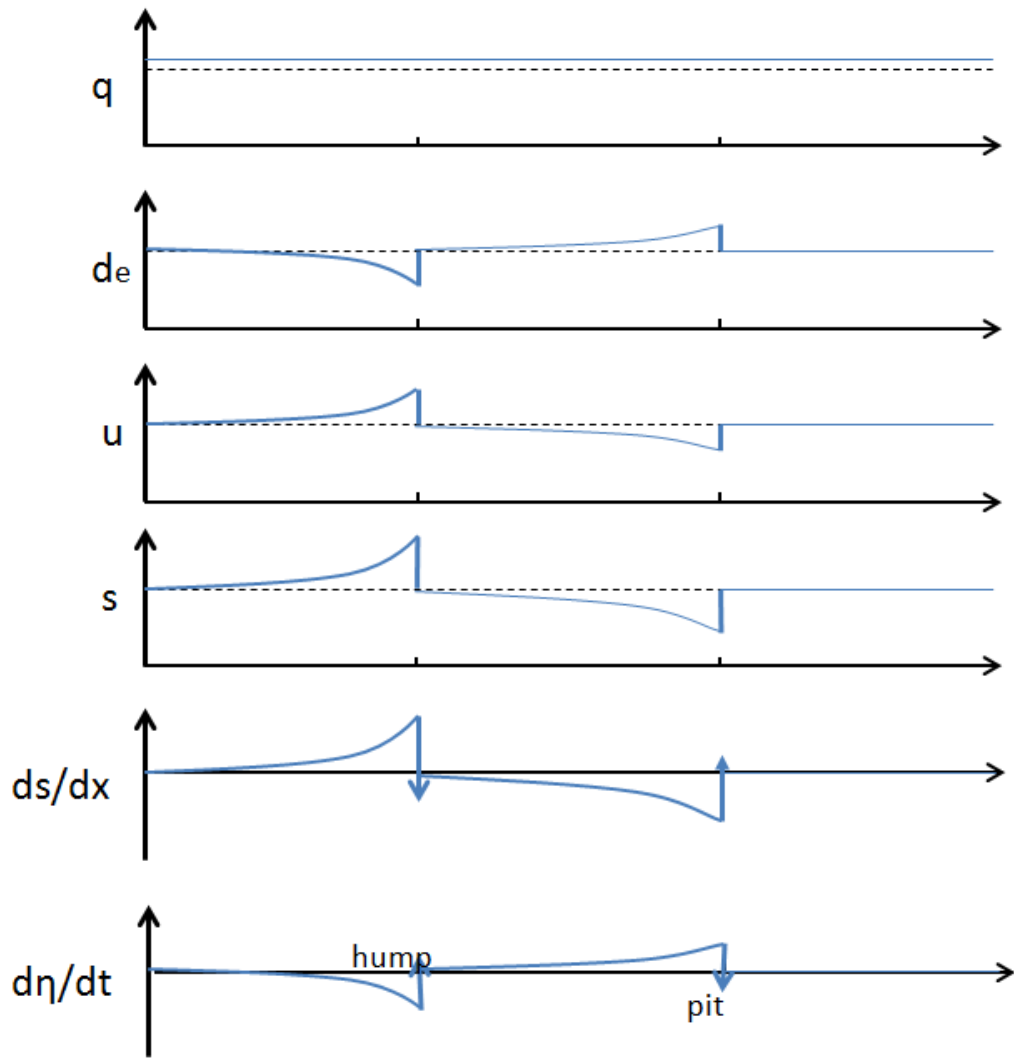
Figure N.4. Overview river case deepening.

PoDeA
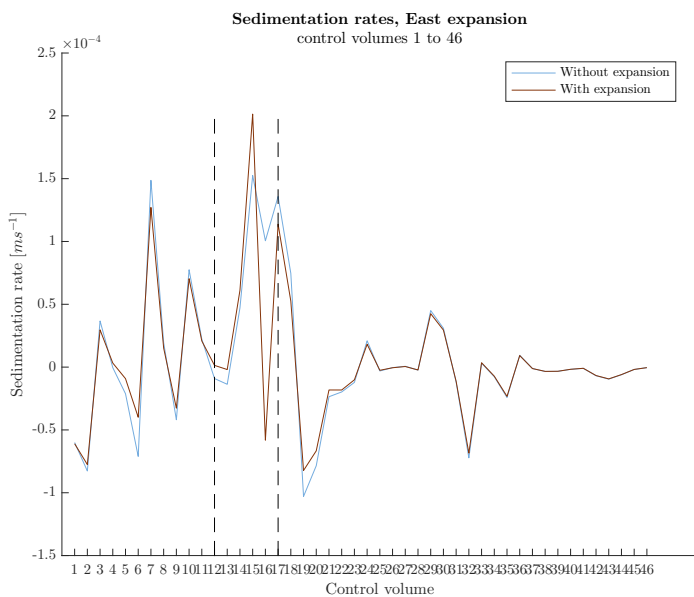
Figure N.5. Sedimentation rates East expansion.
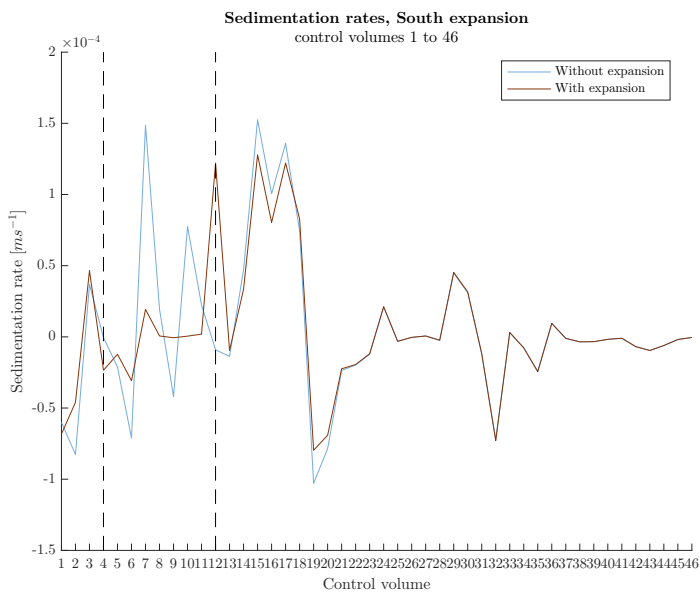
Figure N.6. Sedimentation rates South expansion.
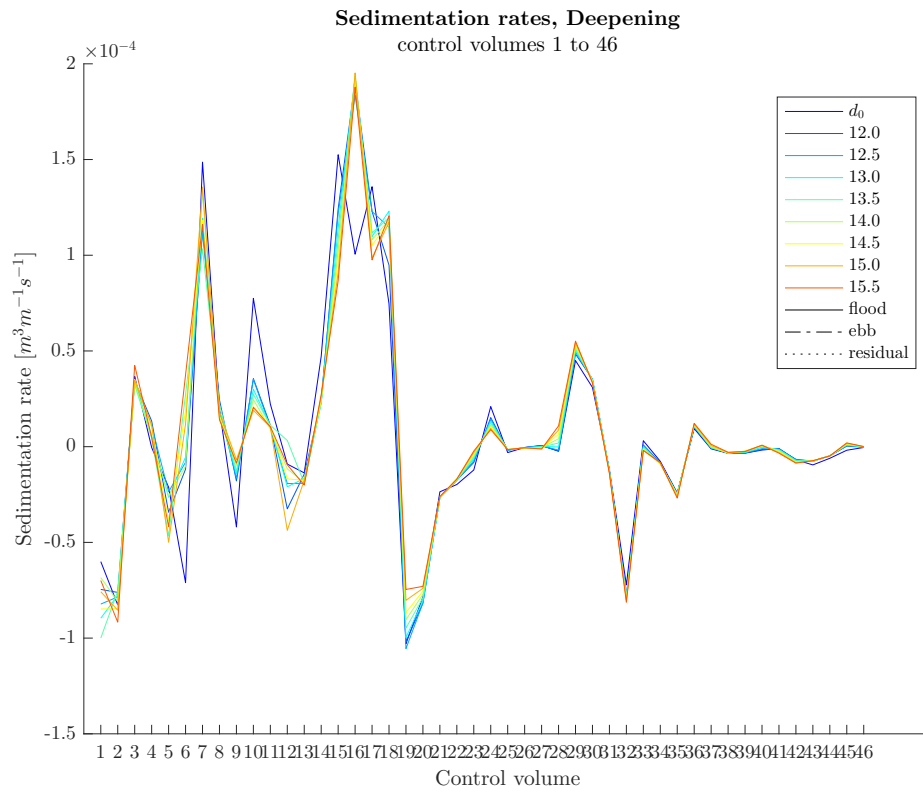
Figure N.7. Sedimentation rates deepening (Virtual Measurement Stations (VMSs) 1 – 46).
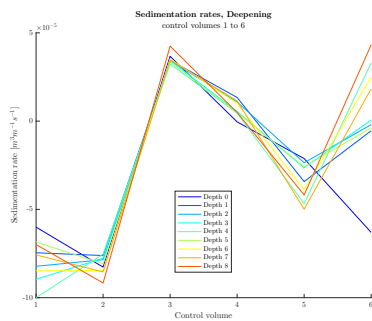
(a)West of the port area (VMSs 1 − 7).
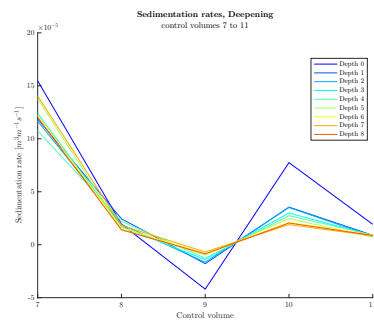
(b)Port area (VMSs 7 − 12).
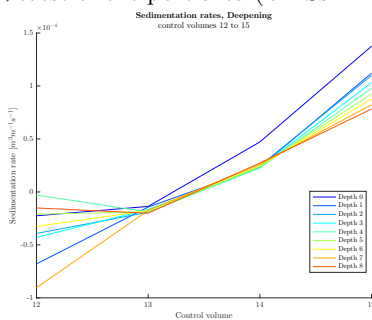
(c)Possible East expansion (VMSs 12 − 16).
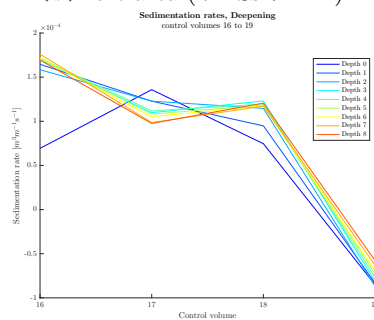
(d)North-south orientated channel section (VMSs 16 − 20).
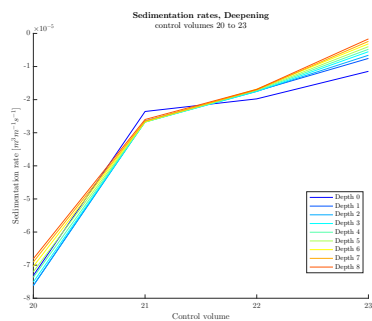
(e)Natural widening main channel (VMSs 20 − 24).
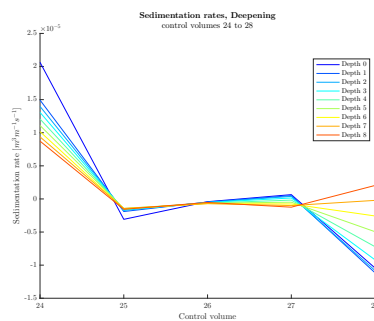
(f)Natural deeper area (VMSs 24 − 29).
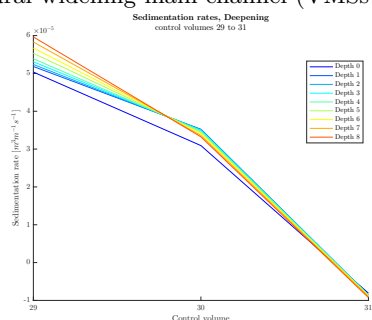
(g)Canal del Toro (VMSs 29 − 32).
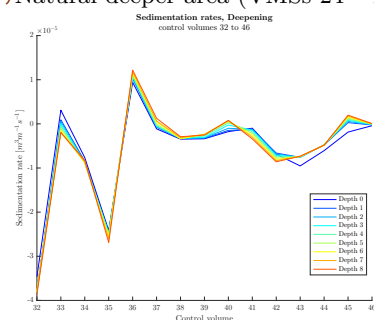
(h)Outer Channel (VMSs 32 − 46).

Figure N.8. Sedimentation rates deepening, per channel section.

0
Maps

In the following chapter larger maps of the different alternatives and final designs are available. First the conceptual designs of Chapter 4 are shown, for east and south. At last a large version of the final design is given.

0.1. East expansion
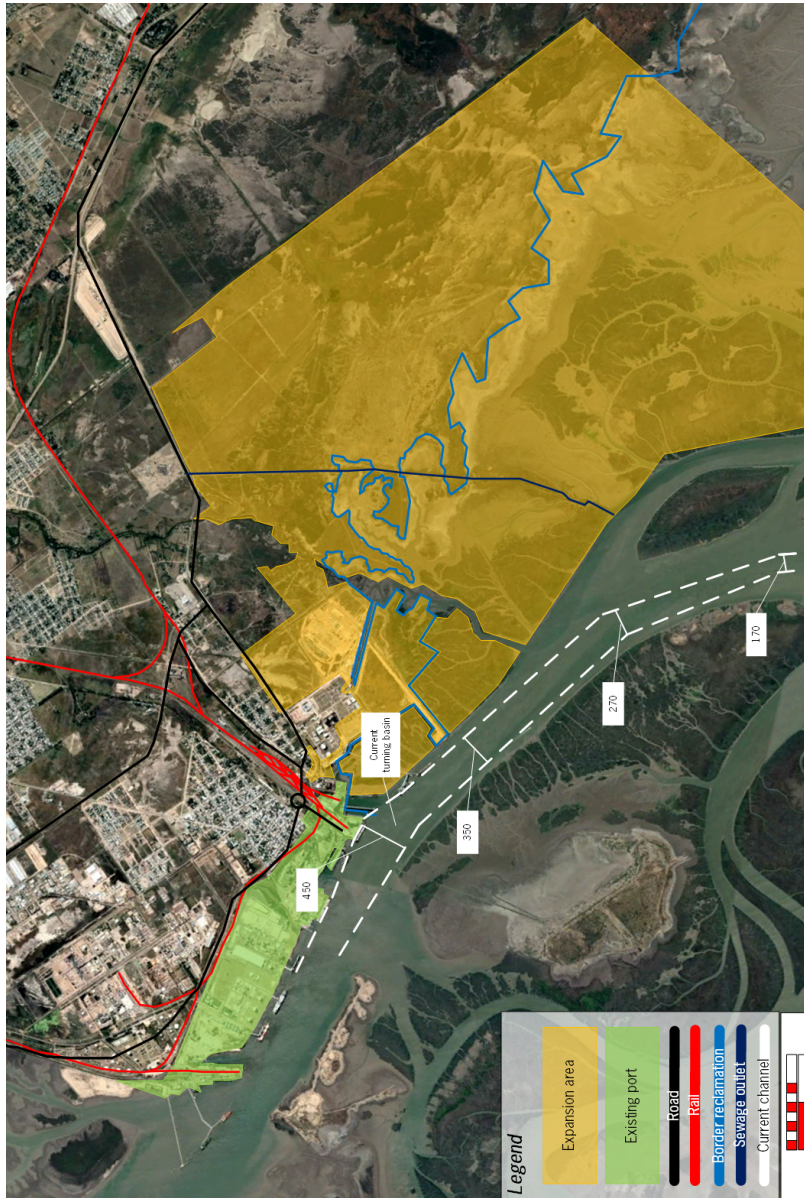
Figure 0.1. The expansion area at the east side with the existing roads, railways and navigation channel.
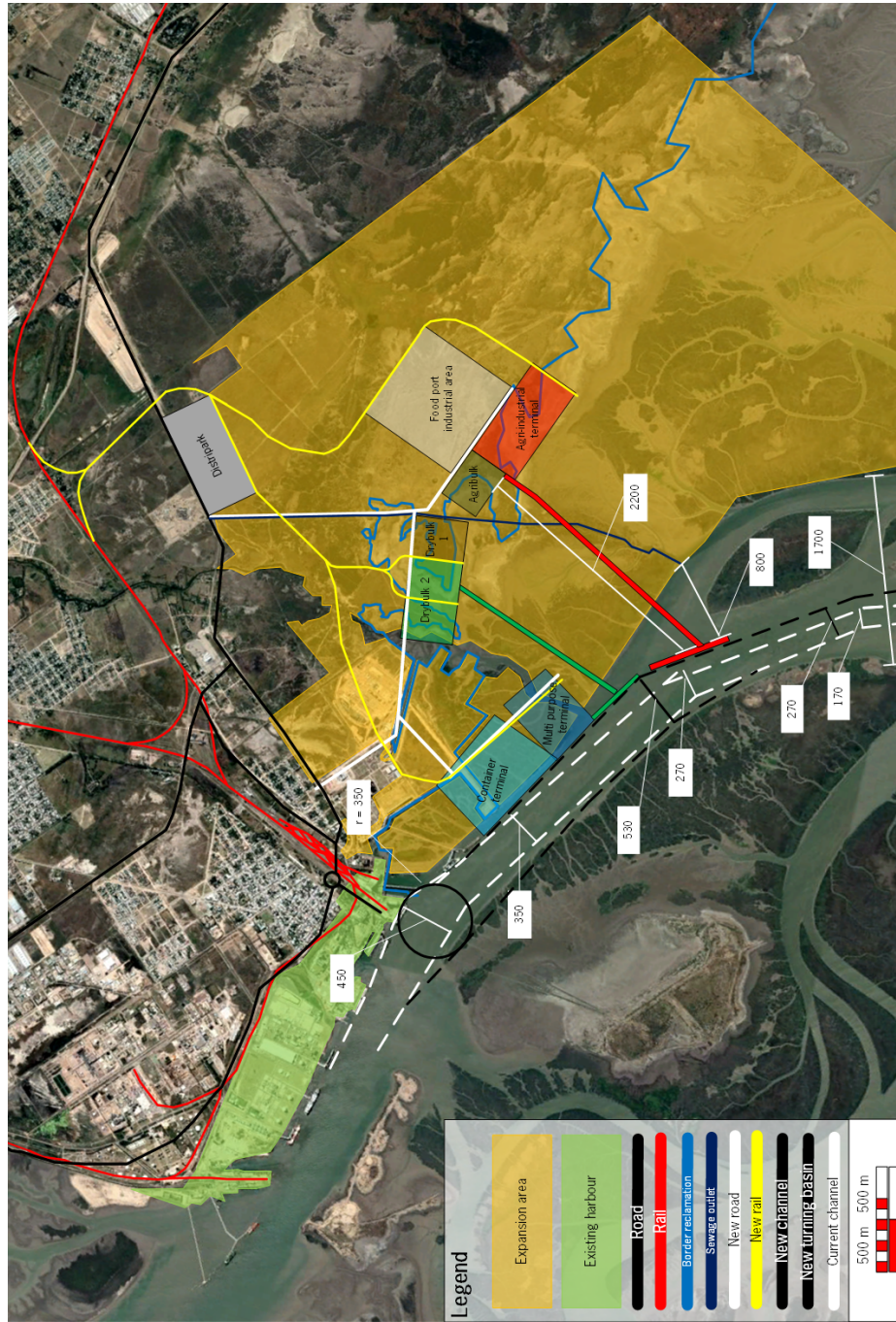
Figure 0.2. Alternative 1 for the east expansion.
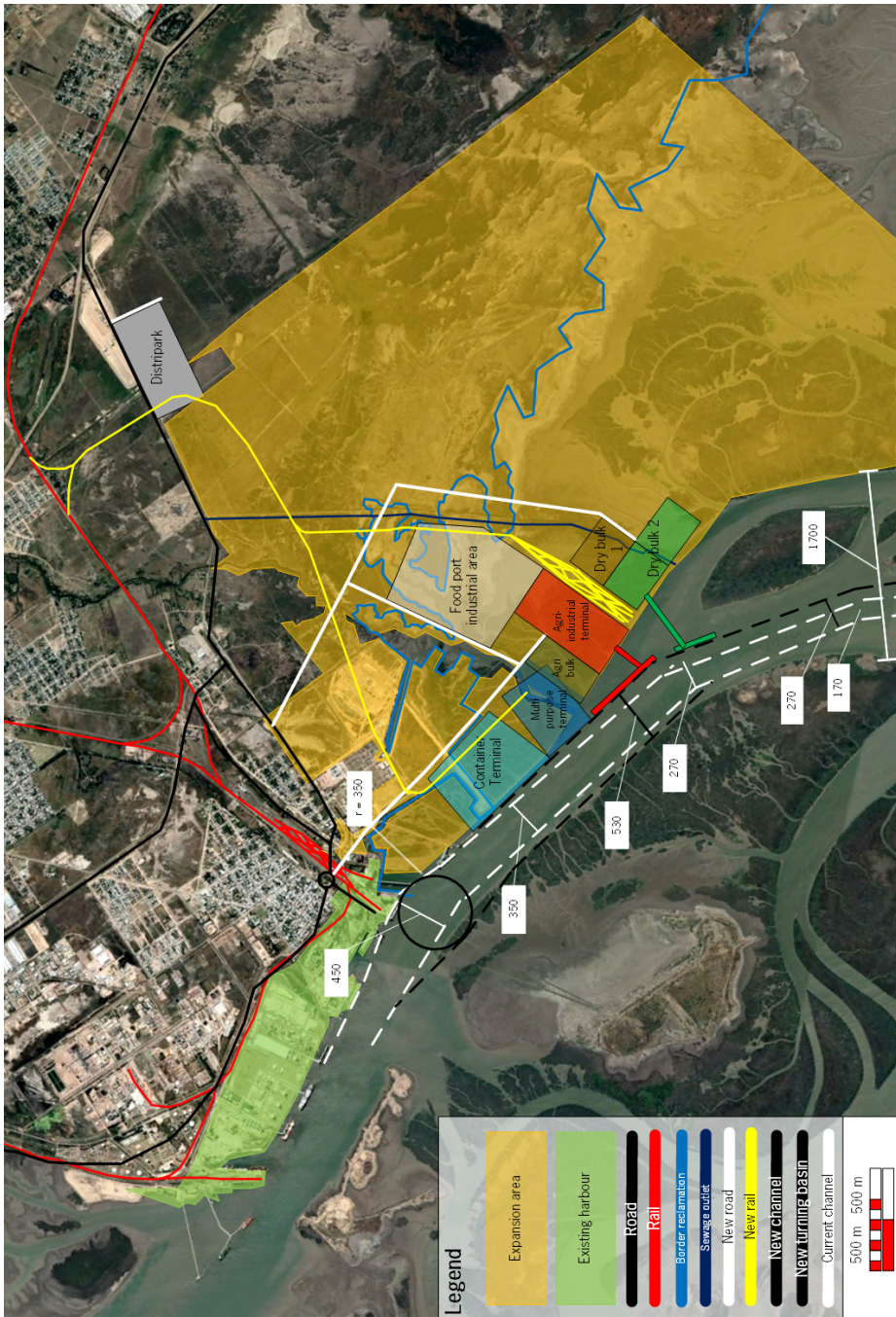
Figure 0.3. Alternative 2 for the east expansion.
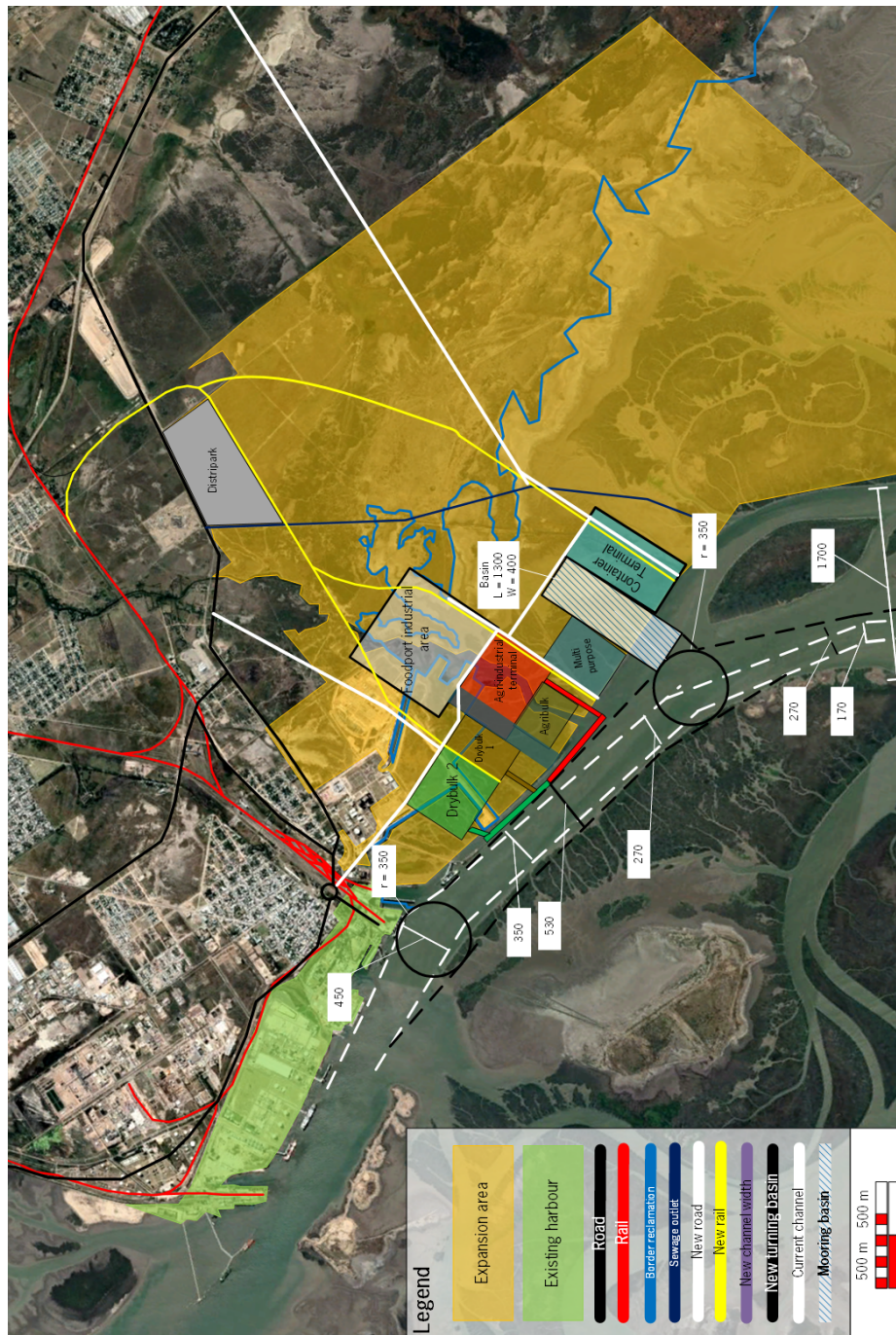
Figure 0.4. Alternative 3 for the east expansion.
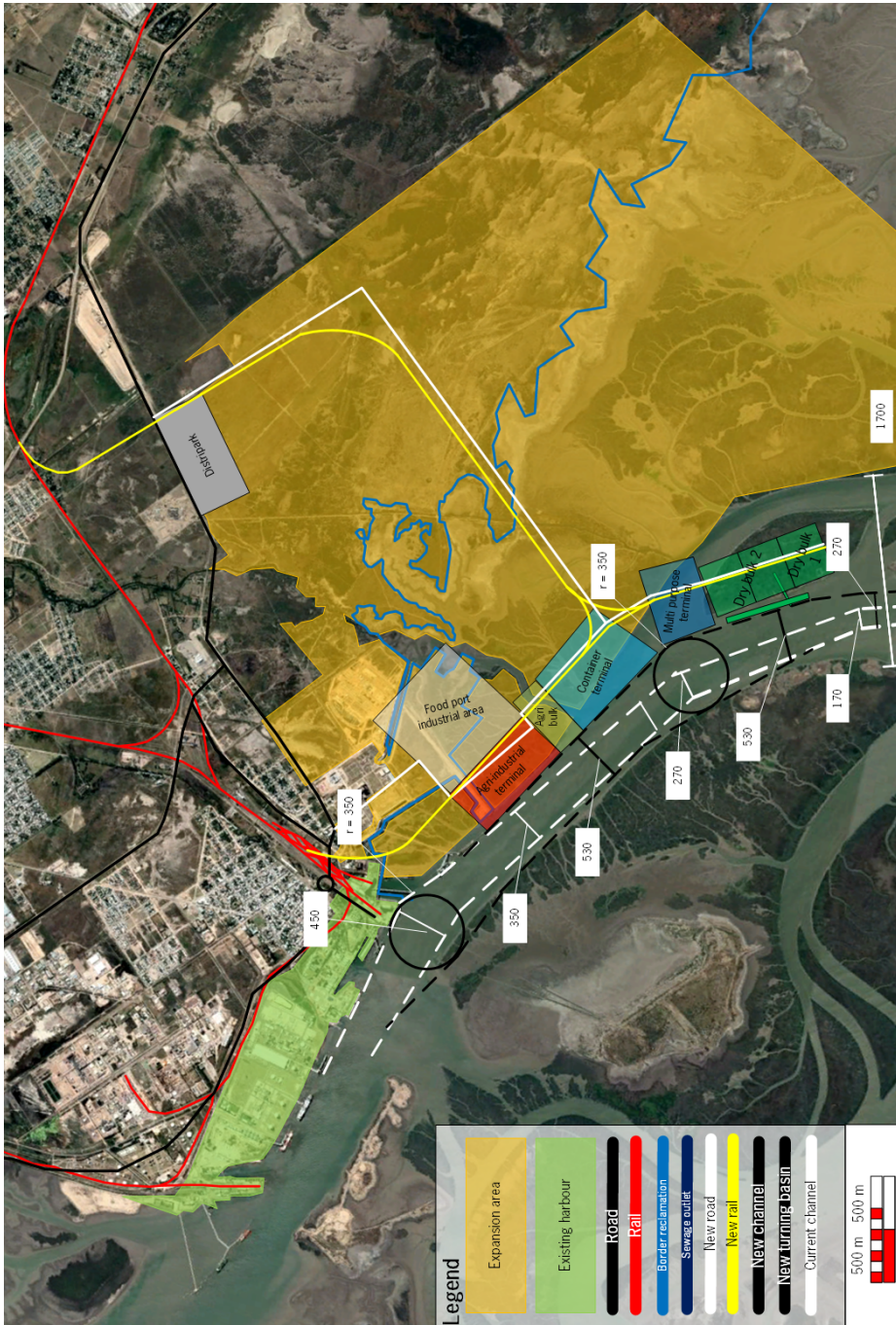
Figure 0.5. Alternative 4 for the east expansion.

0.2. South expansion
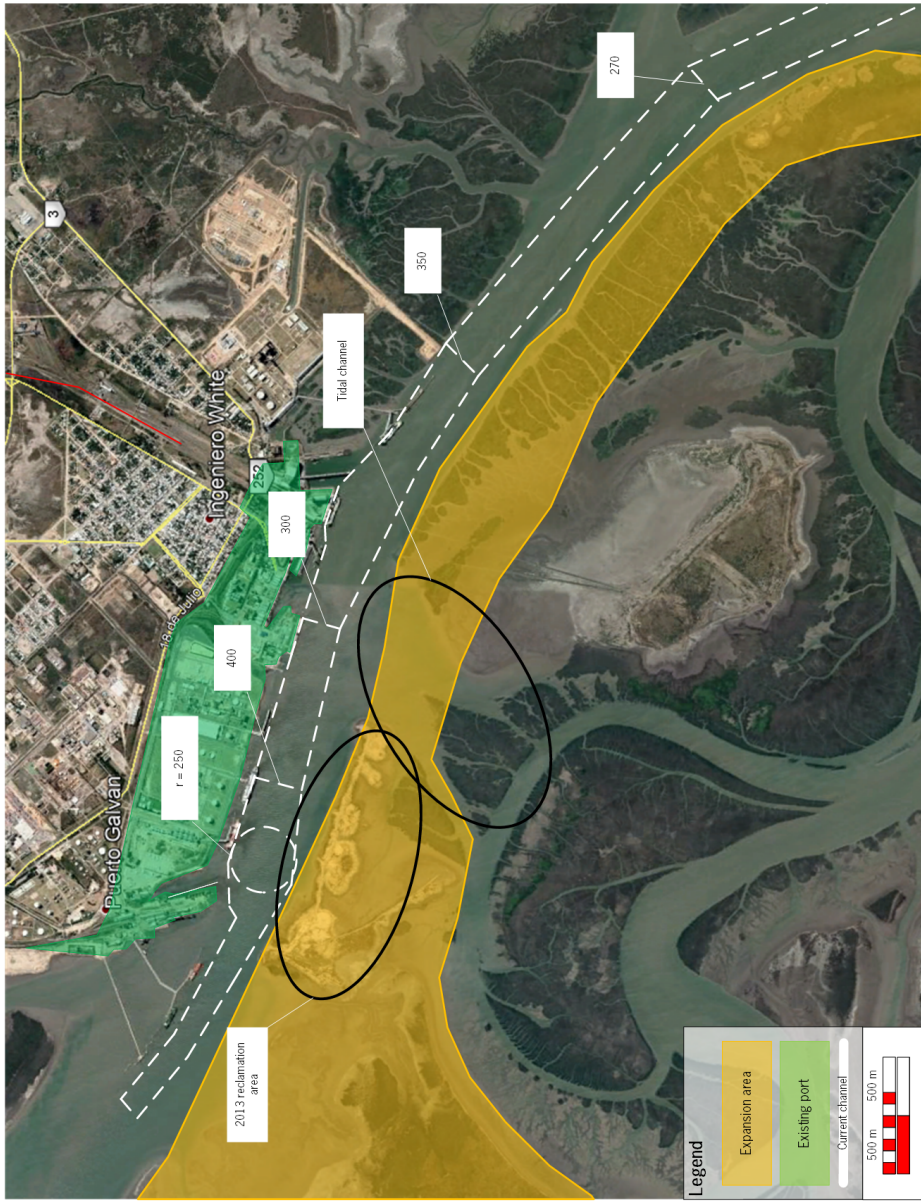
Figure 0.6. General lay-out south position.

Figure 0.7. Options for the infrastructural connections to the current port.
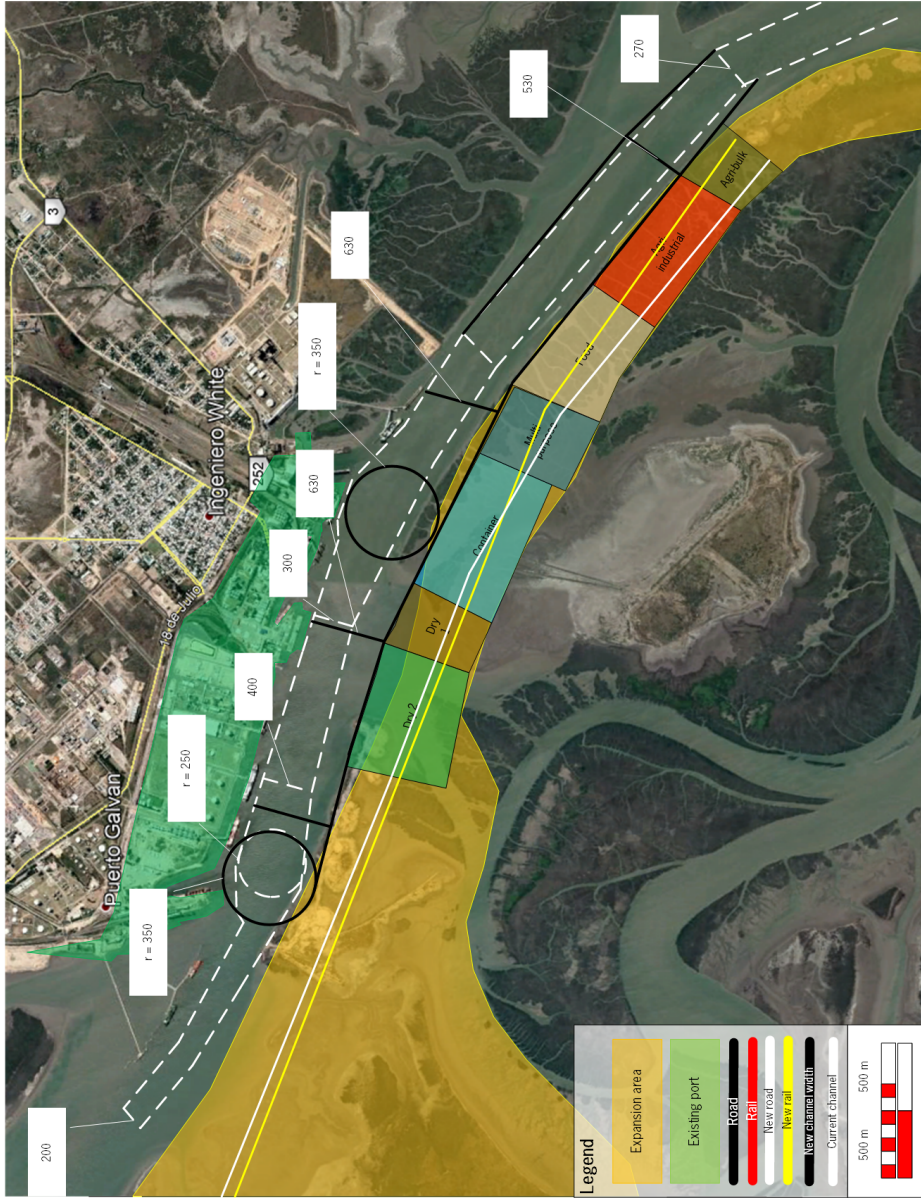
Figure 0.8. Alternative 1 for the south expansion.
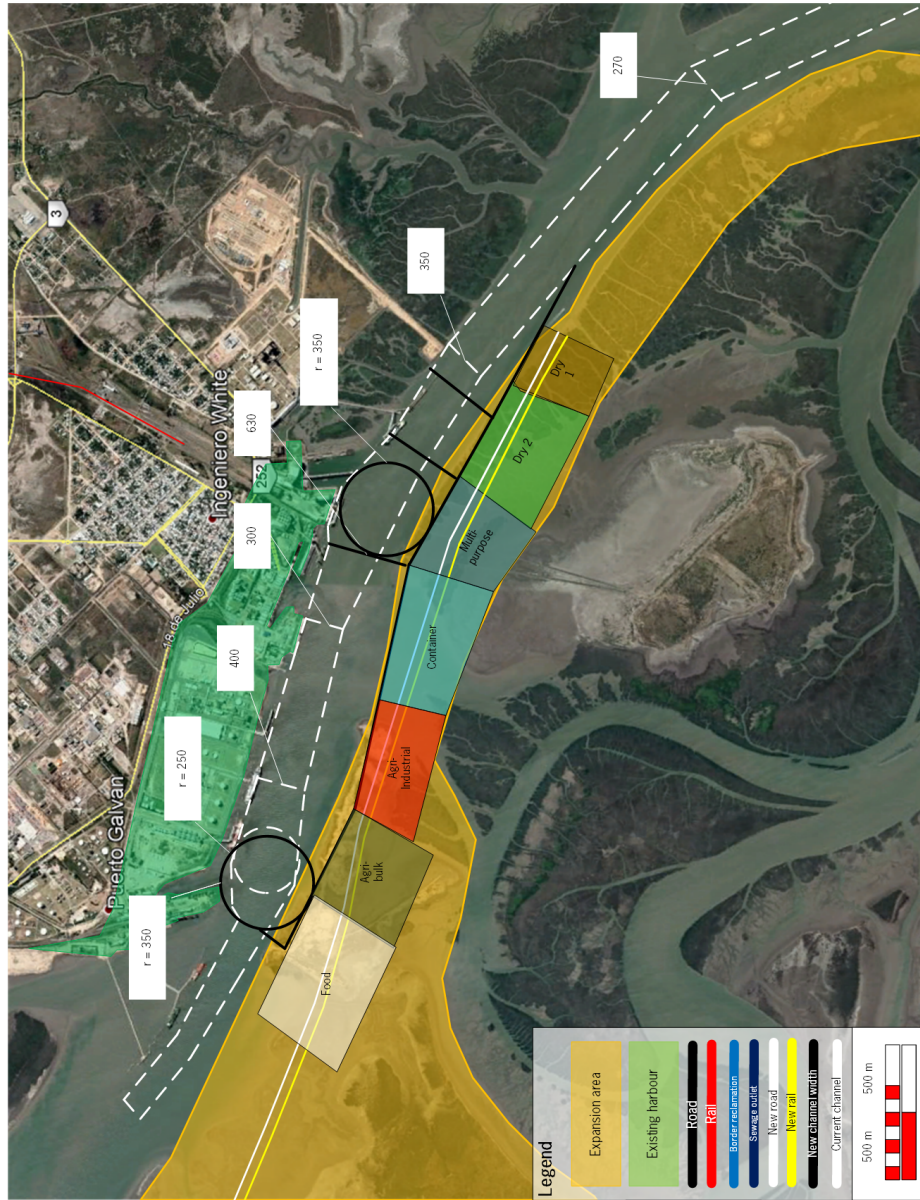
Figure 0.9. Alternative 2 for the south expansion.

Figure 0.10. Alternative 3 for the south expansion.

0.3. Final Design
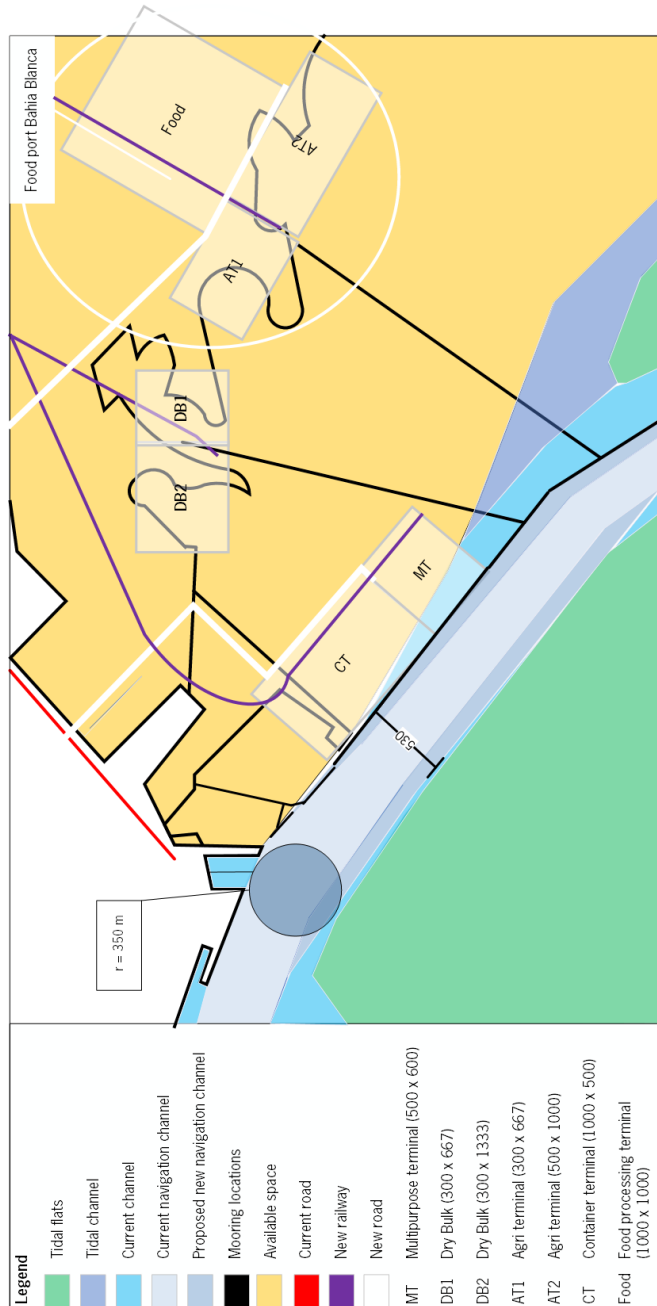
Figure 0.11. Most feasible lay-out for east bank.
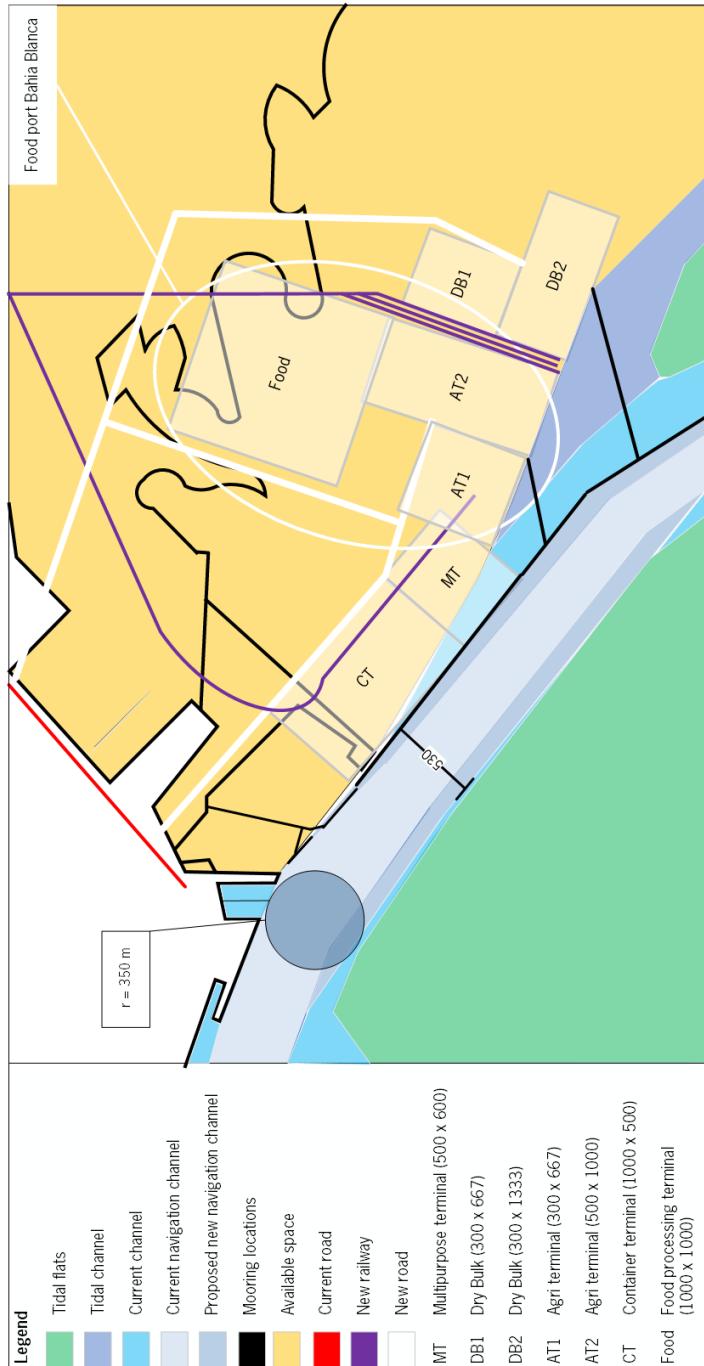
Figure 0.12. Best lay-out for east bank.

Figure 0.13. Most feasible lay-out for south bank.

Legend

- Tidal flats
- Tidal channel
- Current channel
- Current navigation channel
- Proposed new navigation channel
- Mooring locations
- Available space
- Current reclamation
- New railway
- New road

MT — Multipurpose terminal (500 x 600)
DB1 — Dry Bulk (300 x 667)
DB2 — Dry Bulk (300 x 1333)
AT1 — Agri terminal (300 x 667)
AT2 — Agri terminal (500 x 1000)
CT — Container terminal (1000 x 500)
Food — Food processing terminal (1000 x 1000)